Nagra
Nationale
Genossenschaft
für die Lagerung
radioaktiver Abfälle

Cédra
Société coopérative
nationale
pour l'entreposage
de déchets radioactifs

Cisra
Società cooperativa
nazionale
per l'immagazzinamento
di scorie radioattive

TECHNICAL REPORT 87-08

NATURAL ANALOGUE STUDIES IN CRYSTALLINE ROCK: THE INFLUENCE OF WATER-BEARING FRACTURES ON RADIONUCLIDE IMMOBILISATION IN A GRANITIC ROCK REPOSITORY.

W.R. ALEXANDER
A.B. MACKENZIE
R.D. SCOTT
I.G. MCKINLEY

JUNE 1990

Parkstrasse 23 5401 Baden/Schweiz Telephon 056/20 55 11

Der vorliegende Bericht wurde im Auftrag der Nagra erstellt. Die Autoren haben ihre eigenen Ansichten und Schlussfolgerungen dargestellt. Diese müssen nicht unbedingt mit denjenigen der Nagra übereinstimmen.

Le présent rapport a été préparé sur demande de la Cédra.
Les opinions et conclusions présentées sont celles des auteurs et ne correspondent pas nécessairement à celles de la Cédra.

This report was prepared as an account of work sponsored by Nagra. The viewpoints presented and conclusions reached are those of the author(s) and do not necessarily represent those of Nagra.

ABSTRACT

Current Swiss concepts for the disposal of radioactive waste involve disposal in deep mined repositories to ensure that only insignificant quantities of radionuclides will ever reach the surface and so enter the biosphere. The rock formations presently considered as potential candidates for hosting radwaste repositories have thus been selected on the basis of their capacity to isolate radionuclides from the biosphere. An important factor in ensuring such containment is a very low solute transport rate through the host formation. However, it is considered likely that, in the formations of interest in the Swiss programme (eg. granites, argillaceous sediments, anhydrite), the rocks will be fractured to some extent even at repository depth. In the instance of the cumulative failure of near-field barriers in the repository, these hydraulically connected fractures in the host formation could be very important far-field routes of migration (and possible sites of retardation) of radionuclides dissolved in the groundwaters. In this context, the so-called "matrix diffusion" mechanism is potentially very important for radionuclide retardation.

This report is the culmination of a programme which has attempted to assess the potential influence of these water-bearing fractures on radionuclide transport in a crystalline rock radwaste repository. Four rock drill-cores, which intersected suspected water-conducting fractures, were examined for indications of rock-water interactions. Elemental migration (or lack of migration) in the vicinity of the fractures has been examined by means of disequilibrium in the natural decay series. The distributions of a suite of other elements were also established for each core in an attempt to define more clearly the precise nature of any observed rock-water interactions. In general, the processes involved in the transport of any of the elements studied out of the bulk rock are analogous to those which could cause retardation of dissolved radionuclides, released from the repository, by their transport into the rock - the matrix diffusion mechanism previously mentioned.

Data are presented which indicate that a significant depth of rock (up to 0.5 m) behind a water-bearing fracture may be accessible to radionuclides in the groundwaters. Detailed petrographic examination of some of the material analysed suggests that large-scale (often hydrothermally altered) damaged zones associated with the water-bearing fractures probably allow groundwater flowing in the fractures greater access to the rock matrix in the immediate vicinity. Simple calculations imply that transport in the matrix is, however, advective and not purely diffusive as envisaged in the matrix diffusion scenario. The presence of potentially large volumes of "accessible rock" are clearly very significant for radionuclide retardation in the geosphere and the implications for safety assessment are discussed briefly.

ZUSAMMENFASSUNG

Das gegenwärtige Konzept für die Entsorgung von radioaktiven Abfällen in der Schweiz stützt sich auf eine Endlagerung im tiefen Untergrund, um sicherzugehen, dass höchstens unbedeutende Mengen von Radionukliden je an die Oberfläche und somit in die Biosphäre gelangen. Die in Frage kommenden Formationen wurden aufgrund ihres Vermögens ausgesucht, Radionuklide möglichst vollständig im Endlager einzuschliessen. Dabei spielt eine niedrige Transportrate gelöster Stoffe durch die Geosphäre eine grosse Rolle. Es wird angenommen, dass die in Frage kommenden Gesteine (z.B. Granite, tonige Sedimente, Anhydrit), die in den schweizerischen Programmen untersucht werden, bis zu einem gewissen Masse auch in Endlagertiefe geklüftet sein werden. Im Moment des Versagens der technischen Barrieren eines Endlagers bekommen die hydraulisch verbundenen Klüfte im Wirtgestein eine wichtige Bedeutung für den Transport (und mögliche Retardierungsfaktoren) von gelösten Radionukliden im Grundwasser. In diesem Zusammenhang sind die Matrixdiffusions-Effekte möglicherweise ein sehr wichtiger Faktor für den verzögerten Transport von Radionukliden.

In diesem Bericht werden die Ergebnisse eines Programmes zusammengefasst, das versucht hat den Einfluss dieser wasserführenden Klüfte auf den Transport von Radionukliden im kristallinen Gestein eines potentiellen Endlagers festzustellen. Es wurden vier Bohrkerne, welche wasserführende, geklüftete Zonen durchfahren, auf Hinweise von Gestein-Wasser-Interaktion untersucht. Die Migration von Elementen (oder deren Fehlen) in der unmittelbaren Umgebung der Klüfte wurde mit Hilfe von Aktivitätsungleichgewichten innerhalb der natürlichen Verfallsreihen untersucht. Für jeden Bohrkern wurden ebenfalls Konzentrationsverteilung einer Reihe anderer Elementen festgestellt um die Natur der beobachteten Gestein-Wasser-Interaktion klarer festlegen zu können. Generell sind die Vorgänge die am Transport jeglicher Elemente aus dem Gestein - d.H. Mobilität im wassergesättigten Porenraum der Gesteinsmatrix - beteiligt sind, vergleichbar mit jenen, die zur Retardierung freigesetzter Radionuklide führen können.

Es werden Daten präsentiert, die zeigen, dass eine relativ breite Zone (bis zu 0.5 m) entlang einer wasserführenden Kluft für im Grundwasser gelösten Radionulide erreichbar ist. Detaillierte petrographische Untersuchungen des analysierten Materials deuten an, dass grosse (oft hydrothermal umgewandelte) Störzonen, in Verbindung mit wasserführenden Klüften, dem Grundwasser aus den Klüften wahrscheinlich verstärkten Zugang zur unmittelbar anstehenden Gesteins-Matrix ermöglichen. Einfache Berechnungen bedingen advektiven Transport in der Gesteinsmatrix wo üblicherweise jeweils nur mit Diffusionsvorgängen gerechnet wurde. Ein grösstmögliches Volumen an "erreichbarem Gestein" ist für die Retardierung von Radionukliden in der Geosphäre von grösster Wichtigkeit. Die Bedeutung solcher Phänomene für die Sicherheitsanalyse wird kurz diskutiert.

RESUME

Le concept suisse actuel d'évacuation des déchets radioactifs prévoit leur stockage final dans des dépôts excavés en profondeur dans le sous-sol, conçus de sorte à ce que des quantités significatives de radionucléides ne puissent jamais atteindre la surface et de la sorte pénétrer dans la biosphère. Les formations considérées aujourd'hui comme roches d'accueil potentielles pour recevoir des déchets radioactifs ont été sélectionnées sur la base de leur aptitude à isoler les radionucléides de la géosphère. Un facteur important pour assurer un tel confinement est un très faible taux de transport des radionucléides en solution dans l'eau à travers la formation rocheuse d'accueil. On pense cependant qu'il est vraisemblable que, dans les formations rocheuses considérées dans le programme suisse (par ex. granites, sédiments argileux, anhydrite), les roches seront fracturées dans une certaine mesure, même à la profondeur du dépôt. En cas de défaillance cumulative des barrières du champ proche du dépôt, ces fractures dans la roche d'accueil, hydrauliquement connectées les unes aux autres, pourraient représenter des routes de migration très importantes (et d'éventuels sites de retardement) pour les radionucléides dissous dans les eaux souterraines. Dans ce contexte ledit mécanisme de "diffusion matricielle" représente un élément potentiel très important pour le retardement de radionucléides.

Ce rapport représente le point culminant d'un programme qui cherchait à évaluer l'influence potentielle de ces fractures aquifères sur le transport de radionucléides issus d'un dépôt pour déchets radioactifs implanté dans une roche cristalline. Quatre carottes rocheuses, qui coupaient des fractures soupçonnées être aquifères, ont été examinées en vue de détecter des indices d'interactions roche/eau. La migration (ou l'absence de migration) d'éléments dans le voisinage des fractures a été étudiée par le biais du déséquilibre de séries de désintégrations naturelles. On a également établi pour chaque carotte les distributions d'une chaîne d'autres éléments afin d'essayer de mieux définir la nature précise de toutes interactions roche/eau observées. D'une façon générale les phénomènes impliqués dans le transport de chacun des éléments étudiés à l'extérieur de la roche massive sont analogues à ceux qui peuvent être à l'origine du retardement de radionucléides dissous, relâchés du dépôt, par leur transport dans la roche - le mécanisme de diffusion matricielle mentionné précédemment.

Des données sont présentées qui montrent qu'une profondeur significative de roche (jusqu'à 1/2 m) en arrière d'une fracture aquifère peut être accessible aux radionucléides transportés par les eaux souterraines. Un examen pétrographique détaillé d'une partie des matériaux analysés suggère que de vastes zones endommagées (souvent avec altérations hydrothermales) associées à des fractures aquifères permettent vraisemblablement aux eaux souterraines circulant dans ces fractures de mieux accéder à la

matrice rocheuse au voisinage immédiat. On déduit cependant de calculs simples que le transport dans la matrice se fait par advection et non purement par diffusion comme envisagé dans le scénario de diffusion matricielle. La présence de grands volumes potentiels de "roche accessible" est évidemment très importante pour le retardement de radionucléides dans la géosphère et ses implications lors de l'évaluation de la sûreté sont brièvement discutées.

TABLE OF CONTENTS Page

LIST OF FIGURES Page

LIST OF TABLES

1. INTRODUCTION

1.1 Prolegomena

The rock formations considered as potential candidates for the disposal of nuclear waste have been selected on the basis of their capacity to isolate radionuclides from the geosphere. A major factor in assuring such isolation is a very low solute transport rate through the system. This, however, inherently makes the study of transport processes very difficult - the solute migration distances are simply too small to be measured accurately on a laboratory timescale. This problem is particularly acute when attempting to measure matrix diffusion, which has been shown to play a very important role in assuring repository safety, in fissured media. Even in individual fissures where flow velocities may be reasonably fast, there is considerable evidence that flow is localised in channels in the fissure plane. It is not known, however, if such channels are ephemeral entities or if they are stable over long periods of time - ie. can they be "averaged" over the entire plane or must they be considered as discrete?

One approach which circumvents the timescale problem is the examination of "natural analogues" (CHAPMAN et al. 1984). The observed distribution of many species can be interpreted in terms of long timescale migration processes, with the additional advantage that the processes involved have occurred in a relatively unperturbed system. Naturally occurring radionuclides are particularly favourable in this regard as the process of radioactive decay may provide an inbuilt "clock" which allows a more quantitive analysis of hydrochemical processes and their rates.

1.2 The rôle of matrix diffusion in Swiss safety assessment

Current Swiss concepts for the disposal of radioactive wastes involve disposal in mined repositories to ensure that insignificant quantities of radionuclides will ever reach the surface and so enter the biosphere. The host rock provides physical protection for the repository structures and acts as a barrier to radionuclides migrating from the waste. It is considered likely that, in the formations of interest in the Swiss programme (e.g. granites, argillaceous sediments, anhydrite), the rocks will be fractured to some extent even at repository depth. In the instance of the cumulative failure of near field barriers in the repository, these hydraulically connected fractures in the host formation could be very important far-field routes of migration (and possible sites of retardation) of radionuclides dissolved in the groundwaters. In this context, matrix diffusion is an important retardation mechanism.

The term matrix diffusion is applied to the process by which solute in a hydrologic system, dominated by flow in distinct fissures, penetrates the surrounding rock (e.g. NERETNIEKS, 1980). The cases of matrix diffusion of interest in the nuclear waste field represent an extreme case of the general dual porosity hydraulic medium in which advective flow occurs entirely in the fissure (or primary) porosity while all solute transport in the bulk rock (or secondary) porosity occurs by diffusion (e.g. BARENBLATT et al., 1960; GRISAK and PICKENS, 1980). The diffusion into the rock occurs in a connected system of pores or microfractures; diffusion through the solid phase is insignificant by comparison.

The importance of matrix diffusion in the context of repository safety analysis is that it provides a mechanism for enlarging the rock surface in contact with advecting solute from fracture surfaces and infill to a portion (or all) of the bulk rock. The sorption of radionuclides in the rock matrix can greatly increase retardation which, if the resulting transport time is greater than the nuclide half-life, can decrease total releases by orders of magnitude (e.g. KBS, 1983; NAGRA, 1985a). Additionally, pulse releases of radionuclides to the biosphere can be spread over a longer time period - thus decreasing release concentrations by a process of temporal dilution. Even non-sorbing nuclide releases can be decreased by dilution in the reservoir of matrix pores. Although radionuclide retardation is generally of most concern, it has also been noted that the bulk rock can also serve as an important chemical buffer - especially for oxidants produced by radiolysis in the near field (e.g. NERETNIEKS, 1983, 1986).

Redox buffering reactions within the rock matrix have been invoked as a retardation mechanism within the Swedish KBS-3 project (e.g. NERETNIEKS, 1983, 1986) and thus information about such processes is of direct relevance to repository safety assessment. Buffering of radiolytically produced oxidant within the rock matrix is not only directly significant in terms of decreasing the solubility and mobility of some important radionuclides, but if such a "redox front" (cf. sandstone roll-front U deposits and marine U horizons; COWART, 1980; COLLEY et al., 1984; COLLEY and THOMPSON, 1985) is predominantly confined within the (micro-)porous structure of the host rock, then any formation of colloids at this location would be less problematic than if such colloids formed in an open feature in which advective transport occurs. In this study an attempt has been made to examine possible radionuclide immobilisation by redox fronts through the relationship between U and other redox sensitive elements.

In order to incorporate matrix diffusion into a transport model two key parameters are required - the depth to which interconnected porosity extends from the fissure into the bulk rock and the diffusivity of the solute of interest in the rock (possibly as a function of distance from the fissure). The first parameter is obviously very rock- and site-dependent but, even for particular rock types, the conceptual model adopted can vary considerably. For granite, it is assumed by KBS (1983) that a network of connected porosity extends through the entire rock and that diffusivity is constant throughout this region. Alternative models assume that

diffusion occurs predominantly (or entirely) in dead-end pores (GLUECKAUF, 1980) or in a microfractured damage zone (HADERMANN and ROESEL, 1985) which corresponds to a limited matrix diffusion extending only in the order of centimetres from the fracture.

Matrix diffusion can be readily studied in the laboratory only for rock types with large diffusivities (e.g. fractured sandstones) whereas most rocks of relevance to nuclear waste applications (e.g. crystalline rocks, argillaceous sediments) have very low diffusivities. The main problems arise from sampling and preparation. Sampling almost inevitably involves allowing the rock to de-stress, from which it may not recover completely, even if the rock is re-stressed prior to measurement. Sample preparation usually involves either cutting or splitting along a natural fracture which can cause extensive surface damage and, in the latter case, loss of secondary hydrothermal alteration products which may naturally seal some (or all) of the fissure surface porosity. Surface damage is particularly important for crystalline rocks as it will inevitably extend to at least a depth comparable with the grain size (as the rock minerals are generally stronger than the rock matrix). For a coarse grained rock, this depth would be comparable to the diffusion distance of a tracer on a manageable laboratory timescale. It should be noted that these problems also, in principle, apply to field tracer tests to examine diffusion (e.g. ABELIN et al., 1986; BIRGERSSON and NERETNIEKS, 1988).

Further, the potential errors caused by these perturbations all tend to cause overestimation of the diffusivity. As overestimation of diffusivity leads to a better performance of the geosphere as a retardant, it is non-conservative in the safety assessment sense.

One approach which does, however, circumvent both the problems of sample perturbation and slowness of the diffusion process involves the study of natural series radionuclide profiles perpendicular to a water-carrying fissure. The preferential mobility of the daughters of U and Th, relative to their parents, allows them to be mobilised from the bulk rock if connected porosity extends to an advective flow. The diffusion of such nuclides from the rock into the fissure is thus analogous to diffusion of solute from the fissure into the rock as considered in the safety analysis models. Natural series daughter mobilisation, as reflected by isotope ratios, can thus, at the simplest level, provide unambiguous evidence of the minimum depth of interconnected porosity. Additionally, however, information on the rate of diffusion can also be derived from the "clock" provided by the radioactive decay process. In principle, models of natural series radionuclide release and transport into the fissure could be derived which used laboratory diffusivity data and hence could be validated by observations. In real life, however, it is very difficult to determine the boundary conditions in the system in sufficient detail for full validation (HERZOG, 1987). Nevertheless, at least semi-quantitative data on the order of magnitude of the diffusion rate might be derived by curve-fitting a simpler model.

1.3 Natural analogue application to fracture-flow systems

This report is the culmination of a programme which has attempted to assess the potential influence of water-bearing fractures on radionuclide transport in a crystalline rock radwaste repository (see also SMELLIE et al., 1986a). Four rock drillcores, which intersected suspected water conducting fractures, were examined for indications of rock-water interactions. Two cores were take from NAGRA's underground test site (FLG) at Grimsel, southern Switzerland, one from NAGRA's exploratory borehole at Böttstein which penetrates the crystalline basement of northern Switzerland and another from a SKB test hole in the Götemar granite, at Kråkemåla on the southeastern coast of Sweden.

The intention of this study was to appraise past elemental migration (or lack of migration) in the vicinity of the fractures by means of disequilibrium in the natural decay series in profiles taken perpendicular to the suspected water-bearing zones (cf. SMELLIE and ROSHOLT, 1984). The distributions of the rare earth elements (REE) and several redox sensitive species (e.g. Fe, Mn) were also established for each core in an attempt to define, more clearly, the precise nature of any observed rock-water interactions. In general, the processes involved in the transport of any of the above species out of the bulk rock are analogous to those which could cause retardation of dissolved radionuclides, released from the repository, by their transport into the rock - the previously described matrix diffusion mechanism.

The four cores have been analysed for members of the natural decay series and rare earth elements (REE). These are useful natural (chemical) analogues for various radionuclides of interest in a nuclear waste management context. The trivalent lanthanides, for example, have ionic radii very close to those of Am^{3+} and Cm^{3+} while the sorption behaviour of Nd is similar to that of Am. U and Ra are, clearly, of direct interest for safety assessment while Th^{4+} can be considered as a generic analogue of the actinides in the IV oxidation state.

Of course, care must be taken with all chemical analogues, especially for redox sensitive elements, and it is essential in this regard to define, as precisely as possible, the prevailing (and historical) geochemical conditions of the environment studied.

1.4 Natural decay series disequilibria

In a closed geological system all of the nuclides in the natural decay chain studied here (i.e. ^{238}U-^{234}U-^{230}Th-^{226}Ra) will attain radioactive equilibrium in about 1.7 My from an initial disequilibrium with the $^{234}U/^{238}U$, $^{230}Th/^{234}U$, $^{226}Ra/^{230}Th$ activity ratios all equal to unity.

However, if the rock-water system is open to transfer processes, the differing solubility characteristics exhibited by the various members of the natural decay series will result in their chemical fractionation and so lead to isotopic disequilibrium. In general, the mechanisms involved are well documented with α-recoil (FLEISCHER and RAABE, 1978; ROSHOLT, 1983), sorption (LANGMUIR and HERMAN, 1980, BARNEY et al., 1985), preferential leaching (EYAL and FLEISCHER, 1985; LATHAM and SCHWARCZ, 1987a), cation exchange (TANNER, 1964) and complexation reactions (ZUKIN et al., 1987) all recognised as being of importance in this context.

It has thus become standard practise to utilise isotopic disequilibria in the natural decay series as a sensitive indicator of the timing of recent rock-water reactions (e.g. CHERDYNSTEV, 1955, 1971; IVANOVICH and HARMON, 1982; SMELLIE et al., 1986b; ALEXANDER et al., 1987). In theory, at least, the timing of any mobilisation of U or Ra (in most rock-water systems Th is considered to be relatively immobile; LANGMUIR and HERMAN, 1980) can be determined simply from the half-life of the nuclide involved by examination of the daughter/parent activity ratios. For example, a disturbance in the $^{226}Ra/^{230}Th$ system will be detectable for some 8000 years because the ingrowth of ^{226}Ra will be controlled by its own half-life ($\approx$1600 y) and would be measurably, in the case of a severe disturbance, far from equilibrium for around 5 half-lives.

However, to date any leaching or depositional event in this way requires that the rock-water system has remained closed since the disturbing event and that the event itself lasted a very short time relative to the half-lives used - something which is often impossible to assess (e.g. THIEL et al., 1983; SCOTT and MACKENZIE, 1989). In this report the interpretation of U-Th-Ra activity ratios is examined somewhat more rigorously than is usual with the aim of identifying ambiguities in the standard evaluation of measured data. It is evident that, in many cases, unambiguous results can only be achieved with the backing of information from other sources such as petrographic examination and stable isotope studies.

2. SAMPLE DESCRIPTION

2.1 Introduction

Four rock drillcores from three granite terrains are discussed in this report, two from NAGRA's underground test site (FLG) at Grimsel in southern Switzerland (Fig. 1), one from the granite basement in the NAGRA exploratory borehole at Böttstein, northern Switzerland (Fig. 2) and one from the SKB pilot borehole in the Kråkemåla area of the Götemar granite in southeastern Sweden (Fig. 3). In all four cases the drillcore is believed to have intersected a water-conducting fracture in the granite.

2.2 FLG site drillcores, AU96.90W and SB80.001 (94.12-94.52 m)

The Grimsel underground laboratory is situated under the Juchlistock Massif, about 1 km inside the mountain at an elevation of some 1730 metres above sea level. The experimental drifts lie under about 450 m of overburden and both rock cores were obtained by drilling directly into the tunnel walls.

The regional geology is detailed in LABHART (1977) while the Grimsel area and the FLG site are comprehensively covered in STECK (1968), CHOUKROUNE AND GAPAIS (1983), NAGRA (1981), NAGRA (1985b) and MEYER et al. (1989). Briefly, the FLG is situated in the Aare Massif which consists of gneissose zones, Hercynian granites and Carboniferous volcanoclastics with core SB80.001 taken from the Central Aare granite. Core AU96.90W is from further south (Fig. 4) in the Grimsel granodiorite.

The granitic rocks of this area have a complex post-emplacement history (summarised in MEYER et al., 1989) which includes intrusion, firstly by aplitic dykes and then by mafic lamprophyres. The interfaces between these latter dykes and the Aare granitic rocks provide the main control on present groundwater flow in the bedrock (OHSE, 1983). Structurally, the sample sites are relatively straightforward with the fractures belonging to the Alpine greenschist facies shear zones (MEYER et al., 1989). The rocks are generally representative of the Grimsel granite/granodiorite as described by STALDER (1964) and, in hand specimen, are light- to mid-grey, medium to coarse grained, slightly gneissose, mineralogically homogeneous and unaltered. Major constituents are quartz, K-feldspar > plagioclase, biotite muscovite, hornblende and epidote with accessory sphene, allanite, apatite and zircon.

The sub-sampling of the granodioritic core AU96.90W is detailed in Figure 5 while the mineralogical composition of the core is displayed in Table 1. This core intersects the plane of a fracture which has measured flow rates, in various channels, of between 20 and 2000 ml min^{-1} (McKINLEY et al., 1988). The fracture face was observed to be wet on inspection and water was released when the fracture zone was intersected during drilling. This zone is presently packed off and has maintained a flow rate of some 2000 ml min^{-1} for several years.

Figure 1: Simplified geological cross-section of the FLG, southern Switzerland

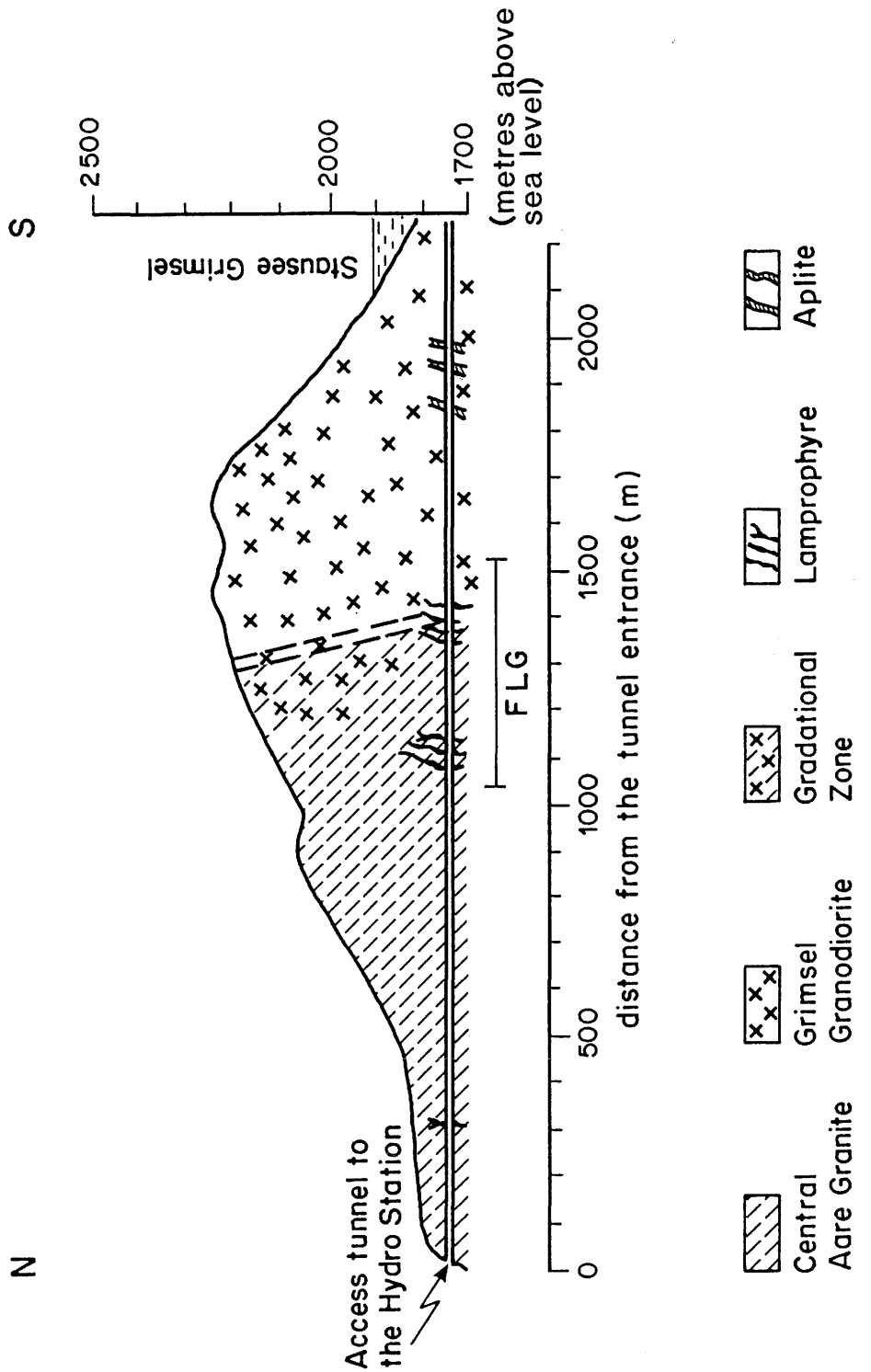

Figure 2: Sampling site of core BOE, Böttstein, northern Switzerland

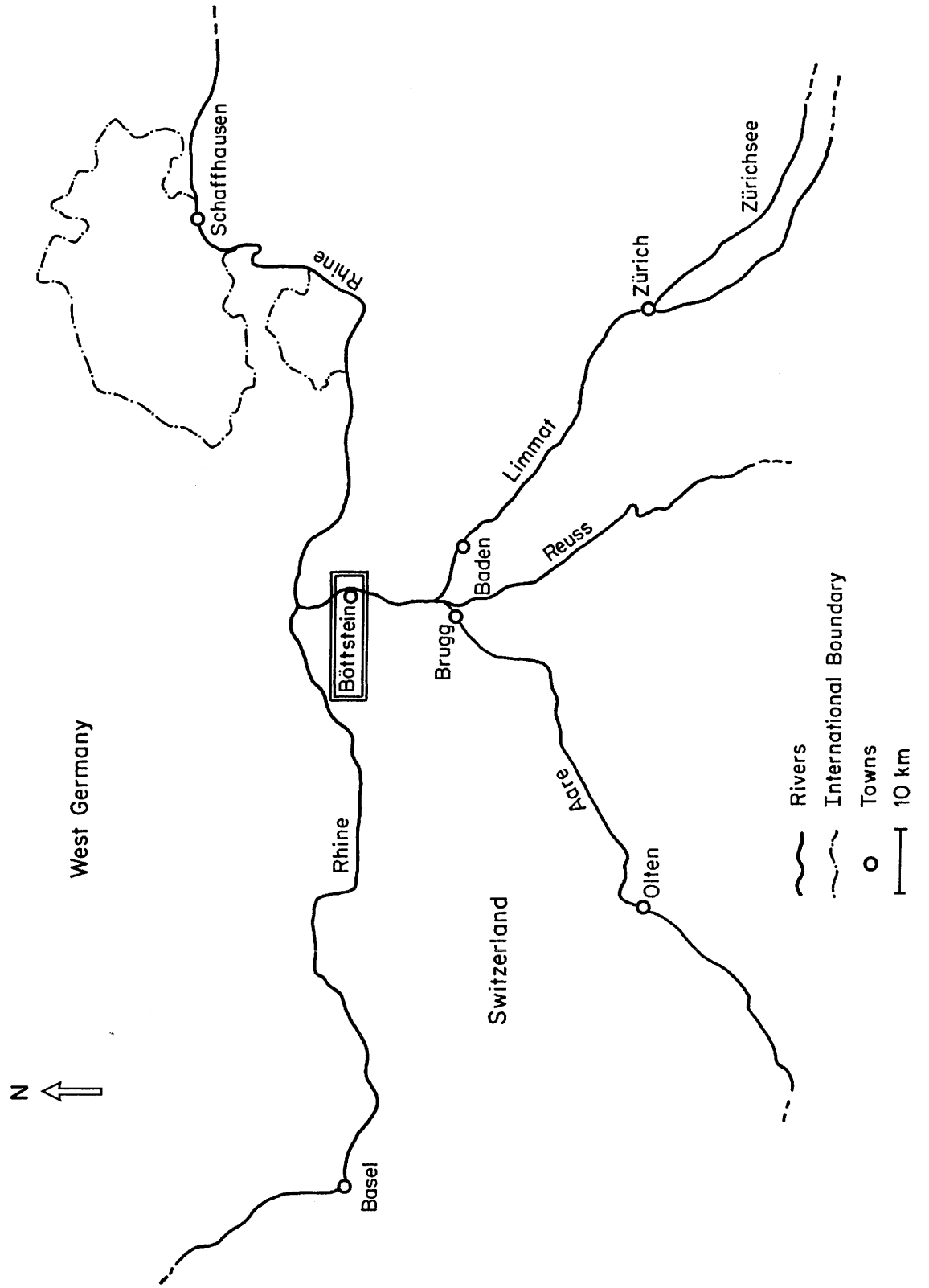

Figure 3: Geological map of the Götemar Massif, South-East Sweden

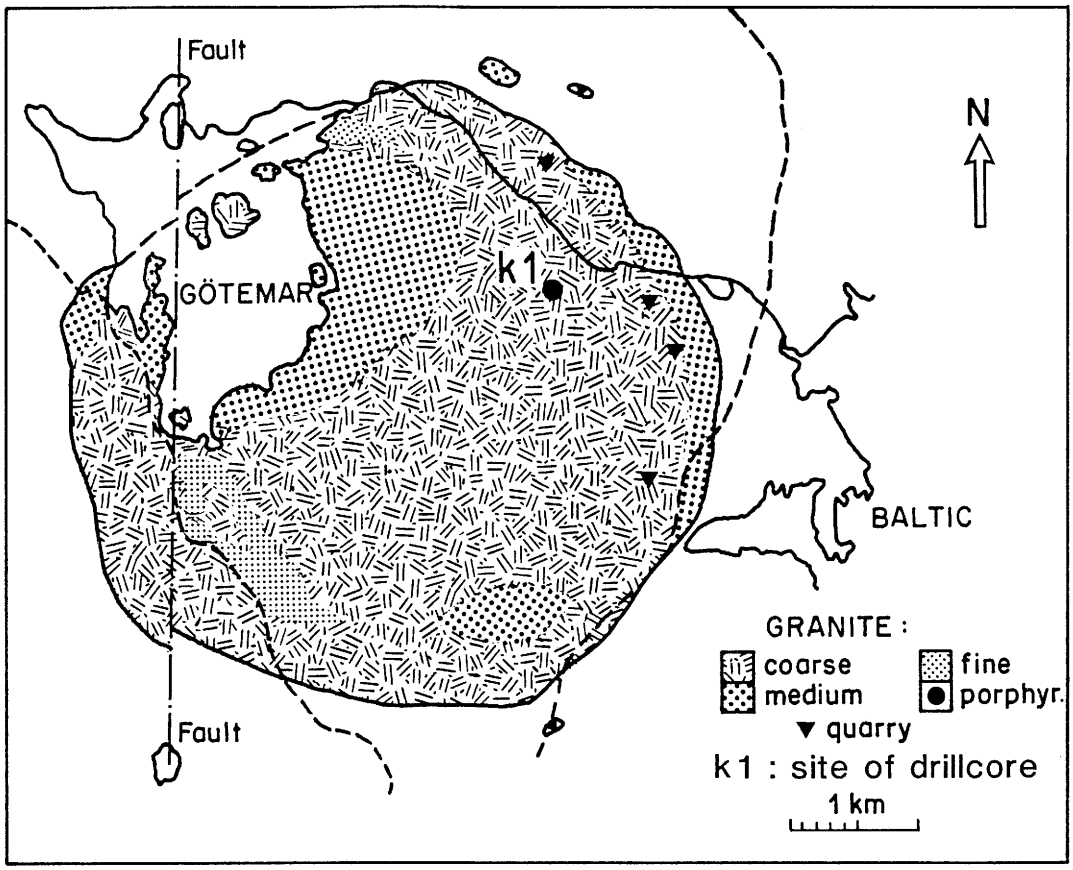

Figure 4: Sampling sites in the FLG

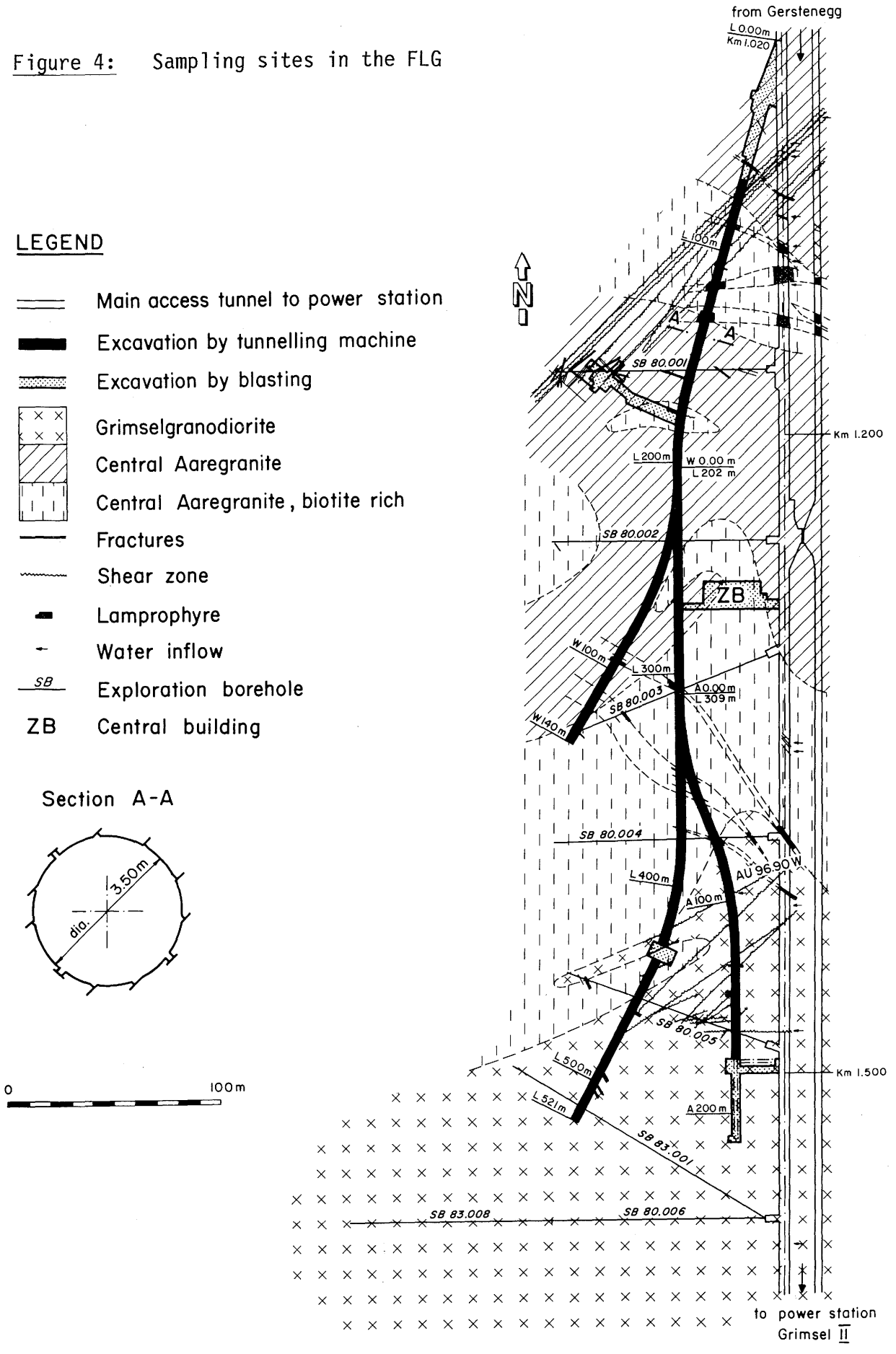

Figure 5: Simplified core map of drillcore AU96.90W (FLG). (DOLLINGER, pers. comm.) Figures 7-13 refer to the samples indicated here.

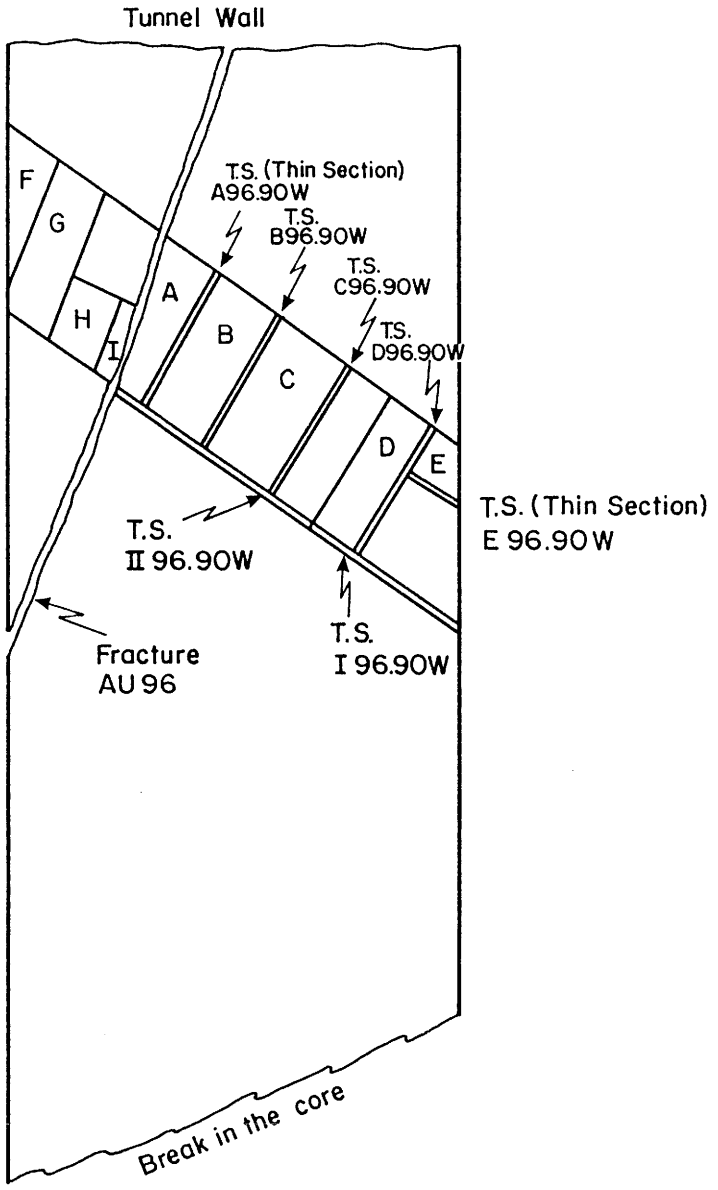

Sample Nº	Distance from fracture (cm)
A	+ 0.45
B	+ 1.60
C	+ 3.00
D	+ 4.80
E	+ 5.50
F	− 2.25
G	− 1.60
H	− 0.75
I	− 0.15

Of note in this core is the intense sericitisation and saussuritisation of the plagioclase, often accompanied by complete alteration of the crystal rims to muscovite (DOLLINGER, pers. comm.). The biotite is similarly heavily altered with secondary titanite, allanite, apatite, epidote and chlorite common. The allanite crystals generally produce intense pleochroic haloes in the biotite implying U-enrichment.

This core intersects the fracture of interest in the NAGRA/PSI radionuclide migration experiment (described in McKINLEY et al., 1988) and, therefore, the fracture associated material has been studied in great detail (see MEYER et al., 1989). In summary, at fracture AU96, the main shear zone is indicated by a dark grey, fine grained (schistose) band of 0.5 - 2 cm wide protomylonite surrounded by smaller, secondary shear zones which may merge into the main fracture (Fig. 6). The fracture associated material consists of fine-grained (microbrecciated or re-crystallised) muscovite, biotite and epidote (Figs. 7 and 8), but the bulk mineralogy and modal composition of the fracture zone is identical to "normal" Grimsel granodiorite (MEYER et al., 1989). The smaller shear zones run approximately parallel to the main fracture (Figs. 9 - 11) and, although the highest density of microfractures appears to be within the first 3 cm of the main fracture, there is clearly evidence of the influence of the microfractures to some 6 - 7 cm from the main zone.

Although several of the microfractures are clearly shown to be open by fluorescent dye impregnation (see section 3 for discussion of this technique), it is not clear how much water flow might occur in them (see ALEXANDER et al., 1989a; MEYER et al., 1989 for comments). Certainly, inspection of the main fracture where it intersects the FLG tunnel indicates that, at present, water flows not only in one discrete zone but rather "branches off" in a random fashion within a larger, disturbed zone. Figures 12 and 13 indicate the presence of interconnected pores perpendicular to the main plane of damage which may aid the development of such multiple flow paths (see section 5.2 for further discussion).

Unfortunately, very little of the protomylonitic material is available for analysis so similar material from a much larger fracture (AU126) was collected. This site has been studied in detail (BRADBURY, 1989) because the material is being used to represent the AU96 protomylonite in a large series of rock-water interaction and sorption experiments (see McKINLEY et al., 1988 for details). According to MEYER et al. (1989) this material is a mylonite and differs from the protomylonite (AU96) in that it has a higher content of sheet silicates, especially muscovite, no chlorite, ilmenite, or allanite, little calcite, and is enriched in SiO_2, K_2O, H_2O, Rb and depleted in Al_2O_3, CaO, Na_2O, Sr, Ba and Th. However, from the point of view of this study, the minerals and elements of interest are sufficiently alike to validate the use of mylonite as an analogue of the protomylonite (see BRADBURY 1989 for a detailed discussion).

Figure 6: Sketch of the outcrop of fault zone AU96, FLG (after MEYER et al., 1989).

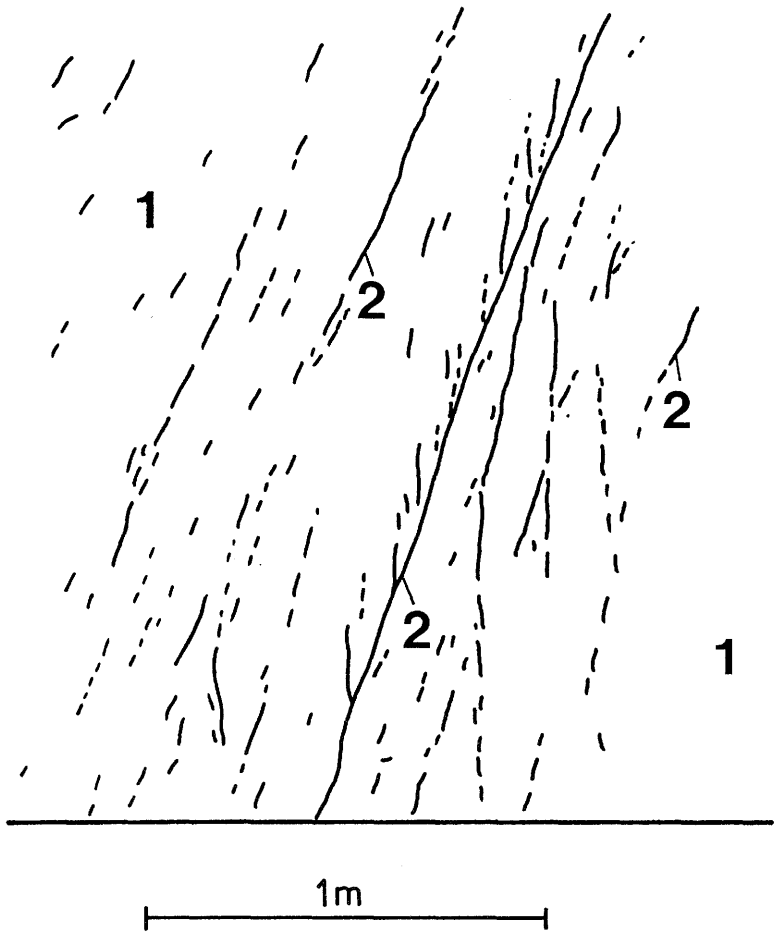

1: "Normal" Grimsel granodiorite, slightly gneissose.

2: Shear zones (0.5 - 3 cm thick) with chlorite, biotite, muscovite and epidote.

Figure 7: Photomicrograph of that part of sample II96.90W (core AU96.90W, Fig. 5) which intersects the main fracture. Crossed polars. Note the mica-rich shear zone.

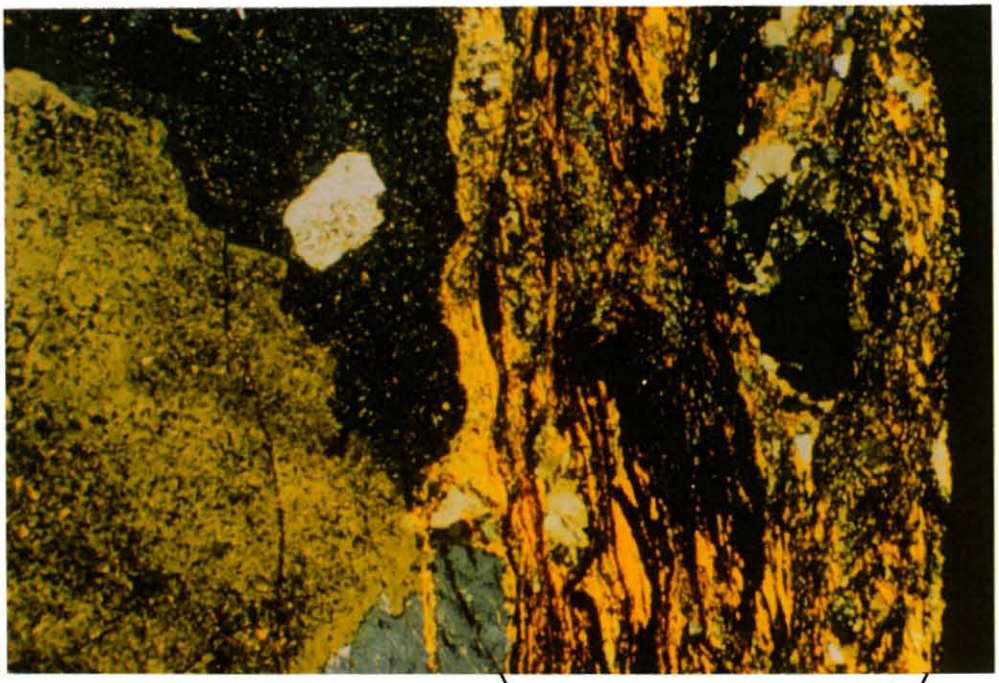

Figure 8: Photomicrograph of the same sample (96.90W) in U.V.-light after dye impregnation to illuminate the open fractures (see section 3). Note that the actual open porosity of the main fracture is highly localised.

Figure 9: Photomicrograph of the whole of sample II96.90W (see Fig. 5). Plane polarised light. Faint microfractures are visible parallel to the protomylonitic main fracture (several are marked ---).

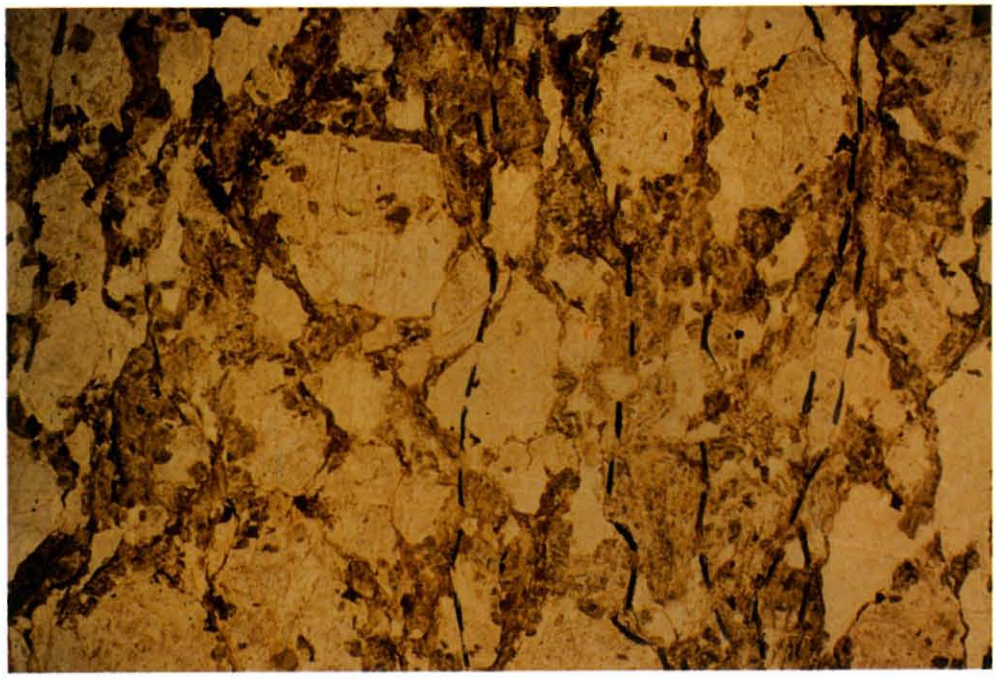

Figure 10: Photomicrograph of the whole of sample II96.90W (Fig. 9 in crossed polars). Microfractures more readily distinguished with clear "crush zones" of micro-crystalline quartz (white) and mica (orange) lineated perpendicular to the fracture.

Figure 11: Photomicrograph of sample I96.90W (Fig. 5). Crossed polars. The microfractures, which are indicated by the mica (yellow) and microcrystalline quartz (white), clearly extend to at least 7 cm from the main fracture (Fig. 7).

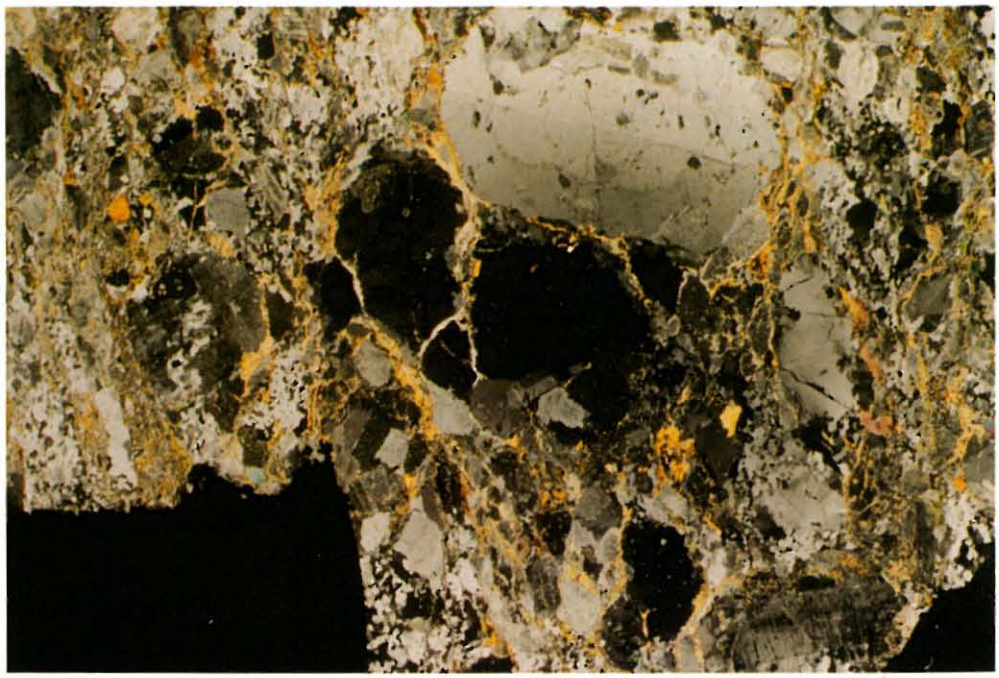

Figure 12: Photomicrographs of B96.90W (core AU96.90W; Fig. 5). Plane polarised light. Although this sample lies parallel to the main fracture there are indications of lineations (e.g. horizontally across the middle of the photomicrograph) which could, by analogy with Figures 7 - 11, represent potential water bearing zones perpendicular to the main fracture.

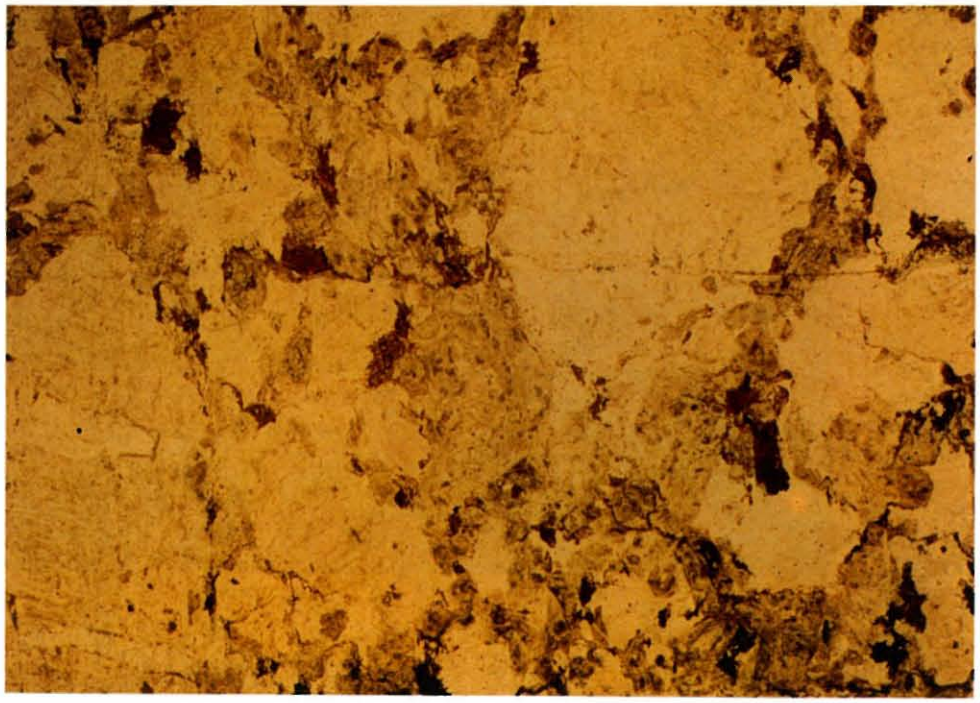

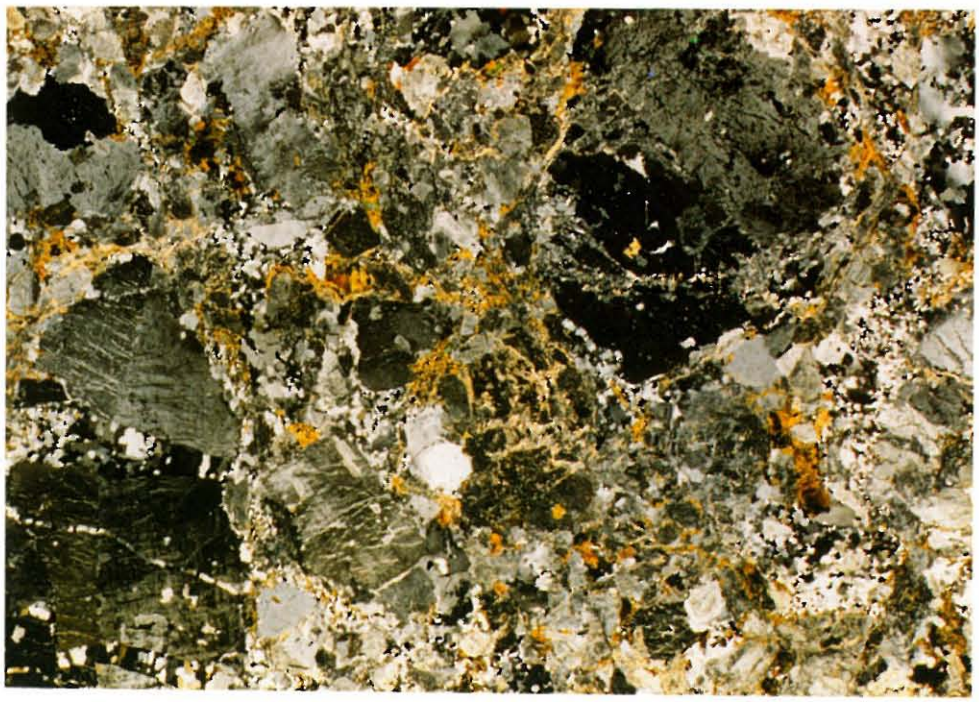

Figure 13: Photomicrograph of B96.90W, Figure 12 in crossed polars. The potential water bearing zones are highlighted by stringers of microcrystalline quartz (white) and mica (yellow-orange).

The sub-sampling of the granitic core SB80.001 is detailed in ure 14 and the mineralogy in Table 1. The chosen fracture was fresh with no alteration visible on a macro-scale and no evidence of any fracture filling material (SMELLIE et al., 1986b). The fracture's water-conducting properties were suspected on the basis of a large release of ground water when the fracture zone was penetrated during drilling. Several other fractures were observed over a short distance (Fig. 14), although they were probably produced during core recovery (FRICK, pers. comm.).

Table 1: Mineral abundance in the two FLG cores

Mineral	AU96.90W[a] (vol %)	SB80.001[b] (vol %)
Quartz	35 - 40	33
K-feldspar	25 - 30	34
Plagioclase	30 - 35	21
Biotite	5 - 7	7
Chlorite		
Muscovite		1 - 2
Epidote		-
Hornblende	-	1
sphene	trace (titanite)	trace
allanite	trace	-
apatite	trace	trace
zircon	trace	trace
calcite	-	trace
opaques	trace (ilmenite cores in titanite)	trace (oxidised magnetite)

a) Sub-sample A, core AU96.90W (see Fig. 5); Dollinger, pers. comm

b) Average modal content of the whole core; SMELLIE et al., 1986b.

The core mineralogy is detailed in SMELLIE et al. (1986b) and is not dissimilar to that of core AU96.90W. However, alteration is generally more pervasive (Figs. 15 and 16) and includes heavily sericitised feldspars, almost complete alteration of biotite to chlorite and, often extensive, oxidation of magnetite. Although no study of the micro-fractures or pore spaces has been carried out on this core, it is of note that much of the chlorite in sample 1 (i.e. between the two obvious fractures; Fig. 14) appeared to be lineated (MEYER, pers. comm). This was mainly along grain boundaries but, less frequently, was also clearly observed cutting across feldspars (e.g. Fig. 16). Although there is no direct evidence to validate the suggestion, it may well be that the lineation and stringers of chlorite are analagous to the mica in core AU96.90W in that they indicate old (and possibly still active) zones of stress release and water flow. However, it is likely that, for both of the FLG cores, these alteration products are the end point of a very complex metamorphic history and therefore cannot, by themselves, be interpreted as being due to geologically recent rock-water interaction (see ALEXANDER et al., 1989a for further discussions).

2.3 Kråkemåla drillcore K1 (317.85-318.40 m)

The Kråkemåla area within the Götemar granite has been studied by SKB as part of a programme of radwaste disposal feasibility studies for several years. Consequently, the geology of the area has been described in some detail (eg KRESTEN and CHYSSLER, 1976: ÅBERG, 1978) and the petrography and mineralogy of this particular drillcore reported elsewhere (SMELLIE and STUCKLESS, 1985; SMELLIE et al., 1986b).

Briefly, the Götemar granite is a highly differentiated alkali-rich granite of Precambrian age. Drillcore K1 is representative of the coarse grained Götemar granite variety which, according to KRESTEN AND CHYSSLER (1976), is predominantly a biotite granite although K1 appears to be more representative of a muscovite variety (SMELLIE and STUCKLESS, 1985). The granite is mineralogically variable on the scale of a thin section, consisting of plagioclase (30-42 vol. %), K-feldspar (25-50 vol. %) and quartz (15-50 vol. %) with subordinate biotite, chlorite and muscovite. Accessory minerals include isolated crystals of galena, pyrite and molybdenite with interstitial magnetite, apatite, zircon, fluorite, sphene and monazite (SMELLIE and STUCKLESS, 1985).

The granite has been weakly but uniformly altered with feldspars breaking down to muscovite/sericite and magnetite to haematite or chlorite pseudomorphs. In some sections of the core, alteration of magnetite with subsequent dispersion of the Fe has resulted in quartz pseudomorphing the magnetite. The dispersed Fe has re-accumulated locally as interstitial Fe-oxyhydroxides. Biotite is commonly altered to chlorite and muscovite occasionally to chlorite or epidote plus opaques. Replacement generally advances along cleavage planes.

Figure 14: Simplified core map of drillcore SB80.001 (FLG). Approximately half-scale (FRICK, pers. comm.).

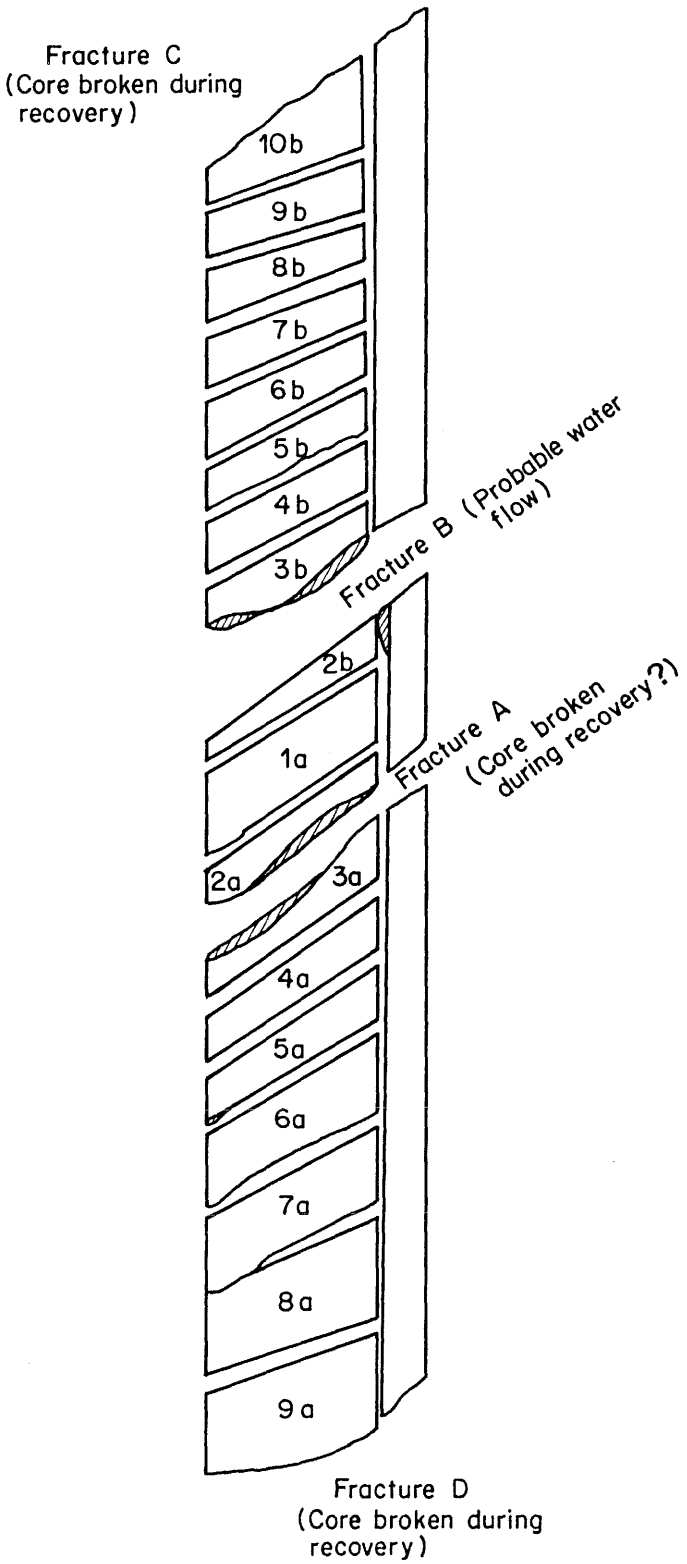

Figure 15: Photomicrograph of sample 1A from drillcore SB80.001 (see Fig. 14). Lineations of mica and secondary chlorite (often with microcrystalline quartz) run horizontally across the field of view. By analogy with core AU96.90W (section 5.2) these may represent zone of water penetration. Crossed polars.

1 cm

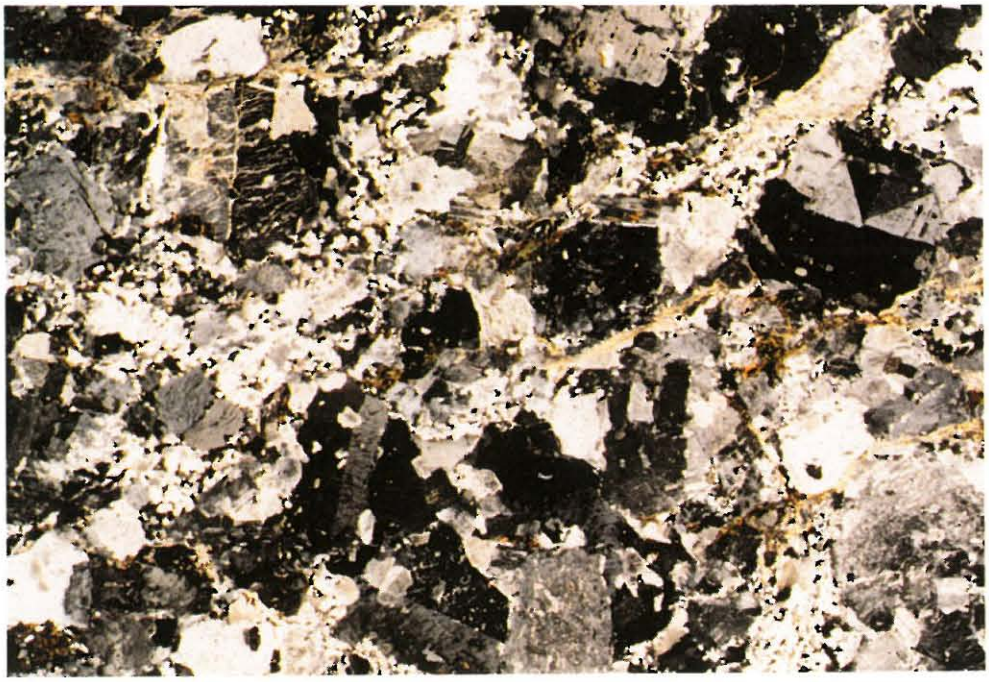

Figure 16: Photomicrograph of sample 2A from drillcore SB80.001. Note the intense alteration of the feldspares and the lineation cutting across grain boundaries (right of centre). Crossed polars.

The particular section of drillcore K1 examined here (312.85-318.40 m) intersects a fractured zone (≈1 cm wide) of sub-parallel microfractures coated with Fe-oxyhydroxides with the largest (1.5 mm wide) fracture also including an infilling of haematite and chlorite. The influence of the fracture zone visibly extends up to 2 cm into the host granite with clearly altered K-feldspar, biotite and muscovite and associated interstitial Fe-oxyhydroxides. Hydraulic conductivity tests suggest that the fracture zone is water conducting (MAGNUSSON and DURAN, 1984).

2.4 Böttstein drillcore BOE (618.34-618.70 m)

The geology of the Böttstein granite complex is detailed in two NAGRA reports (NAGRA, 1984, 1985c) and this particular section of drillcore is described in SMELLIE et al (1986b) and ALEXANDER et al (1988). The sub-sampling procedure is detailed in Figure 17.

In summary, core BOE is a coarse-grained, biotite rich, porphyritic granite with K-feldspar phenocrysts. There is a contact between the granite and a pegmatite and a (suspected water bearing) fracture occurs in the pegmatite a few centimetres from the contact. The water conducting properties of the fracture are suggested by its open nature and idiomorphic quartz fillings. Certainly fluid logging identifed a major water flow between 618 and 621 m but, as this zone also includes a potentially water bearing mylonite, the data remains equivocal.

Major constituents of the granite are K-feldspar >, quartz >, plagioclase and biotite with accessory apatite and zircon (Fig. 18). Some late magmatic muscovite has formed from the breakdown of K-feldspar and biotite and pseudomorphs of pinite after cordierite are common. Numerous microfractures are also clearly visible in thin section. The pegmatite (Fig. 19) is coarse-grained with quartz, K-feldspar and albite with accessory muscovite and tourmaline. The fracture filling consists of calcite, quartz, clays (illite and smectite) and apatite.

Hydrothermal alteration of the granite extends for ≈ 8 cm from the pegmatite contact and the granite is strongly argillised with illite/smectite, calcite (in K-feldspar) and dispersed Fe-oxyhydroxides as secondary phases. A sealed fissure (0.5-2.00 mm wide) containing calcite and clays occurs at 8 cm after which the granite is less altered and the biotite content is higher. A third fracture, again sealed, was present at the end of the core (Fig. 17).

Figure 17: Simplified core map of drillcore BOE (Böttstein). Approximately half scale (Frick, pers. comm.).

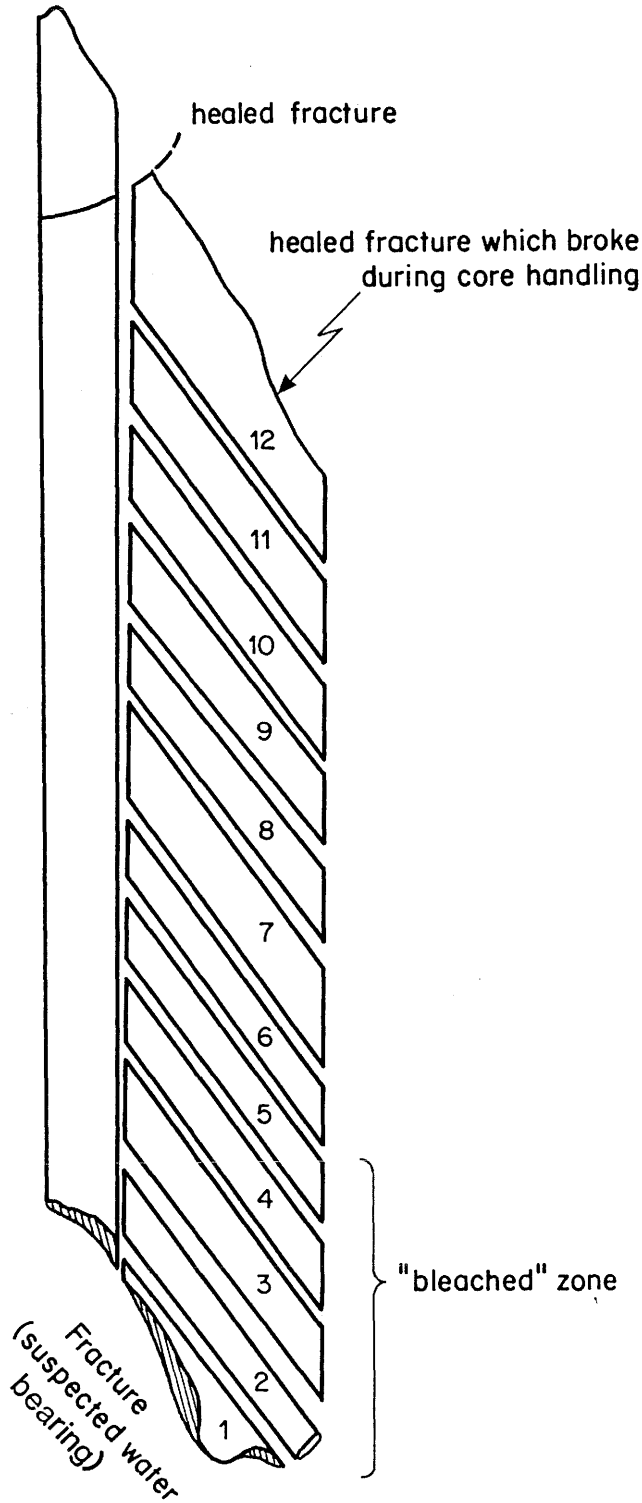

Figure 18: Photomicrograph of BOE-7, granite from the Böttstein drillcore. Note the numerous inter- and intra-granular microfractures. Crossed polars.

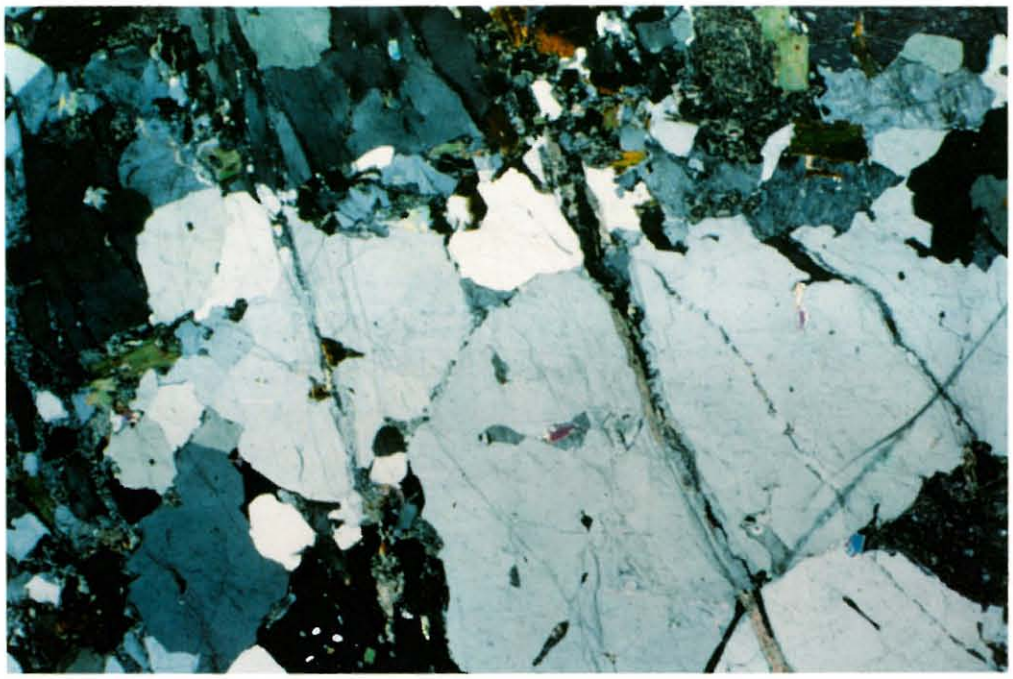

0.5 cm

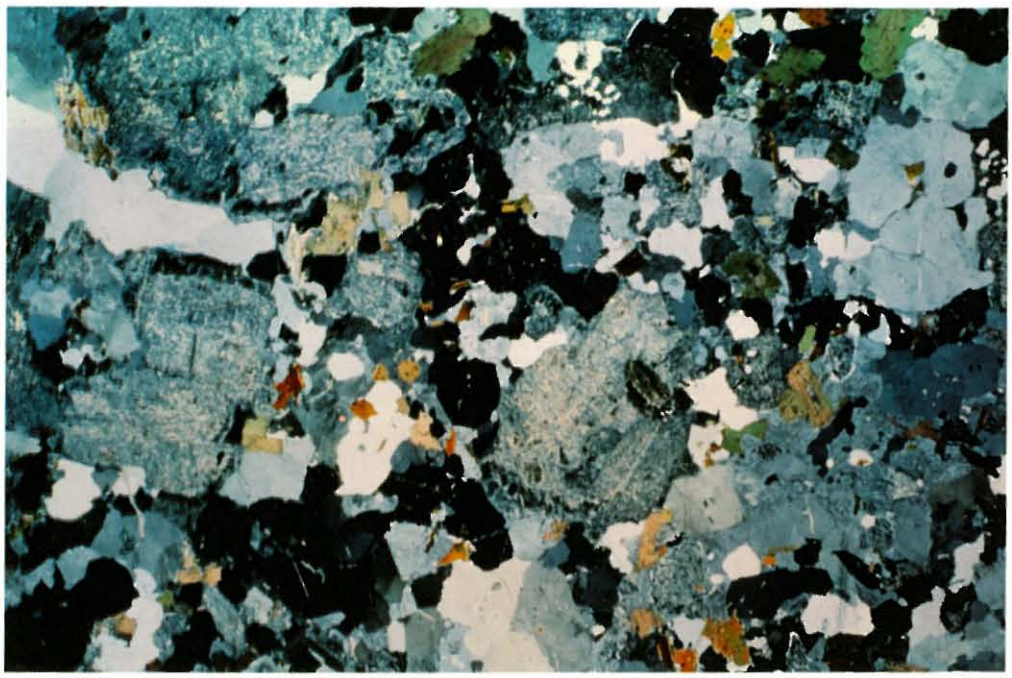

Figure 19: Photomicrograph of BOE-1, pegmatite from the Böttstein drillcore. Note the heavily altered feldspars (speckled blue-yellow). Crossed polars.

3. METHODS

Sub-samples from the rock drillcores were crushed and powdered prior to analysis for natural decay series nuclides and instrumental neutron activation analysis (INAA) as described below. 1 kg of fissure material (mylonite; AU126) was collected by hand in the FLG, and this bulk sample was also crushed and powdered (<500 μm; cf. BRADBURY 1989) prior to analysis.

U and Th were analysed by radiochemical separation and α-spectrometry using methods based on those of BACON and ROSHOLT (1982). 2 g. sub-samples of the powdered granite were spiked with ^{232}U in equilibrium with ^{228}Th and then digested in aqua regia and hydrofluoric acid, a high pressure digestion being used for the dissolution of obdurate minerals. For core AU96.90W the digestion was carried out in a vented microwave oven (after LAMOTHE et al., 1986) and the insoluble material was further dissolved in a microwave transparent, high pressure digestion bomb. As a check on this method, replicate (Böttstein) samples were dissolved by both the standard and microwave technique and no significant differences in samples were observed (Tab. 2 and discussion in ALEXANDER and SHIMMIELD, 1989). Note that, throughout this report the errors are quoted at the 2σ confidence level and represent total errors (including counting statistics, an assumed a priori error etc.).

Table 2: Comparison of U and Th results for two Böttstein samples dissolved by the standard and microwave oven techniques (from ALEXANDER and SHIMMIELD, 1989).

Specimen	U (ppm)	Th (ppm)	Th/U	^{238}U (Bq kg^{-1})	^{234}U (Bq kg^{-1})	$^{234}U/^{238}U$	^{230}Th (Bq kg^{-1})	$^{230}Th/^{234}U$	^{232}Th (Bq kg^{-1})
BOE 7[1]	3.60±0.10	22.89±0.69	6.4	44.50±1.00	43.50±1.00	0.99±0.05	46.33±0.67	1.06±0.07	92.17±1.67
	3.35±0.07	-	-	41.00±0.67	40.83±0.67	1.00±0.03	-	-	-
BOE 7[2]	3.33±0.07	22.35±0.58	6.7	40.83±0.33	40.83±0.50	1.00±0.04	44.17±0.50	1.05±0.03	90.00±0.83
	3.60±0.14	-	-	44.17±0.67	44.80±0.67	1.01±0.03	-	-	-
BOE 8[1]	3.60±0.10	21.44±0.62	6.0	44.17±1.17	44.00±1.17	1.00±0.04	42.00±1.67	0.95±0.07	86.33±2.50
	3.40±0.14	23.52±0.72	6.9	41.67±1.67	41.17±1.67	0.99±0.05	46.33±1.33	1.13±0.07	94.67±2.83
BOE 8[2]	3.56±0.08	24.05±0.60	6.7	43.67±0.67	43.67±0.67	1.00±0.04	45.67±0.67	1.05±0.04	96.83±2.50

1) Standard dissolution technique
2) Microwave oven method

The samples were then dissolved in 9M hydrochloric acid, Fe extracted into di-isopropyl ether and the U extracted on to a 10 cm x 1 cm^2 column of Bio-Rad AG 1 x 8 ion exchange resin. U was recovered from the column by elution with 1.2 M hydrochloric acid and, after a second ion exchange "clean up", U was electrodeposited from a slightly acidified NH_4Cl solution onto stainless steel discs for α-spectroscopy. The residual solution containing the Th was reduced to a volume of about 40 ml and a mixed hydroxide precipitate was prepared by addition of excess NH_4OH solution. After washing with distilled water, the precipitate was redissolved in about 5 ml of concentrated HNO_3 and made up to a volume of approx. 75 ml with 10M HNO_3. Th was extracted from this solution on a 10 cm x 1 cm^2 column of Bio-Rad AG1 x 8 resin and was eluted with 0.1 M HNO_3. The ion exchange purification was repeated before electrodeposition from a slightly acidified NH_4Cl solution onto stainless steel discs. Alpha particles were detected by silicon surface barrier detectors and the spectra recorded in a conventional multi-channel analyser (see SCOTT and MacKENZIE, 1984, 1985).

In the Th analysis it is important to note that both spike and sample contain ^{228}Th, and that the concentrations of U and Th and their isotope ratios are measured on the assumption that the ^{228}Th in the sample is in secular equilibrium with ^{232}Th. However, recent work by LATHAM and SCHWARCZ (1987a) shows that this is not always the case so this assumption was checked with several unspiked samples and was found to be valid for the cores examined here.

^{226}Ra analyses were carried out by direct counting of the 609 keV peak in the gamma-spectrum of ^{226}Ra decay products in a 4g. sub-sample of the untreated powdered rock. The CANMET ^{226}Ra reference material DL-1a was used as a standard (SMITH and STEGER, 1983). It should be stressed that using this peak, produced by ^{214}Bi decay, assumes no significant loss of ^{222}Rn from the sample.

The concentrations of the rare earth elements (REE) and a suite of other elements was carried out by INAA on 0.2 g of untreated, powdered rock by the method of MacKENZIE et al (1983, 1984). The samples, from the same part of the core as those used for U, Th etc. analyses, were irradiated for 6 hours in a thermal neutron flux of 3 x 10^{12} neutrons cm^{-2} s^{-1} after which a series of gamma-spectroscopy measurements were performed with co-axial Ge(Li) detectors and a planar Ge(Li) detector. The IAEA reference materials SOIL-5 and SOIL-7, along with the USGS reference material AGV-1 and the National Museum of Antiquities (UK) reference material EDINBURGH CLAY (E4) were used as multi-element standards. Gamma spectra were recorded on an E.G. and G. Ortec 7032 analyser and were analysed by the Ortec peak search programme Gamma 2. INAA calculations were performed by the SURRC programme NAA (HARRIS, 1985).

Tables 3 and 4 show the results obtained for analyses of samples of two of the reference materials (SOIL-5 and AGV-1) which were included with some of the samples during INAA.

Table 3: Results for analysis of samples of the IAEA reference material SOIL-5 included with samples in the analytical programme (all concentrations are in ppm unless stated).

ELEMENT	CONCENTRATIONS OBTAINED DURING ANALYSES			REFERENCE CONCENTRATIONS
	KRAKEMALA SAMPLES	BOTTSTEIN SAMPLES	GRIMSEL SAMPLES*	
Na(%)	1.91 ± 0.07	1.90 ± 0.06	1.94 ± 0.2	1.9 ± 0.2
K (%)	2.5 ± 0.2	2.3 ± 0.2	2.9 ± 0.4	1.9 ± 0.2
Sc	16.4 ± 0.5	16.4 ± 0.6	17.1 ± 0.5	14.8 ± 0.7
Cr	-	24 ± 2	23 ± 2	28.9 ± 2.8
Fe(%)	4.6 ± 0.2	4.7 ± 0.2	4.7 ± 0.2	4.5 ± 0.2
Co	15.8 ± 0.6	15.9 ± 0.6	16.3 ± 0.5	14.8 ± 0.8
Rb	126 ± 6	130 ± 6	127 ± 6	138 ± 7.4
Sb	-	12.8 ± 0.6	14.2 ± 0.6	14.3 ± 2.2
Cs	45 ± 5	46 ± 4	53 ± 4	56.7 ± 3.3
Ba	582 ± 40	609 ± 59	640 ± 70	562 ± 53
La	32 ± 2	33 ± 2	33 ± 2	28.1 ± 1.5
Nd	40 ± 8	33 ± 2	-	30 ± 2
Sm	4.8 ± 0.2	4.9 ± 0.2	5.2 ± 0.2	5.4 ± 0.4
Eu	1.13 ± 0.07	1.30 ± 0.06	1.41 ± 0.05	1.18 ± 0.08
Tb	-	0.71 ± 0.07	0.61 ± 0.05	0.67 ± 0.08
Lu	0.27 ± 0.03	0.27 ± 0.07	0.24 ± 0.08	0.34 ± 0.04
Hf	5.4 ± 0.2	6.1 ± 0.2	6.6 ± 0.2	6.3 ± 0.3
Ta	0.7 ± 0.1	0.62 ± 0.07	0.88 ± 0.07	0.76 ± 0.06
Th	10.3 ± 0.4	10.2 ± 0.3	10.4 ± 0.3	11.3 ± 0.7

*SB80.001

Table 4: Results for analysis of samples of the USGS reference material AGV-1 included with samples in the analytical programme (all concentrations are in ppm unless stated).

ELEMENT	CONCENTRATIONS OBTAINED DURING ANALYSES			REFERENCE CONCENTRATIONS
	KRAKEMALA SAMPLES	BOTTSTEIN SAMPLES	GRIMSEL SAMPLES*	
Na(%)	3.0 ± 0.1	3.2 ± 0.1	3.3 ± 0.1	3.2
K (%)	2.7 ± 0.3	2.4 ± 0.3	3.5 ± 0.5	2.4
Sc	11.7 ± 0.4	12.9 ± 0.4	13.6 ± 0.4	12.5
Cr	-	8 ± 1	9.9 ± 1.0	10
Fe(%)	4.3 ± 0.2	4.7 ± 0.2	4.8 ± 0.2	4.7
Co	15.5 ± 0.6	17.4 ± 0.7	17.9 ± 0.6	16
Rb	62 ± 3	73 ± 5	77 ± 6	67
Sb	-	3.7 ± 0.2	4.5 ± 0.2	4.3
Cs	1.1 ± 0.2	1.4 ± 0.2	1.2 ± 0.1	1.3
Ba	1040 ± 50	1100 ± 90	1300 ± 100	1200
La	41 ± 2	48 ± 3	50 ± 3	36
Ce	-	51 ± 2	53 ± 2	71
Nd	43 ± 6	-	-	37
Sm	5.2 ± 0.2	5.9 ± 0.2	5.8 ± 0.2	5.9
Eu	1.56 ± 0.07	1.66 ± 0.07	1.84 ± 0.08	1.6
Tb	-	0.59 ± 0.09	0.42 ± 0.08	0.7
Lu	0.19 ± 0.02	-	-	0.3
Hf	3.9 ± 0.2	4.7 ± 0.2	4.9 ± 0.2	5
Ta	0.83 ± 0.08	1.0 ± 0.1	0.9 ± 0.1	1.4
Th	5.6 ± 0.2	6.3 ± 0.2	6.2 ± 0.2	6.4

* Core SB80.001

A series of replicate analyses for natural decay series nuclides (Tab. 5) were also carried out and both sets of data indicate a satisfactory acuracy and precision for the analyses. A closer agreement could probably be produced by grinding the samples much finer and, for future studies, it is recommended that the samples are crushed to pass through a 63 μm mesh sieve. The independent analysis of Th by INAA and by chemical separation and α-spectroscopy gives a further verification of the accuracy of analyses (Tab. 6). This is discussed in detail in MacKENZIE et al., (1986).

Table 5: Replicate analyses of samples for natural decay series nuclides

Specimen	U (ppm)	Th (ppm)	Th/U	^{238}U Bq kg^{-1}	^{234}U Bq kg^{-1}	$^{234}U/^{238}U$	^{230}Th Bq kg^{-1}	$^{230}Th/^{234}U$	^{226}Ra Bq kg^{-1}	$^{226}Ra/^{230}Th$	^{232}Th Bq kg^{-1}
AU96.90W[1]											
(sub-sample G)	5.22±0.15	18.26±1.22	3.5	64.00±1.79	66.50±1.86	1.04±0.04	67.50±4.74	1.02±0.09	48.0±8.7	0.71±0.18	73.50±4.92
	4.95±0.18	-	-	60.67±2.24	59.83±2.21	0.99±0.05	-	-	-	-	-
AU126[2]	7.56±0.19	20.78±0.66	3.7	95.17±2.38	85.33±2.13	0.90±0.30	92.67±5.42	1.08±0.08	109.5±10.4	1.18±0.18	83.67±2.67
	8.30±0.24	-	-	101.67±2.94	103.83±3.01	1.02±0.04	-	-	147.5±16.2	-	-
SB80.001[3]											
(sub-sample 5B)	6.80±0.18	21.49±0.83	3.2	83.33±2.17	87.17±2.17	1.05±0.03	84.00±3.33	0.96±0.07	95.0±15.0	1.13±0.17	86.50±3.33
	6.77±0.27	-	-	83.00±3.33	81.83±3.33	0.99±0.03	-	1.03±0.08	-	-	-
Kråkamalå[4]											
(sub-sample 11)	18.63±0.54	-	-	228.3±6.7	190.0±5.0	0.83±0.03	-	-	-	-	-
	19.31±0.41	-	-	236.7±5.0	190.0±3.3	0.80±0.02	-	-	160.0±23.3	-	-
Böttstein[5]											
(sub-sample 1)	4.20±0.11	0.95±0.12	0.2	57.50±1.33	52.83±1.33	1.03±0.04	50.00±2.00	0.95±0.07	36.7±5.0	0.73±0.11	4.00±0.50
	3.98±0.11	0.74±0.25	0.2	48.83±1.33	44.17±1.33	0.90±0.05	47.00±1.83	1.06±0.08	-	-	3.06±0.99
Böttstein[6]											
(sub-sample 8)	3.60±0.10	21.44±0.62	6.0	44.17±1.17	44.00±1.17	1.00±0.04	42.00±1.67	0.95±0.07	45.0±6.7	1.07±0.16	86.33±2.50
	3.40±0.14	23.52±0.70	6.9	41.67±1.67	41.17±1.67	0.99±0.05	46.33±1.33	1.13±0.07	-	-	94.67±2.83

1. granodiorite
2. mylonite
3. granite
4. muscovite granite
5. pegmatite
6. granite

Table 6: Th content of the four cores by Neutron Activation (INAA) and Radiochemical analyses.

AU96.90W (FLG)

Sample	INAA Th(ppm)	Radiochemical Th(ppm)
F	14±1	10.2±0.5
g	28±2	18.3±1.2
H	18±1	-
I	19±1	12.8±0.6
A	18±1	13.8±0.8
B	16±1	14.5±0.5
C	22±1	13.6±1.2
D	24±1	18.1±0.9
E	22±1	16.3±0.6

SB80.001 (FLG)[a]

Sample	INAA Th(ppm)	Radiochemical Th(ppm)
9A	16±1	16.0±0.8
8A	19±1	21.1±0.4
7A	16±1	22.5±0.9
6A	18±1	18.9±0.5
5A	18±1	17.0±0.5
4A	18±1	27.4±1.3
3A	13±1	23.0±0.5
2A	13±1	19.2±0.7
1	23±1	22.9±0.7
2B	23±1	25.5±0.5
3B	18±1	25.7±1.3
4B	20±1	18.8±0.5
5B	21±1	21.4±0.8
6B	24±1	23.6±0.6
7B	20±1	20.0±0.7
8B	21±1	18.9±0.5
9B	14±1	20.6±0.7
10B	20±1	22.5±0.5

Table 6: (Cont.)

K1 (Kråkamåla) (a)

Sample	INAA Th(ppm)	Radiochemical Th(ppm)
K1A1	46±2	46.1±2.1
K1A2	64±2	57.7±1.2
K1A3	96±3	74.1±2.1
K1A4	62±2	65.5±0.8
K1A5	92±3	84.0±2.1
K1A6	58±2	61.4±1.2
K1A7	77±3	63.8±1.2
K1A8	71±2	68.8±1.2
K1A9	48±2	47.8±1.2
K1A10	61±2	69.6±1.2
K1A12	89±3	88.9±2.5
K1A13	74±3	82.8±2.1
K1A14	46±2	51.1±08
K1A15	71±2	72.1±2.5

BOE (Böttstein) (a)

Sample	INAA Th(ppm)	Radiochemical Th(ppm)
BOE1	0.58±0.03	0.86±0.1
BOE2	5.9 ±0.2	3.2 ±0.1
BOE3	7.4 ±0.3	7.3 ±0.3
BOE4	11.0 ±0.4	12.5 ±0.3
BOE5	37.0 ±1	34.5 ±0.9
BOE6	28.0 ±1	23.2 ±0.7
BOE7	21.4 ±7	24.5 ±0.7
BOE8	23.1 ±0.8	22.5 ±0.7
BOE9	23.7 ±0.8	25.4 ±0.7
BOE10	19.6 ±0.7	22.2 ±0.4
BOE11	25.3 ±0.9	25.2 ±0.5
BOE12	24.8 ±0.8	24.1 ±0.6

(a) MacKENZIE et al., 1986

A bulk rock, wet-leaching, experiment was carried out on a sub-sample of the mylonite (AU126; see section 2.2) with the aim of defining which phases contained U, Th and Ra (see also section 5.2). For this experiment, a six-step sequential leach was applied to 5 g of sample in 30 ml of reagent. Full details of the leach reagents, duration of leach and "target" phases are included in Table 7. The 5 g sample was placed in a centrifuge vial, and 30 ml of the first reagent, 1 M $MgCl_2$, was added. After the prescribed period of agitation (see Tab. 7) on a mechanical shaker, the vial was removed and centrifuged for 5 minutes at 5000 r.p.m. The supernatent was then drawn off and filtered through a 0.2 µm pore diameter filter. Any residue on the filter was washed back into the reaction vial with the next leach reagent (1M NaOAc in this case)

for further agitation. Note that the bulk sample was not washed in distilled water or otherwise treated between leaches (cf. LOWSON et al., 1986) because the changes in the ionic strength of the solutions to which the rock samples would be exposed are likely to induce rupture of any clays present (ALEXANDER, 1985) causing loss of U and Th to the wash solutions. The collected solution was then spiked with the ^{232}U spike described above and had an equal volume of concentrated HNO_3 added. The solution was taken to dryness, ashed, taken up in a small volume of 9MHCl and a Fe carrier added. The precipitated Fe-oxyhydroxide phase was removed (by centrifugation) from the solution, re-dissolved in hydrochloric acid and exchanged with di-isopropyl ether. The previously described U and Th analytical methodology was then followed. Steps (b) to (e) of Table 7 were then carried out in the same manner.

Table 7: Details of the Reagents used in the sequential leaching experiment and the "target" mineral phases

Reagents (time in brackets refers to the duration of sample agitation)	Phases leached (see text for discussion)	References
(a) 1 M $MgCl_2$ at pH 7.0 (1 hour)	easily exchangeable (or sorbed) ions	O'Conner and Kester (1975) Tessier et al (1979, 1985)
(b) residue of (a) leached with 1M NaOAc at pH 5.0 (5 hours)	carbonates - but not organic matter	Chapman (1965) Tessier et al (1979) van Langeveld et al (1978)
(c) residue of (b) leached with 0.1M $NH_2OH.HCl$ in 0.01M HNO_3 (30 min.)	Mn-oxides - but not Fe-oxides	Chester and Hughes (1967) Chao (1972) Gupta and Chen (1975) Tessier et al (1979, 1985)
(d) residue of (c) leached with Tamm's solution in the dark (4 hours)	amorphous iron and aluminium oxides - also organic Fe and Al phases, chlorite, biotite + illite	Tamm (1934 a,b) Lowson et al (1986)
(e) residue of (d) leached with 5 % Na_2CO_3 (16 hours)	remaining amorphous inorganic compounds (mainly Al + Si)	Follet et al (1965) Lowson et al (1986)
(f) residue of (e) microwave digested in $HCl/HNO_3/HF$ and Parr bomb if required	resistate phases	Anon (1986) Alexander and Shimmield (1989)

The method of producing rock thin sections for the fluorescence microscopy studies is detailed in MEYER et al., (1989). Briefly, sub-samples from a core are polished and that surface is impregnated, under high vacuum conditions, with a fluorescent resin. The rock is then treated in the usual manner to produce a thin section with the impregnated plane preserved on the glass slide. This method allows a qualitative assessment of pore spaces (or isolated pores) of a diameter of greater than 1 μm.

The versatility of the technique is demonstrated in Figures 20 and 21 where the zones of increased porosity (sericite etc.) in and around the altered plagioclase are clearly picked out by the fluorescent dye. However, it should be remembered that the action of drilling the core, impregnating the sample with dye and so on are also likely to induce some degree of fracturing of the rock and, as such, the results of this method should be treated with caution.

Figure 20: Photomicrograph of a heavily altered feldspar, sample II96.90W (core AU96.90W; Fig. 6). the sausseritised plagioclase (yellow-light green) is enclosed in a K-feldspar (dark green). Crossed polars.

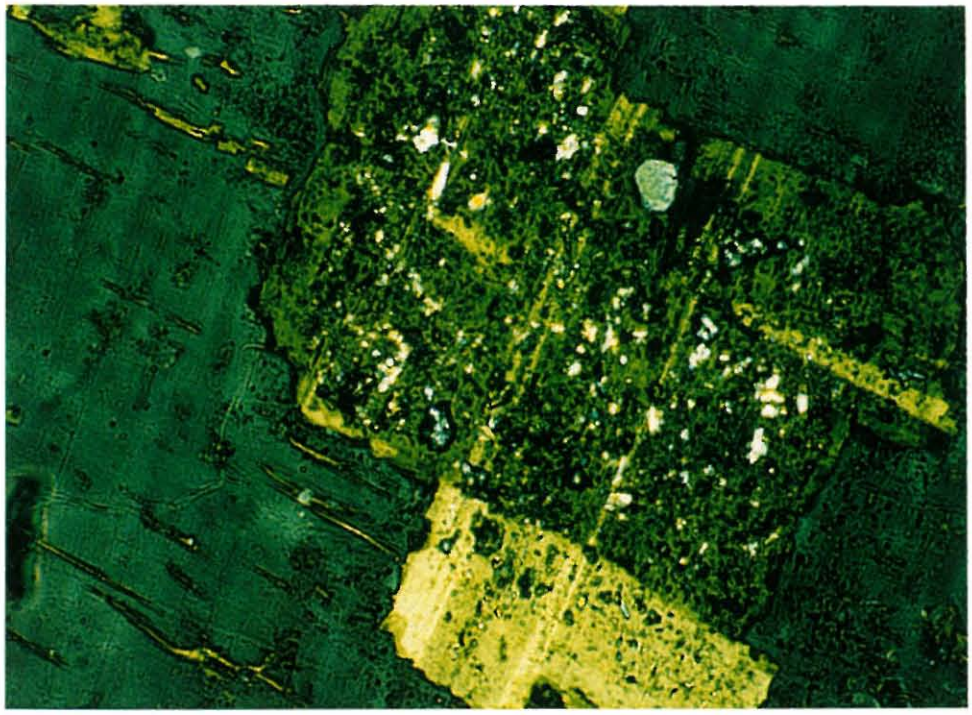

5 mm

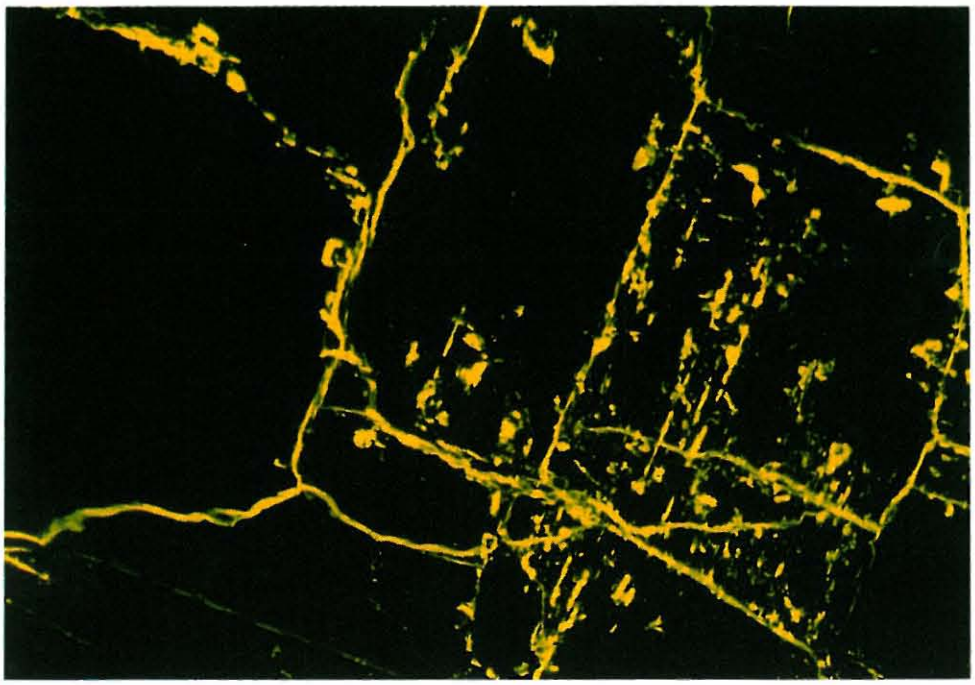

Figure 21: Photomicrograph of the same sample (II96.90W) in U.V.-Light after dye impregnation (cf. Fig. 8). Note the very high internal porosity appears to be connected to the whole rock porosity by grain boundary pores and transgranular microfractures. See also MEYER et. al. (1989).

4. THE INTERPRETATION OF U-TH ACTIVITY RATIOS IN NON-IDEAL SYSTEMS

It is becoming commonplace, in environmental and geohydrological studies, to utilise the natural decay series as a sensitive indicator of the timing of recent rock-water interactions (eg. CHERDYNSTEV, 1955, 1971; IVANOVICH and HARMON, 1982; GASCOYNE and SCHWARCZ, 1986; ZUKIN et al., 1987). In a closed geological system, the ^{238}U-^{234}U-^{230}Th decay chain attains radioactive equilibrium in about 1.7 My with the $^{234}U/^{238}U$, $^{230}Th/^{234}U$ and $^{230}Th/^{238}U$ activity ratios all equal to unity. If, however, the system is disturbed then the differing behaviour of ^{238}U and its daughters can result in fractionation and thus produce activity ratios differing from unity. Groundwaters generally leach ^{234}U from rock preferentially to ^{238}U while ^{230}Th is usually considered to be immobile under most groundwater conditions (LANGMUIR and HERMAN, 1980).

In theory, at least, the timing of any mobilisation of U can be determined from the half-life of the nuclide involved by examination of the daughter/parent activity ratios. For example, assuming there have been no severe disturbances to the system, a disturbance of the $^{234}U/^{238}U$ pair will be detectable for some 1 My while, for the $^{230}Th/^{234}U$ pair, the period is some 300,000 y. This facet of the natural decay series has, in fact, been exploited to study the re-mobilisation of U, with the intention of attempting to date the event which disturbed the system, in many varying environments in recent years (eg. SCHWARCZ et al., 1982; IVANOVICH and HARMON, 1982; ROSHOLT, 1982, 1983; SHIRVINGTON, 1983; IVANOVICH and WILKINS, 1984a,b; GASCOYNE, 1985; IVANOVICH et al., 1986a, b; CANTILLANA et al., 1986; GASCOYNE and SCHWARCZ, 1986; SMELLIE et al., 1986b; ALEXANDER et al., 1987, 1988; LATHAM and SCHWARCZ, 1987a,b,c; LAUL and SMITH, 1988).

In order to date any leaching or depositional event in such studies, it is necessary to make the assumption that the rock-water system has remained closed since the disturbing event and that the event itself lasted a very short time relative to the half-lives used (something which many of the reports quoted above noticeably fail to mention). In this section an attempt is made to examine radionuclide activity ratios in a more thorough manner (after the fashion of THIEL et al., 1983 and LATHAM and SCHWARCZ, 1987b,c) with the aim of identifying ambiguities in the interpretation of measured activity ratios.

Considering, then, only the early members of the ^{238}U natural decay series:

$$^{238}U \xrightarrow[]{} {}^{234}U \xrightarrow[2.45 \times 10^5 y]{} {}^{230}Th \xrightarrow[7.5 \times 10^4 y]{} \ldots$$

it is clear, from the above discussion, that a disturbance to the system can produce four pairs of possible activity ratios for $^{234}U/^{238}U$ and $^{230}Th/^{234}U$ (namely $^{234}U/^{238}U > 1$, $^{230}Th/^{234}U > 1$; $^{234}U/^{238}U > 1$, $^{230}Th/^{234}U < 1$; $^{234}U/^{238}U < 1$, $^{230}Th/^{234}U < 1$ and $^{234}U/^{238}U <$, $^{230}Th/^{234}U > 1$). In this instance, to proceed any further towards defining the timing of the disturbance, it is thus necessary to make several, fundamental, assumptions namely:

a) The decay of ^{238}U is negligible over the time scales of interest, a few My.

b) The rock contains ^{238}U and its daughters initially in secular equilibrium: this counts as an aid towards interpretation since it is easy to incorporate a non-equilibrium starting point in the formalism but difficult then to deduce anything at all from the measurements.

c) The system is perturbed at time zero by
   (I) sudden addition of U,
   or (II) sudden removal of U,
   or (III) continuous addition of U,
   or (IV) continuous removal of U.

By sudden, we mean that the event takes place over a time which is negligible compared with the half-life of ^{230}Th (75 Ky); also, U deposition or leaching can take place either with the ^{238}U and ^{234}U in equilibrium, or with an excess of ^{234}U activity.

d) ^{230}Th is immobile insofar as it is unlikely to be leached by ground waters to any great extent (cf. GABLEMAN, 1977; LANGMUIR and HERMAN, 1980; LATHAM and SCHWARCZ, 1987a,b).

The following symbols will be used throughout this section:

R = initial equilibrium activity level of U.
P = additional activity
subscripts 1, 2 and 3 refer to ^{238}U, ^{234}U and ^{230}Th respectively
t = time
t_M = time of maximum activity of ^{230}Th
A = activity
λ = decay constant
λ' = probability per unit time of removal of an atom. This represents physical (leaching, desorption) removal and is in effect, the same as "C" in the treatment of LATHAM and SCHWARCZ (1987b).
K = deposition rate of the atoms
N = number of atoms.

Consider first a sudden addition of U activity to a rock having U of activity R already present; suppose the ^{238}U and ^{234}U activities are added in amounts P_1 and P_2 respectively, and that P_1 and P_2 are

not necessarily equal (not unreasonable; cf ANDREWS and KAY, 1982; GASCOYNE and SCHWARCZ, 1986; SMELLIE et al., 1986b; ALEXANDER et al., 1987). There is no associated addition of ^{230}Th[1].

In detail, suppose the material has ^{238}U activity = R at t = 0, with ^{234}U and ^{230}Th in equilibrium, and that a pulse P_2 of ^{234}U is added suddenly at t = 0. Then we have subsequently

$$A_1 = R$$

$$A_2 = R + P_2 e^{-\lambda_2 t}$$

$$A_3 = R + 1.44\ P_2\ [e^{-\lambda_2 t} - e^{-\lambda_3 t}]$$

so that $A_2/A_1 = 1 + (P_2/R)e^{-\lambda_2 t}$

Now suppose that there is a sudden, input of both ^{238}U and ^{234}U at t = 0, not neccessarily in equilibrium. Then

$$A_1 = R + P_1$$

$$A_2 = R + P_1[1 - e^{-\lambda_2 t}] + P_2 e^{-\lambda_2 t}$$

$$A_3 = R + P_1[1-e^{-\lambda_3 t}] + \frac{\lambda_3}{\lambda_3 - \lambda_2}(P_2 - P_1)[e^{-\lambda_2 t} - e^{-\lambda_3 t}]$$

(from the half-lifes noted in 4.1, $\lambda_2 = 2.83 \times 10^{-6} y^{-1}$ and $\lambda_3 = 9.24 \times 10^{-6} y^{-1}$).

The expressions for A_2 and A_3 consist in each case of a term describing the growth towards equilibrium with the sudden input of ^{238}U and one for the behaviour of the excess ^{234}U.

We have $$A_2/A_1 = 1 + \left[\frac{P_2 - P_1}{R + P_1}\right] e^{-\lambda_2 t}$$

which has the same functional form as the equation above and this shows that, even if t is known, there is no unique way of assigning

---

FOOTNOTE 1

Note, however, that ^{230}Th grows in from an initially pure source of ^{234}U as

$$A_3 = A_2(o)\ \frac{\lambda_3}{\lambda_3 - \lambda_2}\ [e^{-\lambda_2 t} - e^{-\lambda_3 t}]$$ where $A_2(o)$ is the initial activity of ^{234}U $\lambda_3/\lambda_3 - \lambda_2 = 1.44$ and that $A_2 = A_3$ at the time of maximum ^{230}Th activity (t_M) is given by $1/(\lambda_3 - \lambda_2) \cdot \ln(\lambda_3/\lambda_2) = 0.18$ My.

The activity ratio A_3/A_2 in this case of transient equilibrium is 1.44 and it is clear that a sudden injection of ^{234}U into a system originally in secular equilibrium leads, after some 0,5 My, to a situation in which the activity ratios differ measurably from unity and that this would persist until the excess ^{234}U and ^{230}Th decayed to undetectable levels.

P_1, P_2 and R to produce a given value of A_2/A_1 - another measurement, A_3, is needed. This is a case of having 3 measurements, A_1, A_2, and A_3, but 4 unknowns as t is not usually known, and we note in passing that the ^{234}U - ^{230}Th dating method assumes that R is initially zero so that P_1, P_2 and t can be extracted from A_1, A_2 and A_3.

We find also that $A_2 = A_3$

when $$t_M = \frac{1}{\lambda_3 - \lambda_2} \ln\left[\frac{\lambda_3 P_2 - \lambda_2 P_1}{\lambda_2 (P_2 - P_1)}\right]$$

which reduces to $t_M = 1/(\lambda_3 - \lambda_2) \cdot \ln(\lambda_3/\lambda_2)$ when $P_1 = 0$, as it must, and which is independent of R. Again, this equality of A_2 and A_3 occurs when A_3 attains its maximum value. A_2, on the other hand, is a monotonically decreasing function of time if $P_2 > P_1$.

We illustrate the behaviour of the activity ratios A_2/A_1 and A_3/A_2 in Figure 22 for an initial R = 1 with $P_1 = 0.1$, $P_2 = 0.2$ and $P_1 = 1$, $P_2 = 2$; we also show R = 0 and $P_2/P_1 = 2$. The essential points are:

(a) At early times ($< t_M$ above) $A_3/A_2 < 1$ and $A_2/A_1 > 1$

(b) A_3/A_2 can be experimentally indistinguishable from unity near t_M and at long times while $A_2/A_1 > 1$ in both cases.

(c) Both ratios can be > 1 only at times > t_M

(d) If sudden equilibrium deposition takes place then $P_1 = P_2$ and $A_1 = A_2 \geq A_3$ at all times. This is the only case in which A_3/A_2 is always < 1, but the approach to equilibrium is fast since it goes as $(1 - \exp(-\lambda_3 t))$

(e) A value of unity for A_3/A_2 does not necessarily mean that the ^{234}U and ^{230}Th are in equilibrium in the secular sense; this will only be so if A_2/A_1 also equals unity.

(f) 0.18 My < t_M < ∞, as the ratio P_2/P_1 varies between ∞ and 1. That is to say, t_M has its minimum value for a sudden input of ^{234}U in the absence of ^{238}U and the value increases only logarithmically as equilibrium input is approached so that it is a very insensitive function of P_2/P_1.

Figure 22: Graphical representation of the time dependency of the activity ratios to a sudden U input

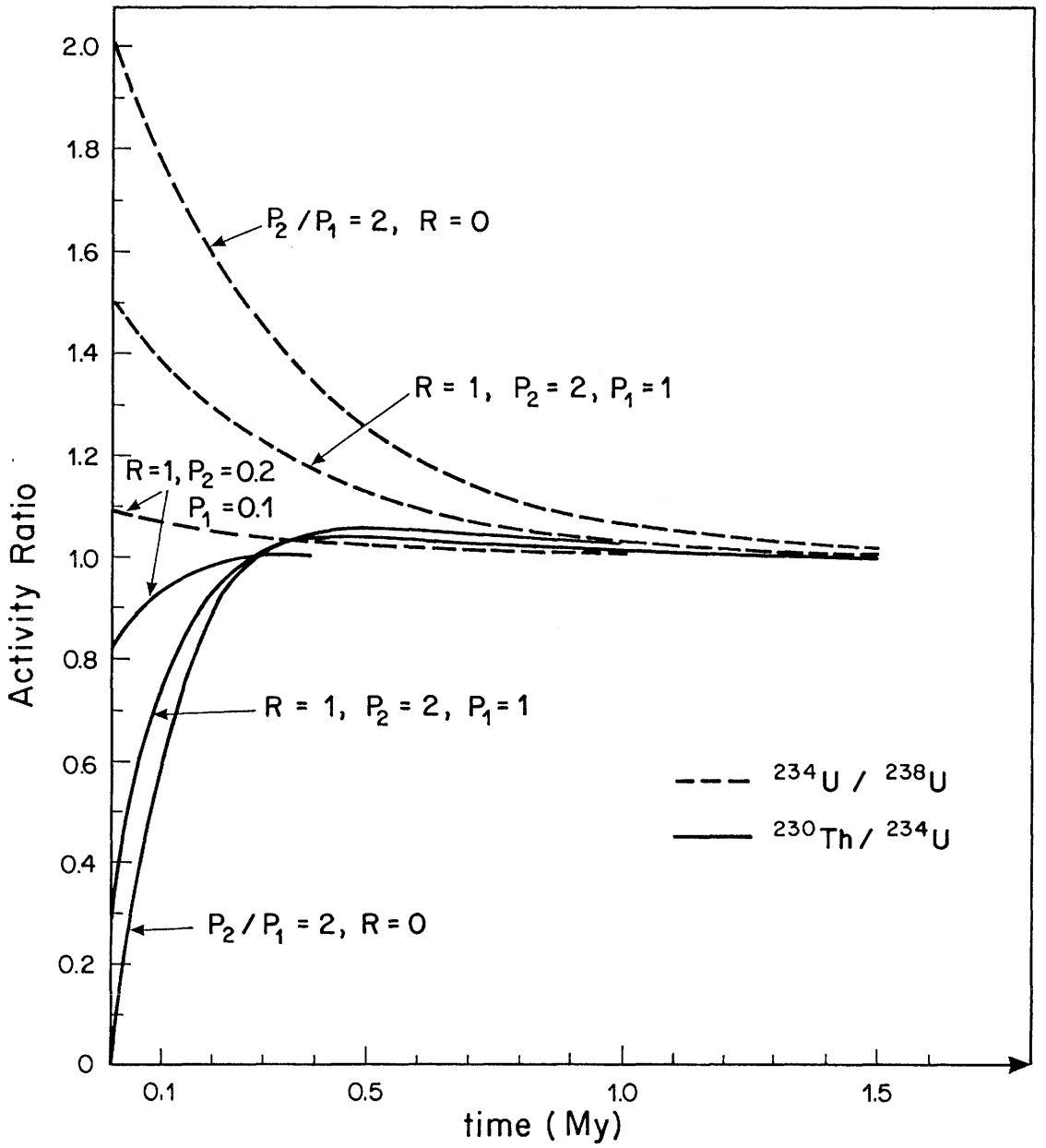

Sudden removal is accommodated merely by making P_1 and P_2 negative, but then t_M represents the time of minimum ^{230}Th activity. In the case of equilibrium deposition, or removal, ^{230}Th adjusts towards the new level at a rate determined by its own half life and effective equilibrium will be restored after some 300 ky (note true equilibrium would require infinite time). The time t_M is significant because, if $t > t_M$, then we have

$A_2/A_1 > A_3/A_2 > 1$ for sudden addition
and $A_2/A_1 < A_3/A_2 < 1$ for sudden removal.

These points are illustrated in Figure 23.

Suppose now that U is added continuously to the rock from a non-depleting source (to simplify the mathematics we will consider deposition rates of U rather than activity ratios) so that supply is at a constant rate of K_1 atoms per unit time for ^{238}U and K_2 per unit time for ^{234}U. Again, we assume that the supply commences at time t = 0 prior to which the material had ^{238}U and its daughters in equilibrium with activity R.

At time t, $\frac{dN_1}{dt} = K_1 - \lambda_1 N_1$

and $A_1 = R + \lambda_1 K_1 t$ (ignoring the decay of ^{238}U as $t \leq 10^8$ y)

Activity of ^{238}U is thus being supplied in amount $\lambda_1 K_1$ per unit time.

For the excess ^{234}U we have $\frac{dN_2}{dt} = \lambda_1 K_1 t + K_2 - \lambda_2 N_2$

which leads to a value of the total ^{234}U activity given by

$$A_2 = R + \lambda_1 K_1 t + (\lambda_2 K_2 - \lambda_1 K_1)(1 - e^{-\lambda_2 t})/\lambda_2$$

$$= A_1 + (\lambda_2 K_2 - \lambda_1 K_1)(1 - e^{-\lambda_2 t})/\lambda_2$$

This tends at long times to

$$A_2 \longrightarrow A_1 + (\lambda_2 K_2 - \lambda_1 K_1)/\lambda_2$$

so that a continuous excess deposition of ^{234}U leads to a constant difference between A_2 and A_1; $A_2/A_1 > 1$ but tends to unity as A_1 increases.

For ^{230}Th we have (considering the excess)

$$\frac{dN_3}{dt} = A_2 - R - \lambda_3 N_3$$

Figure 23: Comparison of the effects of sudden input and sudden removal of U on the activity ratios

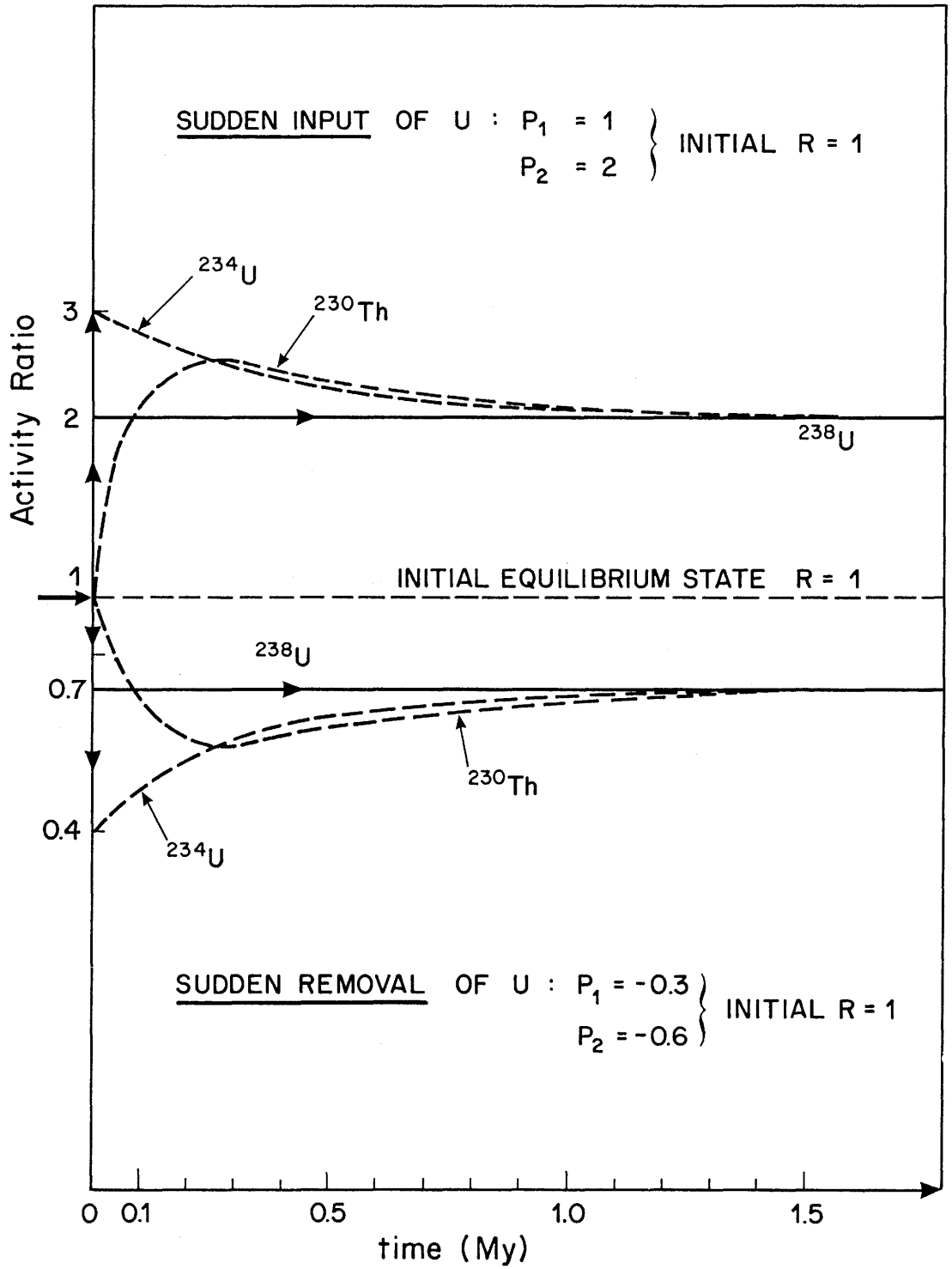

which eventually gives

$$A_3 = A_1 + (K_2 - \lambda_1 K_1/\lambda_2 - \lambda_1 K_1/\lambda_3)(1 - e^{-\lambda_3 t})$$

$$+ \frac{\lambda_3}{\lambda_3 - \lambda_2}\left(\frac{\lambda_1 K_1}{\lambda_2} - K_2\right)(e^{-\lambda_2 t} - e^{-\lambda_3 t})$$

This tends at long times to

$$R + \lambda_1 K_1 t + K_2 - \frac{\lambda_1}{\lambda_2} K_1 - \frac{\lambda_1}{\lambda_3} K_1 \longrightarrow A_2 - \frac{\lambda_1}{\lambda_3} K_1$$

and therefore $A_3 < A_2$ by a constant amount. If the deposition occurs in equilibrium (when $\lambda_1 K_1 = \lambda_2 K_2$) then $A_1 = A_2$ at all times, as it must, and

$$A_3 = A_1 - \frac{\lambda_1}{\lambda_3} K_1 (1 - e^{-\lambda_3 t})$$

If, in addition, ^{230}Th is being deposited then there will be another term in A_3 of the form $K_3 (1 - \exp(-\lambda_3 t))$.

Then if, for instance, ^{238}U and ^{234}U were being deposited in equilibrium we would have $A_2/A_1 = 1$ and

$$A_3 \longrightarrow A_2 - \frac{\lambda_1}{\lambda_3} K_1 + K_3$$

at long times.

The practical situation would be a rock-groundwater interaction where U was being adsorbed from solution onto the rock. Chemical deposition would be proportional to the atomic population and would reflect the activity ratio in the water. The above formalism allows for an extra ^{234}U recoil deposition by suitable adjustment of K_2 and there would probably always be a K_3 term since ^{230}Th would almost certainly be insoluble. In this model of constant replenishment of U in the water which is supplying U to the rock, the K_3 term would just be equal to the ^{234}U activity in the water, and this would be $<<R$. Figure 24 shows the activity ratios A_2/A_1 and A_3/A_2 as a function of time for $\lambda_1 K_1 = 0.1\ R/10^5 y$, $\lambda_2 K_2 = 0.2\ R/10^5 y$ and $K_1 = R/10^5 y$, $K_2 = 2R/10^5 y$ with $R = 1$ and $K_3 = 0$ in each case; we also show $R = 0$, $\lambda_2 K_2/\lambda_1 K_1 = 2$.

Comparing with Figure 22 it is evident that the continuous input curves are damped versions of those for a sudden input. Notice that, at short times, for sudden addition

$$A_2/A_1 \rightarrow \frac{R + P_1}{R + P_2} \longrightarrow P_1/P_2 \text{ if } R = 0 \text{ and } A_3/A_2 \longrightarrow R/R + P_2$$

if $R = 0$, whereas for continuous addition $A_2/A_1 \dashrightarrow 1$ if $R \neq 0$, $\lambda_2 K_2/\lambda_1 K_1$, if $R = 0$, and $A_3/A_2 \longrightarrow 1$, if $R \neq 0$, $\longrightarrow 0$ if $R = 0$

Comparison of Figures 22 and 24 shows that:

(1) A sudden input can generate $A_3/A_2 > 1$ but a continuous input cannot.

Figure 24: Time dependency of the measured activity ratios when subjected to a continuous input of U

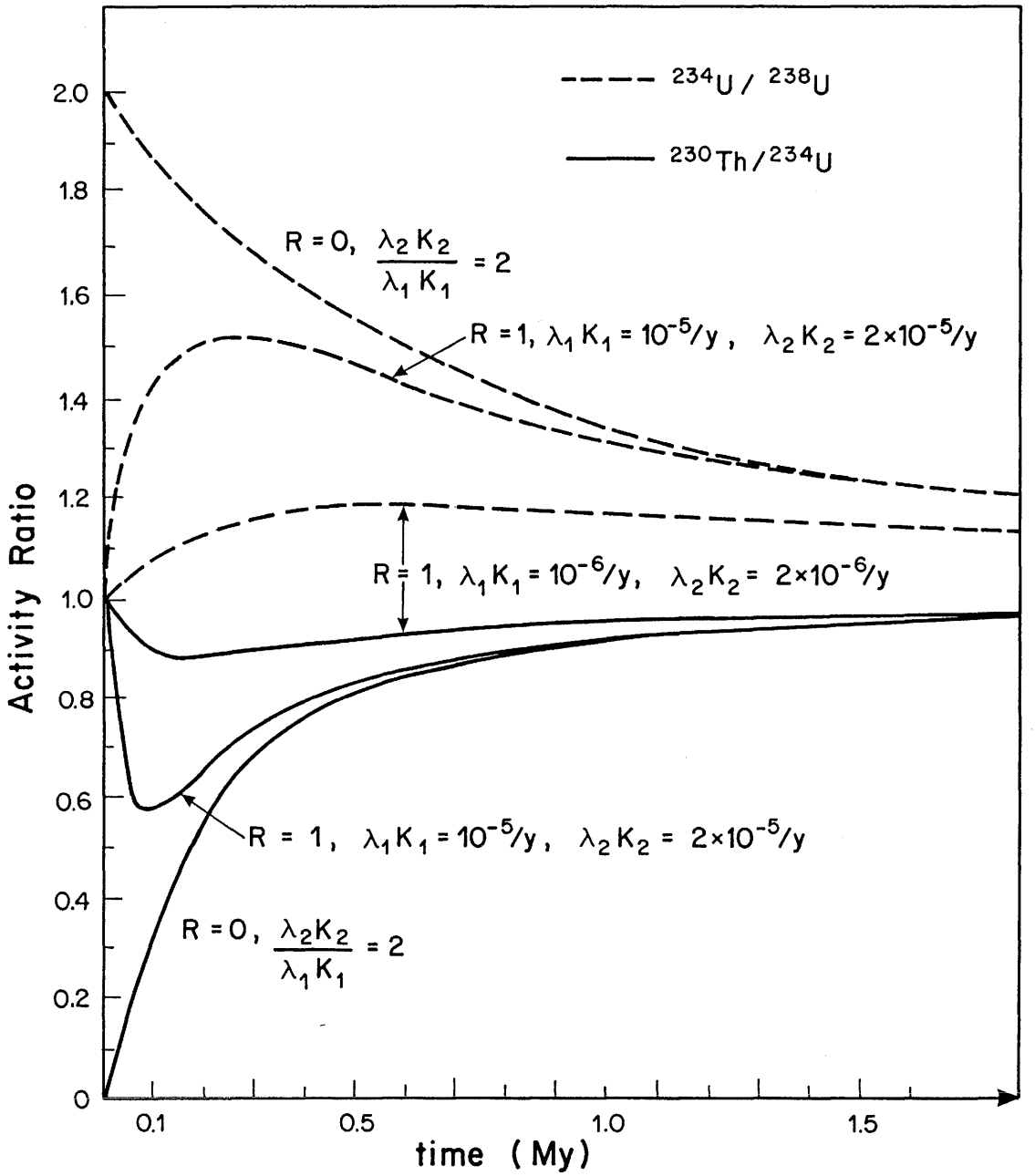

(2) A_3/A_2 can be unity at time t_M after a pulse and A_2/A_1 would be > 1, but the same type of behaviour is possible a long time (2 My) after continuous input has started.

(3) After some 1.5 My the distinction between the values of A_3/A_2 for the two cases of continuous deposition has almost disappeared (i.e. it would be experimentally unmeasurable) whereas the A_2/A_1 ratios are still distinguishable. This is what would be expected, of course, given the difference in half-lives of ^{230}Th and ^{234}U.

(4) if R = 0 initially then the ratios are functions of P_2/P_1 or K_2/K_1 only, and the sudden and continuous input ratios will have the same initial values if

$$P_2/P_1 = \frac{\lambda_2 K_2}{\lambda_1 K_1}$$

The sudden inputs lead much more quickly to equilibrium in both and it is noticeable that after some 0.5 My the activity ratios are insensitive to the value of R.

In the case of continuous removal of U, suppose again that the material originally has ^{238}U - ^{234}U - ^{230}Th in equilibrium and that removal begins at time t = 0.

For ^{238}U we have $\frac{dN_1}{dt} = -\lambda_1' N_1$

so that $A = R \exp(-\lambda_1' t)$, where λ' is the probability per unit time of removal of a ^{238}U atom by leaching or desorption and R is the initial equilibrium activity (^{238}U is not depleted by decay, only by physical removal, over the time scales considered here).

For ^{234}U we have $\frac{dN_2}{dt} = A_1 - \lambda_2 N_2 - \lambda_2' N_2$

The solution subject to $\lambda_2 N_2 = R$ at t = 0 is

$$A_2 = R\left[e^{-(\lambda_2 + \lambda_2')t} + \frac{\lambda_2}{\lambda_2 + \lambda_2' - \lambda_1'}\left(e^{-\lambda_1' t} - e^{-(\lambda_2 + \lambda_2')t}\right)\right]$$

Equilibrium removal corresponds to $\lambda_1' = \lambda_2'$ and the above reduces to $A_2 = Re^{-\lambda_1' t}$, as it must.

In the general case we see that, provided $\lambda_2 + \lambda_2' > \lambda_1'$

$A_2/A_1 \dashrightarrow \lambda_2/(\lambda_2 + \lambda_2' - \lambda_1')$, at long times. Hence if ^{234}U is preferentially removed, so that $\lambda_2' > \lambda_1'$ we have $A_2 < A_1$ and this is a steady state at long times although the activity ratio is not unity. This holds for rapid or slow removal as long as $\lambda_2' > \lambda_1'$.

For ^{230}Th, assuming no leaching of Th,

$$\frac{dN_3}{dt} = A_2 - \lambda_3 N_3 \quad , \text{ subject to } \lambda_3 N_3 = R \text{ at } t = 0.$$

The solution is

$$A_3 = R[e^{-\lambda_3 t} + \frac{\lambda_3(\lambda_2' - \lambda_1')}{[\lambda_3 - (\lambda_2 + \lambda_2')][\lambda_2 + \lambda_2' - \lambda_1']}(e^{-(\lambda_2 + \lambda_2')t} - e^{-\lambda_3 t})$$

$$+ \frac{\lambda_2 \lambda_3}{[\lambda_2 + \lambda_2' - \lambda_1'][\lambda_3 - \lambda_1']}(e^{-\lambda_1' t} - e^{-\lambda_3 t})]$$

For equilibrium removal, we have $\lambda_1' = \lambda_2'$ and so

$$A_3 = R[e^{-\lambda_3 t} + \frac{\lambda_3}{\lambda_3 - \lambda_1'}(e^{-\lambda_1' t} - e^{-\lambda_3 t})]$$

As $t \rightarrow \infty$, $A_2/A_1 \rightarrow \lambda_2/(\lambda_2 + \lambda_2' - \lambda_1')$ and $A_3/A_2 \rightarrow \lambda_3/(\lambda_3 - \lambda_1')$ provided that the conditions $\lambda_1' < (\lambda_2 + \lambda_2')$ and $\lambda_1' < \lambda_3$ are satisfied simultaneously. Both these conditions are necessary if equilibrium ratios are to be set up in the material which is, of course, steadily losing its activity. If ^{234}U is removed preferentially and the removal probabilities satisfy the above inequalities then a steady state is attained where

$A_2/A_1 < 1$ and $A_3/A_2 > 1$.

For the short-term behaviour we have

$A_1 \rightarrow R(1 - \lambda_1' t)$
$A_2 \rightarrow R(1 - \lambda_2' t)$
$A_3 \rightarrow R$

and A_2/A_1 is < 1 if $\lambda_2' > \lambda_1'$; also A_3/A_2 is > 1 if $\lambda_2' \neq 0$ which is, of course, to be expected.

The steady state example is illustrated in Figure 25. The activity ratios in this example are not unity. If there is reason to believe that a steady state has been reached then it is, of course, possible to solve the above equations in the measured quantities A_3/A_2 and A_2/A_1 to obtain values for λ_1 and λ_2.

Finally, it is instructive to note that our approach is equivalent to that of THIEL et al (1983) although these authors do not present explicit formulae for continuous deposition or depletion. Instead, they employ a graphical representation which is quite useful in that it incorporates the points made earlier in this section

concerning sudden processes verses continuous processes, and makes it immediately apparent whether or not certain combinations of activity ratios can be reached (from an initial state of equilibrium) in processess of a single type, sudden or continuous. The essential points are made in Figures 26 and 27; Figure 26 shows the general form of the activity ratio plot. In Figure 26 (a), the arrows represent the result of sudden uranium accumulation or removal and the system, as it returns to equilibrium, traces out a curve in the plane. A continuously perturbed system also traces out a curve in the plane, starting at the origin. The simplest cases, of sudden equilibrium deposition or removal, are shown in Figure 26 (b) where, if it is assumed that the $^{234}U/^{238}U$ activity ratio = 1, it is clear that the return to equilibrium merely proceeds back to the origin along the x-axis. Conversely, continuous deposition or leaching is represented by a similar movement away from the origin. More detail is presented in Figure 27 where a few typical paths for both pulsed and continuous processes are shown and the existence of regions in the plane which are inaccessible by certain processes is illustrated. Thus, the line marked $t = t_M$ cannot be reached by a continuous process, but will be crossed by a system returning to equilibrium after a sudden perturbation; since the other line on the diagram marked x---x is an asymptotic boundary for all single sudden events, it follows that the region between these lines is out of bounds for continuous single events starting out from the origin. By the same token, activity ratio combinations in the cross-hatched regions cannot be reached in single processes, whether sudden or continuous. Unfortunately, of course, all regions of the plane are accessible to complex, that is to say multi-stage, processes in which, for example, a continuous leaching event might be interrupted by a sudden large U-accumulation. It is therefore evident that any interpretation of activity ratios must be backed by deductions from other geological observations such as stable isotope studies, thin section examinations of the rocks and minerals of interest etc.

In the next section the U leaching model described here is applied to data from fracture zones. U leach rates are deduced for several rock types and compared with the results of LATHAM and SCHWARCZ (1987b) for weathered granite.

Figure 25: Time dependency of the measured activity ratios when subjected to a continuous removal of U

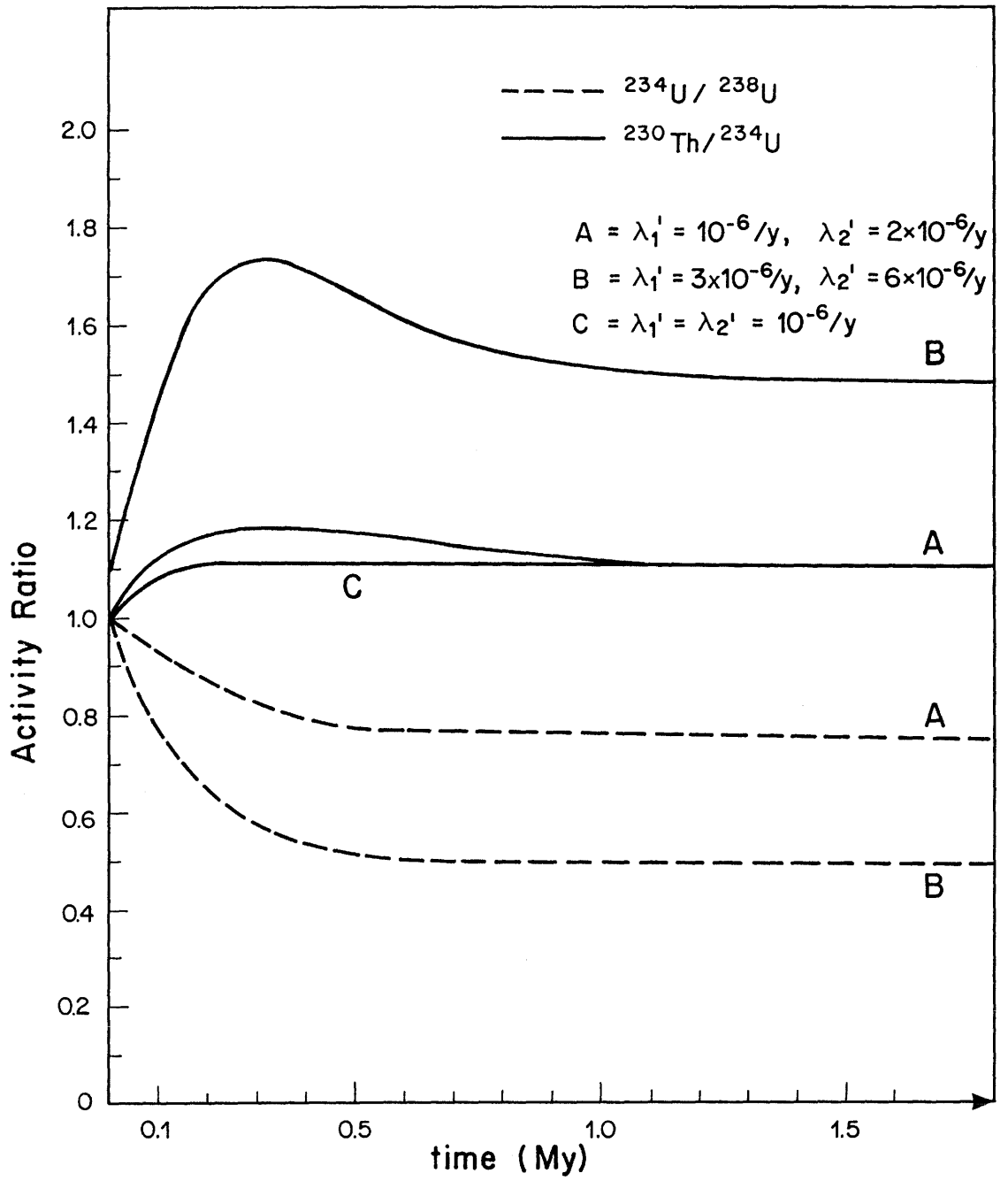

Figure 26: Graphical representation of the effects of U accumulation and U removal on the activity ratios (after THIEL et al., 1983)

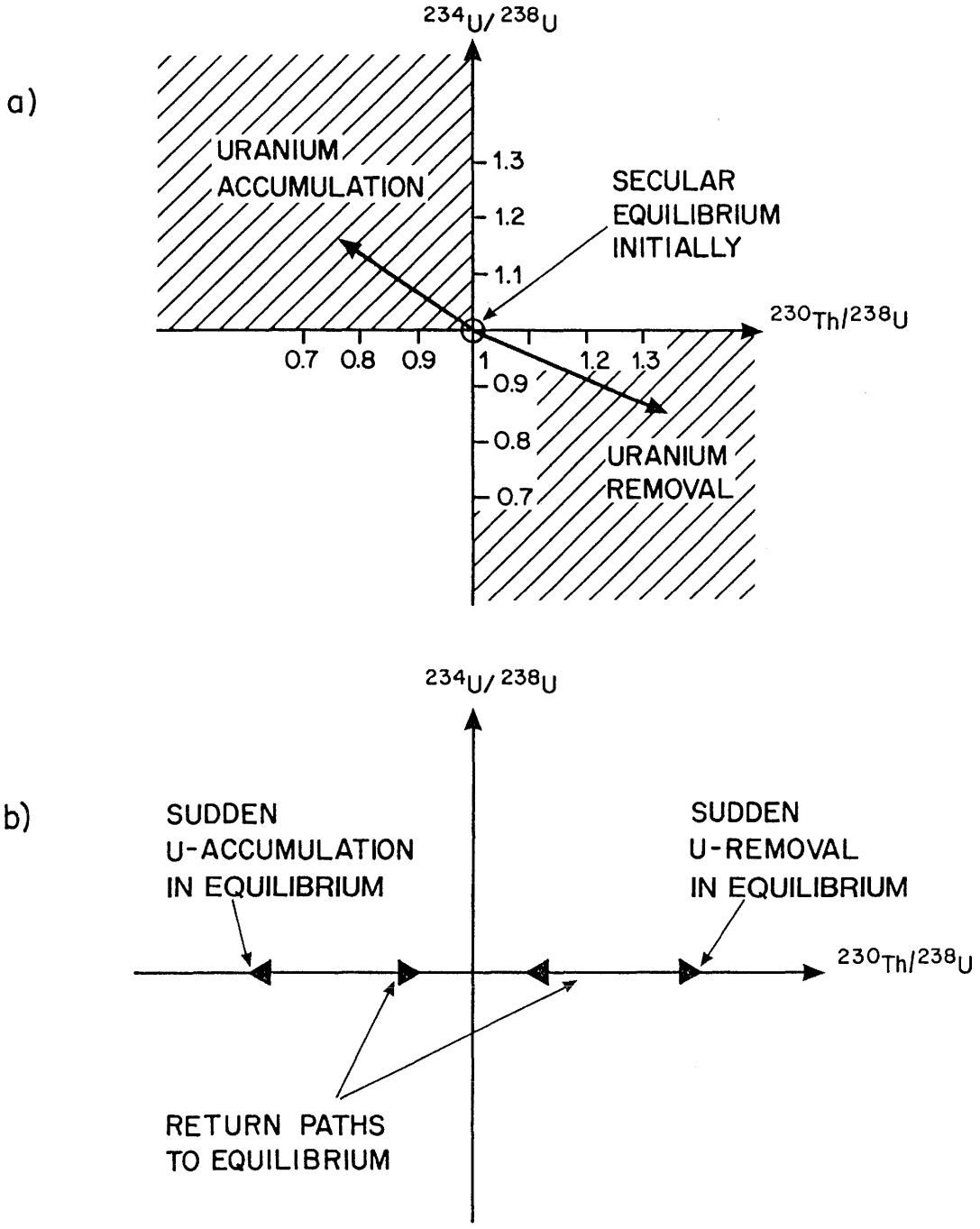

Figure 27: Detailed examples from Figure 26

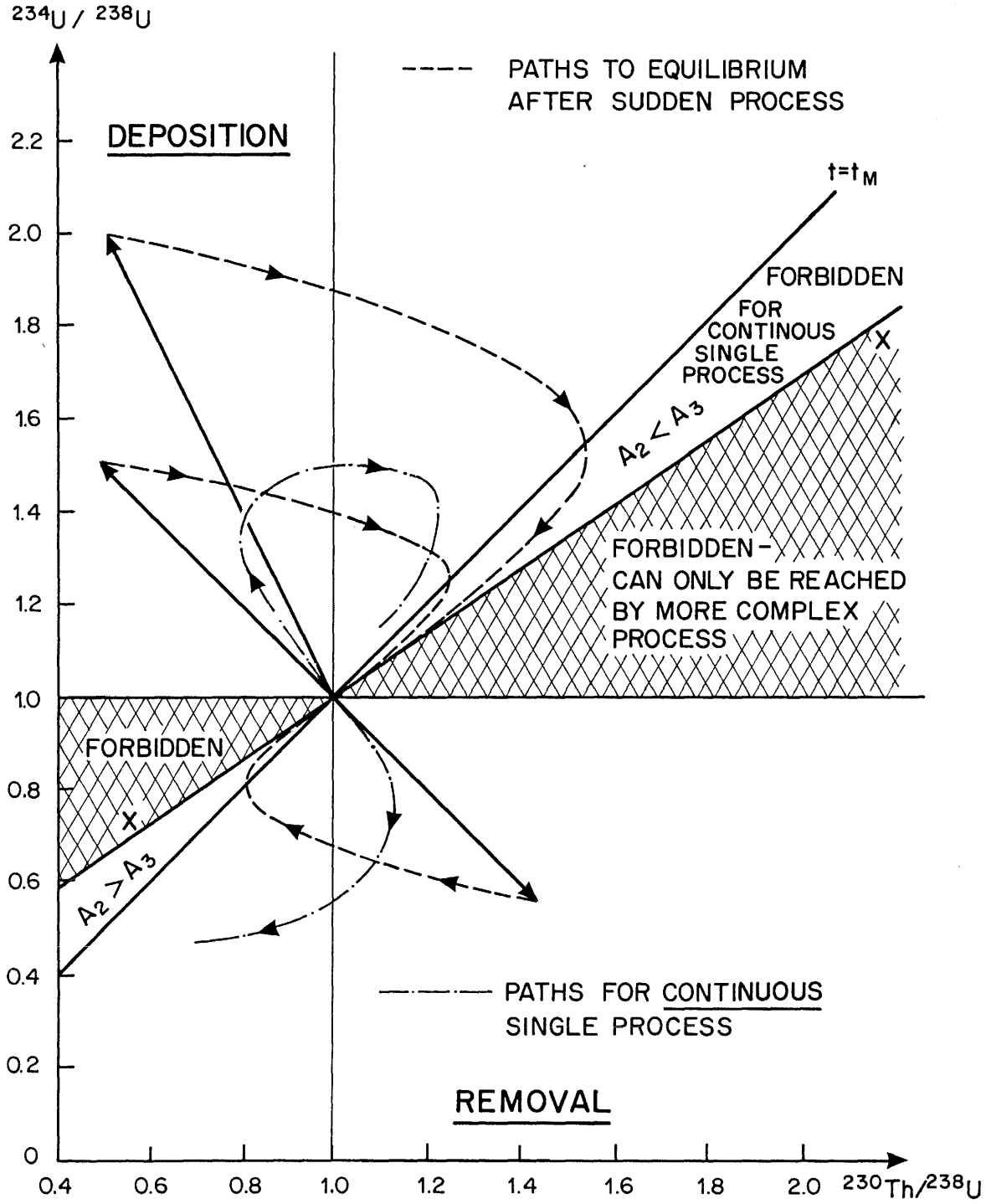

5. RESULTS AND DISCUSSION

5.1 Introduction

Geochemical data from four rock drillcores (two from the FLG, southern Switzerland, one from the Böttstein basement, northern Switzerland and one from Kråkamåla, southern Sweden) are presented in this section along with an interpretation of the material. All four cores were drilled at the perpendicular to supposed water bearing fractures. The distribution patterns of the natural decay series radionuclides, REE, Na, K, Sc, Ba, Hf and Ta were defined. Redox sensitive, or associated, elements (Fe, Mn, Co and Cs) were also examinded for indications of redox fronts in the vicinity of the fractures.

It should be noted that, as in section 3, the error limits quoted here are 2σ values and represent total analytical errors. Although SI units are used throughout this report some of the data presented here have been previously reported in units of $dpmg^{-1}$ (e.g. SMELLIE et al., 1986b) in accordance with the vast majority of similar studies in this field (e.g. LAUL et al., 1985; LOWSON et al., 1986; ZUKIN et al., 1987).

5.2 FLG drillcore AU96.90W

The levels of U and its daughter decay products are displayed in Figure 28 and are tabulated in Table 8. Fe, Mn, Co, Cs and the REE's La, Ce, Eu and La are displayed in Figure 29 and these elements along with Na, K, Sc, Ba, Hf, Ta, Th (by INAA) and the REE's Nd and Sm are listed in Table 9.

The U content of the granodiorite ranges from 4.43 to 6.17 ppm while the Th level ranges from 10.22 to 18.26 ppm; the mean Th/U ratio is 2.8 which compares with an average Th/U ratio of 4.0 for world granites (CLARK et al., 1966). However these U and Th concentrations are similar to the other FLG core discussed here (SB80.001; section 5.3) and to other reported analyses of Grimsel granitic rocks (LABHART and RYBACH, 1976; BAJO, 1980; ALEXANDER et al., 1987). There are no data available on the U/Th phases in the Grimsel granodiorite but fission track studies of samples collected $\sim$ 1 km from the FLG indicate an absence of interstitial U (cf core K1; section 5.4) and identify the major U and Th bearing phases as allanite, titanite, zircon and apatite with rare polycrase (BAJO, 1980).

The distribution patterns of U and Th in the drillcore (Fig. 28) are similar with little variation discernable throughout. Plots of the $^{234}U/^{238}U$ and $^{230}Th/^{234}U$ activity ratios indicate secular equilibrium, within the limits of analytical precision, for most of the core with the possibility of $^{230}Th/^{234}U$ activity ratios of greater than unity in the +3 to + 6 cm zone of the core. This may, however, be a reflection of disequilibrium in the $^{228}Th/^{232}Th$ pair in the rock with the attendant disturbance to the ^{232}U spike utilised in the counting technique (see the comments in section 3) and should be treated with caution.

Figure 28: Distribution of the natural decay series radionuclides in core AU96.90W (FLG)

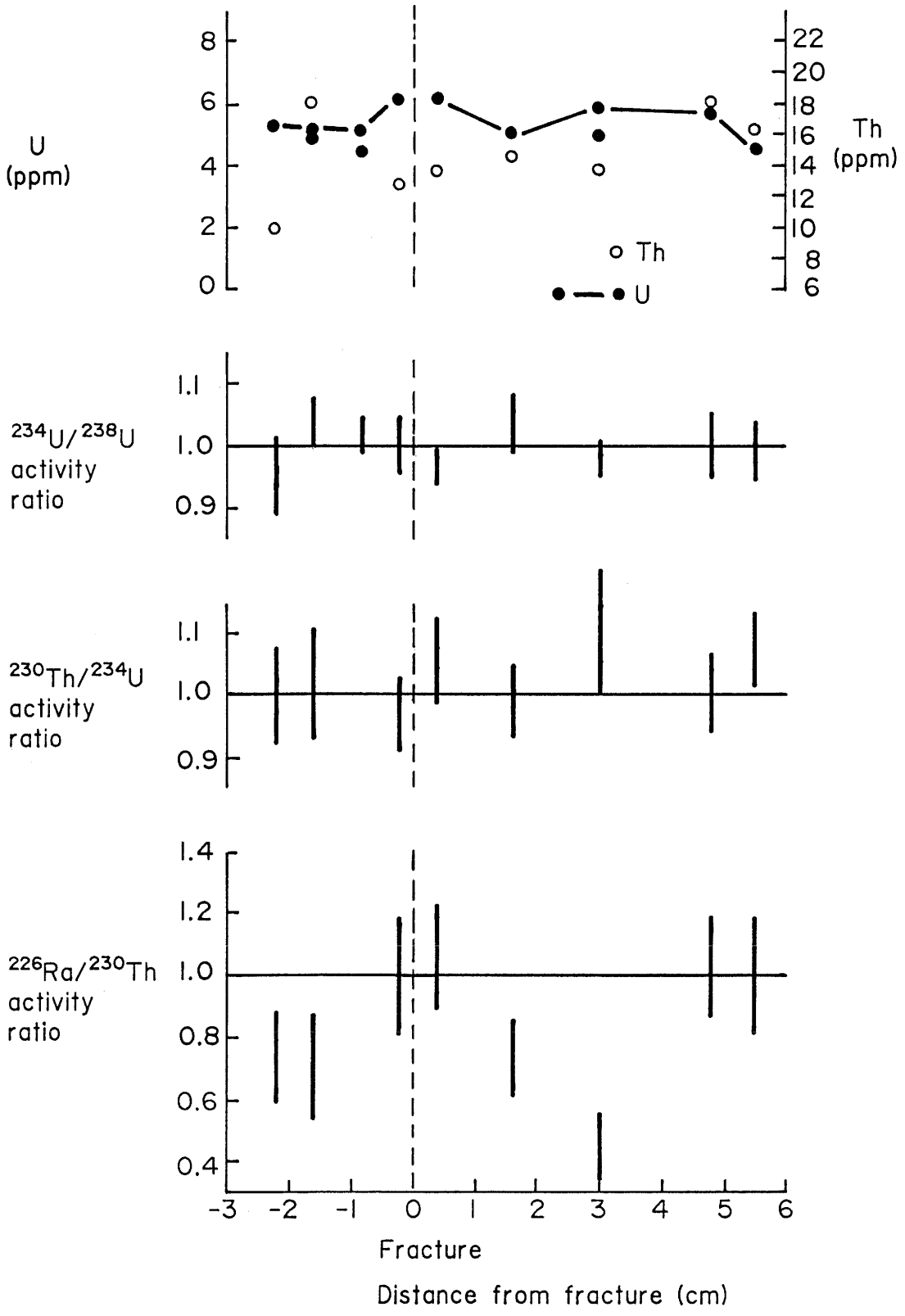

Table 8: Natural decay series results for core AU96.90W from the MI site, FLG.

Sample	Distance from fissure (cm)	U* (ppm)	Th* (ppm)	Th/U	^{238}U (Bq kg^{-1})	^{234}U (Bq kg^{-1})	$^{234}U/^{238}U$	^{230}Th (Bq kg^{-1})	$^{230}Th/^{234}U$	^{226}Ra (Bq kg^{-1})	$^{226}Ra/^{230}Th$	^{232}Th (Bq kg^{-1})
F	-2.2	5.32±0.22	10.22±0.54	1.9	65.17±2.68	62.00±2.60	0.95±0.06	62.00±2.67	1.00±0.08	46.5±7.3	0.75±0.15	41.16±2.18
G	-1.6	5.22±0.15	18.26±1.22	3.5	64.00±1.79	66.50±1.86	1.04±0.04	67.50±4.74	1.02±0.09	48.0±8.7	0.71±0.18	73.50±4.92
		4.95±0.18	-	-	60.67±2.24	59.83±2.21	0.99±0.05	-	-	-	-	-
H	-0.8	4.43±0.11	-	-	54.30±1.36	55.50±1.38	1.02±0.03	-	-	-	-	-
		5.09±0.19	-	-	62.33±2.37	59.00±2.24	0.95±0.05	-	-	54.2±6.8	-	-
I	-0.2	6.15±0.20	12.79±0.60	2.1	75.38±2.50	75.83±2.50	1.00±0.05	73.67±3.85	0.97±0.06	73.8±11.5	1.00±0.19	51.50±2.42
Fracture Material	0	-	-	-	-	-	-	-	-	198.3±6.6	-	-
A	+0.4	6.17±0.17	13.83±0.76	2.2	75.67±2.12	73.17±2.05	0.97±0.03	77.50±3.72	1.06±0.07	82.3±9.0	1.06±0.17	55.67±3.06
B	+1.6	4.94±0.21	14.49±0.46	2.9	60.50±2.54	62.66±2.63	1.04±0.05	61.83±1.90	0.99±0.06	45.7±6.8	0.74±0.13	58.33±1.84
C	+3.0	5.86±0.21	13.60±1.16	2.3	71.83±2.59	70.00±2.52	0.97±0.05	77.00±6.08	1.10±0.10	35.3±6.5	0.46±0.12	63.83±5.49
		4.82±0.13	-	-	59.00±1.65	58.17±1.63	0.98±0.03	-	-	-	-	-
D	+4.8	5.60±0.18	18.05±0.86	3.2	68.67±2.27	69.00±2.21	1.00±0.05	69.33±3.47	1.00±0.07	71.5±8.2	1.03±0.17	72.67±3.49
E	+5.5	4.53±0.15	16.27±0.55	3.6	55.50±1.83	55.17±1.82	0.99±0.05	58.83±2.12	1.07±0.06	58.7±9.3	1.00±0.19	65.50±2.23

*Determined by radioisotope dilution and α-spectrometry

There is, however, a clear deviation from equilibrium in the case of the $^{226}Ra/^{230}Th$ activity ratios with a maximum ratio of 1.06 immediately adjacent to the fracture. It then falls rapidly to a minimum ratio of 0.46 (at +3.0 cm) mirrored by a minimum ratio of 0.71 (at -1.6 cm) on the opposite side of the fracture. Further away from the fracture the activity ratios begin to rise, reaching unity again at +4.8 cm. Note that, while no ^{230}Th data are available for the protomylonitic fracture material to allow a proper comparison, the ^{226}Ra levels attain a maximum level of 198.3 $Bqkg^{-1}$ in this material (Tab. 8). The particular pattern of activity ratios displayed in this core, where the longer-lived daughters ^{234}U and ^{230}Th are in equilibrium with their parents but ^{226}Ra is relatively depleted, may be taken to indicate that the granite has been undisturbed over a period of around 0.2 to 2 Ma prior to a more recent (i.e. less than 8000 years old) event which preferentially mobilised a significant amount of Ra from the bulk rock adjacent to the main fracture (cf SCHWARCZ et al., 1982).

However, as was pointed out in section 4, such models assume a closed-box system i.e. that the mobilisation event was instantaneous (or at least much shorter than the half-life of ^{226}Ra) and, immediately the Ra had been removed from the bulk rock, that the system was then closed to any further loss or addition of ^{226}Ra (or ^{230}Th). Clearly, in most natural systems, this is too great a simplification. In this particular fracture system there is evidence of repeated (and perhaps current) movement and, presumably, water flow. In that case it is equally as likely that the mobilisation of the Ra has been a slow, continuous process (or a series of sudden events) which is now impossible to date in any realistic manner (similar situations were discussed in detail in section 4). Possible disturbances could therefore include glacial offloading, contruction of the Grimsel I Power Station access tunnel ($\sim$ 40 years ago) and even contruction of the FLG.

The precise nature of the ^{226}Ra mobilisation in this core is difficult to define because the location of the Ra is unknown. No discrete Ra-rich minerals (such as baryte, strontianite or cerussite) have been reported in these granites nor identified in these samples, so it is likely that the Ra sources are common to those of U and Th although, since ^{226}Ra results from three α - decays, it is likely to be loosely bound in U and Th acccessory minerals (cf. EYAL and FLEISCHER, 1985). The Ra would, of course, also inherit sites from previously mobile U (both ^{234}U and ^{238}U; see sections 5.4 and 5.5) although, as mentioned above (and later), there is no evidence for interstitial U and Th here so this is probably an insignificant source in this particular core.

In a recent study, LATHAM and SCHWARCZ (1987a), have shown that ^{226}Ra (and ^{228}Ra) can be easily leached from weathered granites by groundwaters. The coincidence of the zones of ^{226}Ra depletion with the numerous, probably water conducting, microfractures in this core (Figs. 7-12) suggest this as a likely mechanism here too. Alternatively the Ra could be displaced from the minerals by exchange with Na, Ca, Sr, Ba or Mn in solution (TANNER, 1964) or by chloride complexation (ZUKIN et al., 1987).

Regardless of the mechanism of re-mobilisation, there still remains the important question of the pathways of Ra once in solution. Does the $^{226}Ra/^{230}Th$ profile merely indicate loss of Ra from the rock in the immediate vicinity of the microfractures followed by rapid advective transport away from the site by water flowing in these same microfractures? Or might the profile not equally represent release of Ra from the bulk rock in the vicinity of the microfractures (due to interaction with water present in these zones) followed by migration of the Ra towards the main fracture (i.e. a form of matrix diffusion as recognised by NERETNIEKS, 1980 and HADERMANN and ROESEL, 1985)? Certainly MEYER et al., (1989) have shown the presence of connected pores, running perpendicular to the microfracture system towards the main fracture (Fig. 13), which would facilitate such diffusion and detailed examination of the ^{226}Ra data in Table 8 does indicate a dramatic increase of ^{226}Ra levels towards the main fracture (along with a slight increase in U and Th too) with ^{226}Ra attaining a maximum activity of 198.3 Bq kg^{-1} in the protomylonitic fracture material. Recent studies have indicated that clay minerals (AIREY, 1986; GREY, 1986; GASCOYNE and SCHWARCZ, 1986) and feldspars (LATHAM and SCHWARCZ, 1987a) are likely sinks for Ra in solution. In the granodiorite adjacent to the fracture and in the protomylonitic fracture material it is thus highly probable that the saussuritised plagioclase crystals (e.g. Fig. 18) which show inclusions of sericite, epidote and chlorite and are highly porous will be significant sites of Ra sorption. The micas which are present in the protomylonite may also provide sites for exchange of Ra (cf. BRADBURY, 1989).

Although the data for all other elements analysed in this core are equivocal with respect to the relative influence of the main fracture and the microfractures (Fig. 29 and Tab. 9), it is not inconceivable that local advective flow of water (from the microfractures towards the main fracture) has ocurred. Unfortunately it has proved impossible to determine sufficient boundary conditions in this core for a full validation of matrix diffusion (as envisaged by HADERMANN and ROESEL, 1985 and HERZOG, 1987) but work is proceeding on a simpler model in an attempt to ascertain whether true matrix diffusion or advective flow have dominated the transport of Ra in this rock core (ALEXANDER et al., 1989b).

Of course it is possible that the apparent transport of ^{226}Ra is, in fact, migration of ^{222}Rn, the intermediate step in the decay from ^{226}Ra to ^{214}Bi. While Rn may well be released from U-containing minerals more easily than Ra (RAMA and MOORE, 1984; KRISHNASWAMI and SEIDEMANN, 1988), it does seem unlikely that ^{222}Rn could migrate over a few centimetres in the 3.8 days it would exist before decaying to ^{214}Bi. Diffusion would, clearly, be insignificant and advection rates of the order of a cmd^{-1} also seems highly unlikely considering the physical state of this granodiorite (section 2; MEYER et al., 1989).

However, this does indicate the urgent need for the development of an efficient method for the determination of Ra, at the levels expected in rocks, by α-spectrometric examination of gramme weights of sample (cf. ACEÑA and CRESPO, 1988).

Figure 29: Distribution of Fe, Mn, Co, Cs, Ce, La, Eu and Lu in core AU96.90W (FLG)

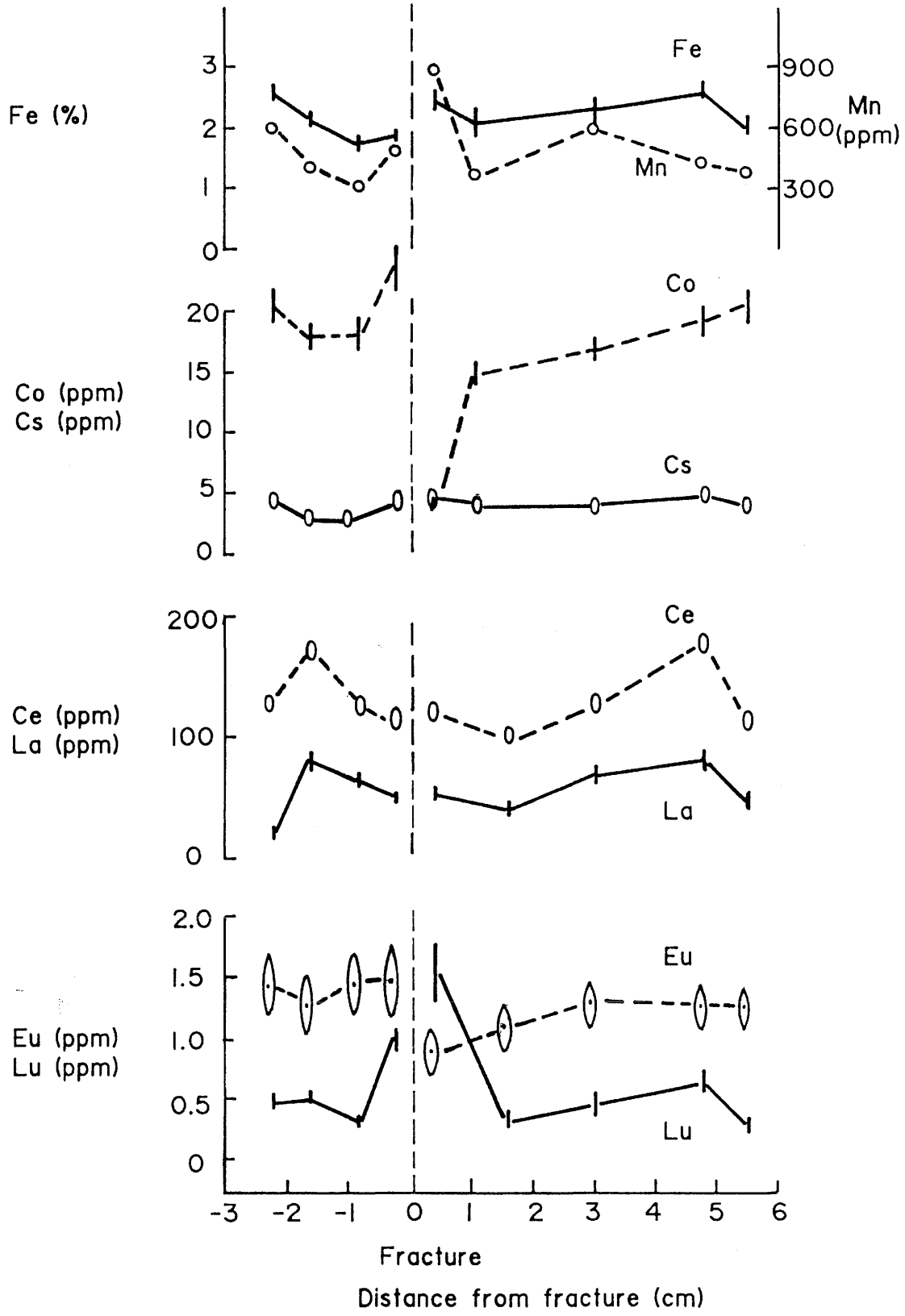

Table 9: INAA results for core AU96.90W from the MI site, FLG (all concentrations are in ppm unless otherwise stated)

Specimen	Distance from fissure (cm)	Na%	K%	Sc	Fe%	Co	Cs
F	-2.2	2.45±0.14	4.43±0.60	6.84±0.36	2.58±0.15	20.6±1.4	4.4±0.6
G	-1.6	2.36±0.14	3.07±0.47	4.90±0.26	2.13±0.12	17.9±1.2	3.1±0.4
H	-0.8	2.42±0.14	3.87±0.52	4.37±0.23	1.77±0.10	18.3±1.2	2.9±0.4
I	-0.2	3.74±0.18	2.62±0.44	8.20±0.42	1.88±0.11	23.5±1.9	4.6±0.7
A	+0.4	2.84±0.14	3.07±0.45	7.18±0.37	2.43±0.45	4.2±0.4	4.3±0.6
B	+1.6	2.46±0.15	3.62±0.52	5.65±0.29	2.05±0.12	15.0±1.0	4.1±0.6
C	+3.0	2.47±0.15	3.32±0.49	5.75±0.30	2.14±0.12	16.9±1.2	3.8±0.5
D	+4.8	2.40±0.14	2.70±0.41	7.27±0.37	2.66±0.15	19.2±1.3	4.7±0.6
E	+5.5	2.26±0.13	3.83±0.52	5.90±0.31	2.04±0.18	20.6±1.4	4.0±0.6

Table 9: (cont.)

Specimen	Distance from fissure (cm)	La	Ce	Nd	Sm	Eu
F	-2.2	19±5	126±7	41±9	2.4±0.4	1.45±0.22
G	-1.6	81±7	173±1	42±9	9.4±0.7	1.30±0.19
H	-0.8	63±7	126±7	42±9	6.7±0.7	1.47±0.21
I	-0.2	49±4	116±8	54±3	6.7±0.3	1.50±0.29
A	+0.4	52±6	121±7	32±8	7.6±0.6	0.90±0.18
B	+1.6	46±6	99±6	39±8	5.6±0.6	1.14±0.18
C	+3.0	68±7	126±7	36±8	7.2±0.6	1.32±0.19
D	+4.8	80±8	175±1	41±9	9.2±0.6	1.29±0.20
E	+5.5	48±6	110±7	34±8	6.4±0.5	1.28±0.19

Table 9: (cont.)

Specimen	Distance from fissure (cm)	Lu	Hf	Ta	Th	Mn
F	-2.2	0.48±0.09	7.3±0.8	2.1±0.4	14±1	609.3±40.9
G	-1.6	0.53±0.09	7.4±0.8	1.8±0.3	28±2	400.5±25.9
H	-0.8	0.33±0.06	5.3±0.6	1.9±0.3	18±1	315.8±20.8
I	-0.2	1.00±0.12	6.0±0.5	2.1±0.4	19±1	474.8±31.2
A	+0.4	1.56±0.23	7.5±0.8	1.7±0.3	18±1	883.4±58.3
B	+1.6	0.36±0.07	6.2±0.6	1.5±0.3	16±1	357.4±23.5
C	+3.0	0.44±0.08	7.2±0.7	1.6±0.3	22±1	594.9±38.1
D	+4.8	0.65±0.10	7.2±0.7	2.3±0.4	24±1	427.4±27.4
E	+5.5	0.37±0.07	6.1±0.6	1.8±0.3	22±1	359.1±23.7

As has previously been mentioned, there is a slight rise of U, Th and Ra near the main fracture (Tab. 8) which may be an indication of an increased ability of the fracture zone to retain the nuclides when compared to the bulk granodiorite (cf sections 5.4 and 5.5). As part of this study it was thus decided to attempt a series of chemical leaches on the fissure material in order to indicate which, if any, secondary phases in the fracture associated material were involved in the uptake of mobile radionuclides. Unfortunately, insufficient material from site AU96 was available so a bulk sample from site AU126 was obtained instead (see section 2 and BRADBURY, 1989 for a discussion on the relevance of this material to the fracture of interest).

Numerous methods have been described for the extraction of trace elements from rocks (e.g. BERGER and TRUOG, 1944; COTTENIE et al., 1979; TESSIER et al., 1979, 1980, 1985; MORTON and LONG, 1980; KRALIK, 1984) and the large number and diversity of analyses are probably indicative of their speculative nature. In this particular experiment a sequence of leaches (see Tab. 7) was chosen with the specific intention of dissolving several of the secondary mineral phases which previously have been reported to either contain U/Th/Ra or have been indicated in association with U/Th/Ra (see, for example, SHIRVINGTON, 1983; THIEL et al., 1983; MICHEL, 1984; LOWSON et al., 1986; BARRETTO and FUJIMORI, 1986; AIREY and

IVANOVICH, 1986; GASCOYNE and SCHWARCZ, 1986; ZIELINSKI et al., 1987; LATHAM and SCHWARCZ, 1987a, KRISHNASWAMI and SEIDEMANN, 1988). In addition to this, leach steps were included which would degrade part of the clays present in the samples to provide information on the accessibility of U/Th/Ra to groundwater solutions once they are associated with clays.

It should be stressed at this point that the particular sequence of leaches applied in this study is by no means unique and that numerous other groupings of leach reagents are possible if it is desirable to examine the relationship between U-decay series radionuclides and other phases in the fracture material (or granodiorite). It must also be emphasised that leaching schemes, such as this, produce operationally defined partition of elements between fractions of the rock and it cannot be necessarily assumed that discrete phases associated with each fraction actually exist in the rock (a point which has been ignored in several recent studies: see McKINLEY et al., 1989, for comments). It should also be noted that, had the mineralogical description of the AU126 mylonite (MEYER et al., 1989) been available earlier, then certain of the target phases would have been changed. For example, the absence of significant amounts of either carbonate minerals or Mn-oxides would probably have precluded the inclusion of steps (b) and (c) in Table 7.

Nevertheless, the data presented in Table 10 does indicate several important features of the mylonite from AU126, even if the failure to develop a satisfactory α-spectrometric method for ^{226}Ra does curtail wider applications. It is clear that, like the granitic parent rock (BAJO, 1980), there is very little detectable interstitial U in the mylonite. In some ways this is surprising because it would be not unreasonable to expect at least some U to be released from mineral lattice sites to interstitial (or clay?) sites during alteration of the rock or simply by α-recoil mechanisms (cf. SHIRVINGTON, 1983; THIEL et al., 1983; LOWSON et al., 1986; LATHAM and SCHWARCZ, 1987a; KRISHNASWAMI and SEIDEMANN, 1988; section 5.4 this report).

MEYER et al., (1989) indicate the complete absence of allanite (the likely major U and Th host; see above) in the mylonite (and the protomylonite from AU96) along with low (<10ppm) Th levels when compared to the Grimsel granodiorite ($\sim$19ppm Th; LABHART and RYBACH, 1976). Based on other geochemical data, MEYER et al., (1989) conclude that the alteration of the granodiorite to the mylonite was a non-isochemical process and therefore the Th was similarly lost from the system (cf. with the data for AU126 presented in Appendix A). However, the data presented here for the mylonite (Tab. 10) shows little difference in the Th (and U) content from that of the granodiorite (Tab. 8) or LABHART and RYBACH's (1976) data.

It is suggested, therefore, that release of Th (and U) by the destruction of allanite during mylonitisation was accompanied by local uptake of Th (and U) in new minerals forming coevally.

Table 10: Natural decay series radionuclides in a series of sequential leaches on mylonitic material from fissure AU126, FLG (leach reagents are detailed in Tab. 7).

Sub-sample A^+

"Target" Phase:	U* (ppm)	Th* (ppm)	Th/U	^{238}U (Bq kg^{-1})	^{234}U (Bq kg^{-1})	$^{234}U/^{238}U$	^{230}Th (Bq kg^{-1})	$^{230}Th/^{234}U$	^{232}Th (Bq kg^{-1})
- easily exchangeable (or sorbed) ions	b.d.l	n.d.	-	b.d.l	b.d.l	-	n.d.	-	n.d.
- carbonates	b.d.l	n.d.	-	b.d.l	b.d.l	-	n.d.	-	n.d.
- Mn-oxides	b.d.l	n.d.	-	b.d.l	b.d.l	-	n.d.	-	n.d.
- amorphous Fe and Al-oxides (also organic Fe and Al phases)	b.d.l	b.d.l.	-	b.d.l	b.d.l	-	b.d.l	-	b.d.l
- remaining amorphous inorganic compounds	b.d.l	b.d.l.	-	b.d.l	b.d.l	-	b.d.l	-	b.d.l
- resistates	7.76±0.19	20.78±0.66	3.7	95.17±2.38	85.33±2.13	0.90±0.30	92.67±5.42	1.08±0.08	83.67±2.67

Table 10: (cont.)

Sub-sample B+

"Target" Phase:	U* (ppm)	Th* (ppm)	$^{Th}/_{U}$	^{238}U (Bq kg^{-1})	^{234}U (Bq kg^{-1})	$^{234}U/^{238}U$	^{230}Th (Bq kg^{-1})	$^{230}Th/^{234}U$	^{232}Th (Bq kg^{-1})
- easily exchangeable (or sorbed) ions	b.d.l	n.d.	-	b.d.l	b.d.l	-	n.d.	-	n.d.
- carbonates	b.d.l	n.d.	-	b.d.l	b.d.l	-	n.d.	-	n.d.
- Mn-oxides	b.d.l	n.d.	-	b.d.l	b.d.l	-	n.d.	-	n.d.
- amorphous Fe and Al-oxides (also organic Fe and Al phases)	b.d.l	b.d.l.	-	b.d.l	b.d.l	-	b.d.l	-	b.d.l
- remaining amorphous inorganic compounds	b.d.l	b.d.l.	-	b.d.l	b.d.l	-	b.d.l	-	b.d.l
- resistates	8.30±0.24	n.d.	-	101.67±2.94	103.83±3.01	1.02±0.04	n.d.	-	n.d.

b.d.l: below detection limit (see BACON and ROSHOLT, 1982)
n.d.: not determined
+: 5 g sub-samples from a homogenised and crushed 200 g aliquot from a 1 kg bulk sample
*: determined by radioisotope dilution and α-spectometry

Certainly alpha autoradiographs of the mylonite indicate radiation sources which are lineated parallel to the foliation of the rock and which may indicate uptake by re-crystallized sheet silicates such as biotite (MEYER, pers. comm.).

The leaching experiments indicate that Th and U are, at present, in strongly bound (lattice) sites in the mylonite, and this (see Tab. 10) suggests that we may consider this system to be a closed box with respect to dating the uptake event from the U-Th system (discussed in detail in section 4). This would then indicate that the $^{234}U/^{238}U$ activity ratio of ~1 represents true equilibrium and therefore the event which concluded in the uptake of U and Th by the new minerals in the mylonite was >1My BP. That the $^{226}Ra/^{230}Th$ activity ratio of 1.18 (see Tab. 5) for the mylonite implies uptake of Ra from solution is not necessarily inconsistent with the above mechanism for U and Th if the same processes (Ra sorption on clay sized material and altered feldspars) are going on in the AU 126 mylonite as are probably occurring in the AU96 protomylonite (see Tab. 8 and comments above). Thus, while U and Th are tightly bound in the lattice sites, ^{226}Ra remains accessible to groundwaters as a consequence of lattice site damage due to α-recoil and a greater susceptibility to exchange reactions (see also BAEYENS et al, 1989 for a detailed discussion of the nature of the sorption processes in the AU126 mylonite).

It is of note that the distribution of the other elements examined in this core (Tab. 9) provide no clear evidence of reaction in the vicinity of the fracture (cf. section 5.5). However, following the study of BRADBURY (1989) it is intended to examine several other elements (e.g. Sr) which have been shown to be significant to the understanding of sorption processes in the AU126 mylonite.

5.3 FLG drillcore SB80.001

This report represents a completely new study of drillcore SB80.001 and reaches significantly different conclusions from those reported in an earlier study (SMELLIE et al., 1986b).

The distribution of U and its daughter decay products are displayed in Figure 30 and listed in Table 11. Fe, Mn, Co and Cs and the REE are presented in Figure 31 and tabulated in Table 12 along with Na, K, Sc, Rb, Ba, Hf, Ta, Th (by INAA) and the REE's Nd, Sm and Tb. Note that these Figures differ from those presented in SMELLIE et al. (1986b) due to a drafting error in the earlier report.

U and Th vary sympathetically throughout the length of the drillcore and display a random distribution with no discernible relationship to the known fractures (cf with Fig. 14). U ranges in concentration from 5.26 to 9.25 ppm and the Th levels vary from 16.06 to 27.53 ppm and, although the mean Th/U ratio of 2.4 is slightly lower than the other FLG core (AU96.90W; section 5.2), the values are similar to other reported analyses of Grimsel granitic rocks (e.g. LABHART and RYBACH, 1976; BAJO, 1980; ALEXANDER et al., 1987). All other elements analysed in this drillcore display

Figure 30: Distribution of the natural decay series radionuclides in core SB80.001 (FLG)

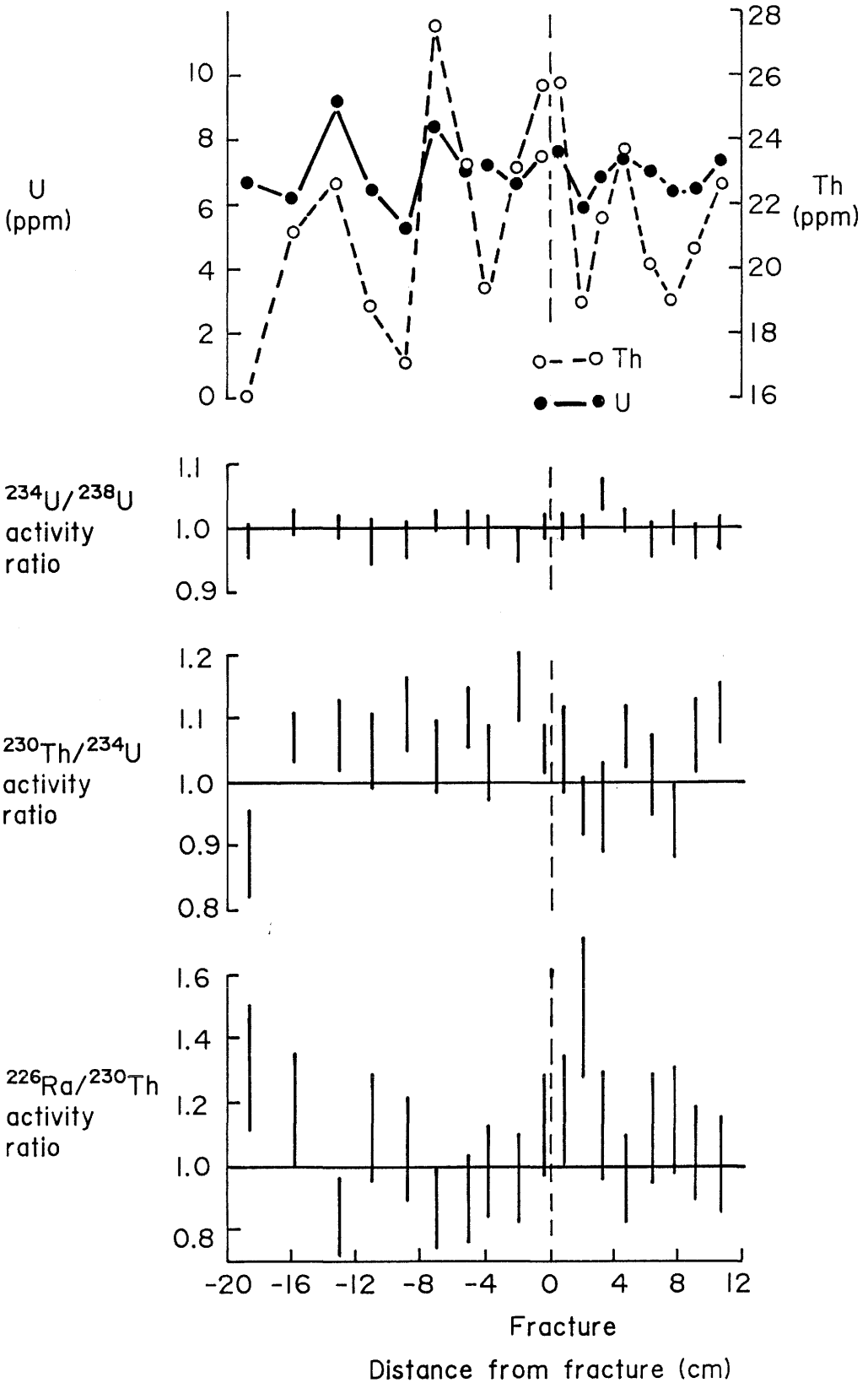

Table 11: Natural decay series results for core SB80.001 from the FLG

Specimen	Distance from fracture face (cm)	U(*) (ppm)	Th(*) (ppm)	Th/U	^{238}U (Bq kg^{-1})	^{234}U (Bq kg^{-1})	$^{234}U/^{238}U$	^{230}Th (Bq kg^{-1})	$^{230}Th/^{234}U$	^{226}Ra (Bq kg^{-1})	$^{226}Ra/^{230}Th$	^{232}Th (Bq kg^{-1})
9A	-18.6	6.69±0.15	16.06±0.83	2.4	82.00±1.83	80.33±1.83	0.98±0.03	71.17±3.50	0.89±0.07	93.3±13.3	1.31±0.20	64.67±3.33
8A	-15.8	6.15±0.07	21.20±0.41	3.4	75.33±0.83	76.33±0.83	1.01±0.02	81.83±1.67	1.07±0.04	96.7±15.0	1.18±0.18	85.33±1.67
7A	-13.0	9.25±0.14	22.65±0.87	2.4	113.33±1.67	113.00±1.67	1.00±0.02	121.33±5.00	1.07±0.06	103.3±15.0	0.85±0.13	91.17±3.50
6A	-10.8	6.47±0.23	18.96±0.54	2.9	79.33±2.83	77.67±2.83	0.98±0.04	81.83±2.33	1.05±0.06	91.6±13.3	1.12±0.17	76.33±2.17
5A	- 8.8	5.26±0.14	17.10±0.50	3.3	64.50±1.67	63.17±1.67	0.98±0.03	70.17±2.00	1.11±0.06	73.3±11.7	1.05±0.16	68.83±2.00
4A	- 7.0	8.38±0.08	27.53±1.28	3.3	102.67±1.00	103.67±1.00	1.01±0.02	107.67±5.17	1.04±0.06	93.3±13.3	0.87±0.13	110.83±5.17
3A	- 5.0	6.99±0.18	23.14±0.54	3.3	85.66±2.17	85.83±2.17	1.00±0.03	94.33±2.17	1.10±0.05	85.0±13.3	0.90±0.14	93.17±2.17
2A	- 3.9	7.15±0.15	19.25±0.75	2.7	87.67±1.83	86.83±1.83	0.99±0.03	89.33±3.50	1.03±0.06	88.3±13.3	0.99±0.15	77.50±3.00
1	- 2.0	6.62±0.12	23.06±0.66	3.5	81.17±1.50	78.67±1.50	0.97±0.03	90.33±2.67	1.15±0.06	86.6±13.3	0.96±0.14	92.83±2.67
2B	- 0.4	7.36±0.15	25.67±0.50	3.5	90.17±1.83	90.00±1.83	1.00±0.02	94.83±2.00	1.05±0.04	108.3±16.7	1.14±0.17	103.33±2.00
3B	+ 0.6	7.60±0.15	25.83±1.28	3.4	93.17±1.83	93.17±1.83	1.00±0.02	98.17±5.17	1.05±0.07	115.0±16.7	1.17±0.18	104.00±5.17
4B	+ 2.2	5.86±0.08	18.92±0.54	3.2	71.83±1.00	71.50±1.00	1.00±0.02	68.67±2.00	0.96±0.05	103.3±15.0	1.50±0.22	76.17±2.17
5B	+ 3.4	(6.80±0.18	21.49±0.83	3.2	83.33±2.17	87.17±2.17	1.05±0.03	84.00±3.33	0.96±0.07	95.0±15.0	1.13±0.17	86.50±3.33
		(6.77±0.27	-	-	83.00±3.33	81.83±3.33	0.99±0.03	-	1.03±0.08	-	-	-
6B	+ 4.8	7.44±0.12	23.68±0.58	3.2	91.17±1.50	92.17±1.50	1.01±0.02	98.50±2.33	1.07±0.05	95.0±15.0	0.96±0.14	95.33±2.33
7B	+ 6.4	6.94±0.20	20.12±0.66	2.9	85.00±2.50	83.67±2.50	0.98±0.03	84.83±2.83	1.01±0.06	95.0±15.0	1.12±0.17	81.00±2.67
8B	+ 7.8	6.31±0.16	18.96±0.54	3.0	77.33±2.00	77.67±2.00	1.00±0.03	72.67±2.17	0.94±0.06	83.3±13.3	1.15±0.17	76.33±2.17
9B	+ 9.2	6.38±0.15	20.66±0.70	3.2	77.50±1.83	76.67±1.83	0.98±0.03	81.83±2.83	1.07±0.06	85.0±13.3	1.04±0.15	83.17±2.83
10B	+10.8	7.29±0.14	22.65±0.54	3.1	89.33±1.67	88.67±1.67	0.99±0.03	98.00±2.33	1.11±0.05	98.3±15.0	1.00±0.15	91.17±2.17

* Determined by radioisotope dilution and α-spectrometry

similar, if not identical, forms (cf. Figs. 30 and 31) and it is assumed that the element distribution patterns merely reflect the distribution of primary minerals in the core. Unfortunately no fission track analyses of this core exist and so it is assumed that the major U and Th bearing phases are the same as those reported by BAJO (1980) for other Grimsel granitic rocks (see previous section).

Plots of measured activity ratios indicate secular equilibrium for the $^{234}U/^{238}U$ pair but clear deviation from equilibrium for the $^{230}Th/^{234}U$ activity ratios with values ranging from 0.89 to 1.15 and the majority significantly greater than unity. The $^{226}Ra/^{230}Th$ activity ratios similarly display significant deviation from equilibrium, ranging from 0.85 to 1.50, again with the majority > 1.

In the conditions encountered in most groundwaters one expects Th to be relatively immobile (see, for example, LANGMUIR and HERMAN, 1980; IVANOVICH and HARMON, 1982; LAUL et al., 1985; LATHAM and SCHWARCZ, 1987a) unless the waters are either organic rich and acidic (MANSKAYA and DROZDOVA, 1968) or highly alkaline (LAFLAMME and MURRAY, 1987; BATH et al., 1987). As there is no evidence of these types of waters, flowing or having flowed, in the FLG then it is assumed that the disequilibria indicated by the $^{230}Th/^{234}U$ activity ratios represent preferential remobilisation of ^{234}U, followed by loss from the system. That the $^{234}U/^{238}U$ activity ratios show no disequilibrium indicates that the U remobilisation was an equilibrium removal with no preferential loss of ^{234}U in comparison with ^{238}U.

The above can be stated more precisely if the nomenclature of section 4 is used here too.

Thus A2/A1 = 1 and A3/A2 $\simeq$ 1.05 and the simplest assumption of equilibrium removal of U over a long (>0.2 My period) yields a value of $\lambda' = 4.4 \times 10^{-7} y^{-1}$ i.e. a removal probability for U, throughout the core, of about 10^{-7} atom^{-1}y^{-1} (cf. sections 5.4 and 5.5). Of course, a similar relationship between the activity ratios can be produced if higher removal rate have been operating for a shorter time or if the activity ratios are attempting to return to equilibrium after a recent, sudden removal of U (cf. the $^{226}Ra/^{230}Th$ activity ratios which suggest a recent disturbance; Fig. 30).

As in the case of the previous core, there is insufficient information on the form of the U phases (mobile verses immobile; pore fluid concentrations etc.) to enable a full validation of matrix diffusion (cf. HERZOG, 1987), although it is still possible to carry out a crude check to determine whether it is feasible or not to transport U out of the granite at the depths observed here in the type of timescale postulated. After HADERMANN and ROESEL (1985), if we assume pure pore diffusion in the rock core (the likely case in unaltered granite), we can define an interaction depth by -

Figure 31: Distribution of Fe, Mn, Co, Cs, Ce, La, Eu and Lu in core SB80.001 (FLG)

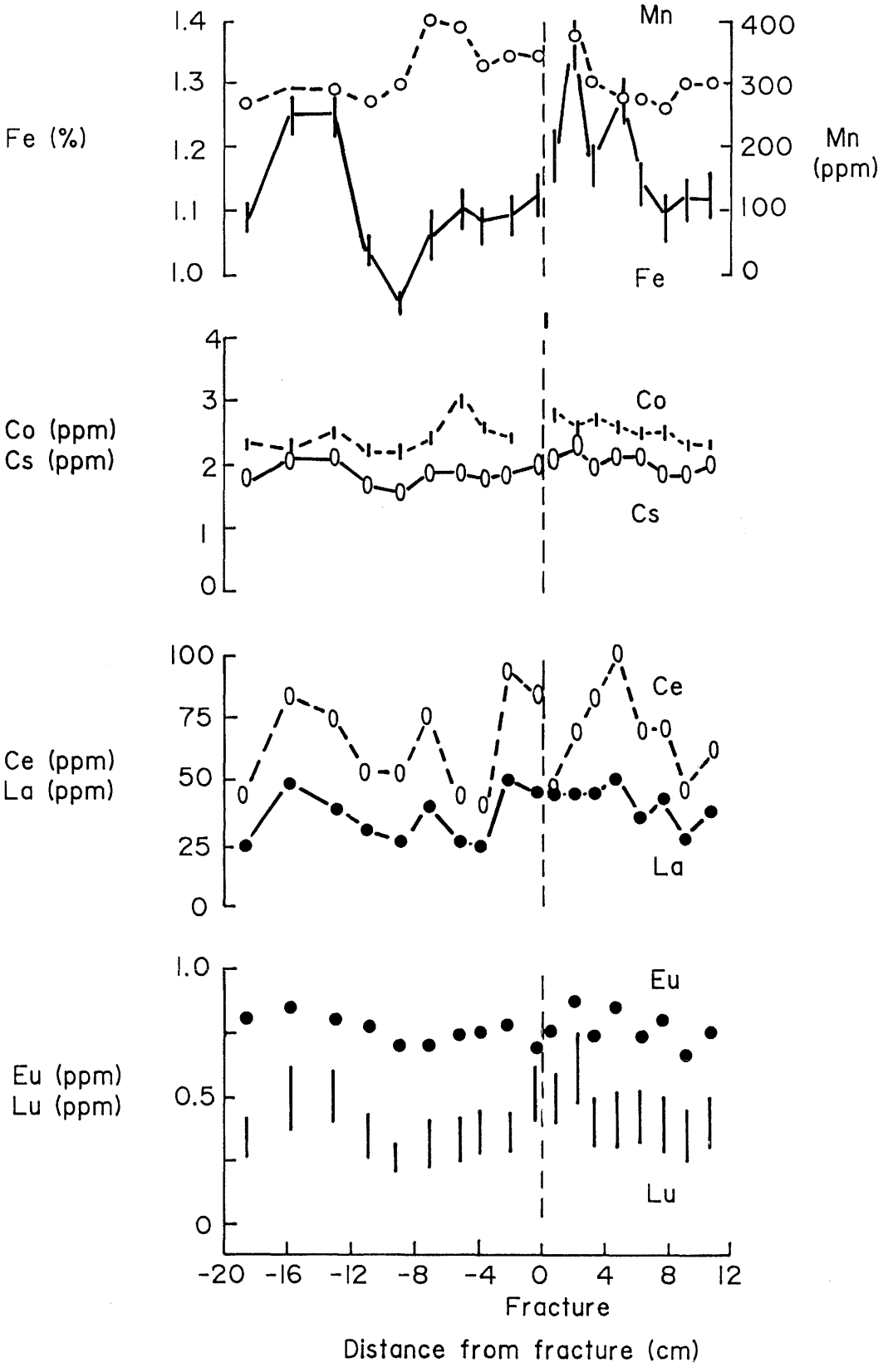

Table 12: INAA results for core SB80.001 (concentrations are in ppm unless stated otherwise)

Specimen	Distance from fracture face (cm)	Na%	K%	Sc	Fe%	Co	Rb
9A	-18.6	2.88±0.09	4.0±0.4	2.42±0.08	1.09±0.03	2.3±0.1	193±7
8A	-15.8	2.83±0.09	4.6±0.6	3.11±0.10	1.25±0.04	2.3±0.1	200±7
7A	-13.0	2.78±0.09	3.5±0.4	3.07±0.10	1.25±0.04	2.5±0.1	198±7
6A	-10.8	2.88±0.09	4.1±0.4	2.48±0.08	1.04±0.03	2.2±0.1	197±7
5A	- 8.8	2.61±0.08	4.0±0.4	2.18±0.07	0.94±0.03	2.2±0.1	183±7
4A	- 7.0	2.64±0.08	4.1±0.4	2.24±0.07	1.06±0.04	2.4±0.1	181±7
3A	- 5.0	3.03±0.09	4.9±0.5	2.66±0.08	1.10±0.04	3.0±0.1	189±7
2A	- 3.9	3.03±0.10	3.7±0.4	2.30±0.07	1.08±0.03	2.6±0.1	176±7
1	- 2.0	2.86±0.09	4.4±0.4	2.51±0.08	1.09±0.03	2.4±0.1	189±1
2B	- 0.4	2.63±0.08	3.4±0.3	3.06±0.09	1.12±0.04	4.3±0.1	177±7
3B	+ 0.6	2.90±0.09	4.4±0.5	2.79±0.09	1.19±0.04	2.8±0.1	188±7
4B	+ 2.2	2.93±0.09	4.1±0.4	3.14±0.10	1.36±0.04	2.6±0.1	204±8
5B	+ 3.4	2.78±0.09	4.0±0.4	2.64±0.08	1.17±0.04	2.7±0.1	190±7
6B	+ 4.8	2.88±0.09	3.6±0.4	3.03±0.09	1.27±0.04	2.6±0.1	191±8
7B	+ 6.4	2.53±0.08	3.7±0.4	2.49±0.08	1.14±0.04	2.5±0.1	183±7
8B	+ 7.8	2.79±0.09	4.1±0.4	2.33±0.07	1.09±0.04	2.5±0.1	189±8
9B	+ 9.2	2.58±0.08	3.8±0.4	2.49±0.08	1.12±0.04	2.3±0.1	176±7
10B	+10.8	2.75±0.09	3.5±0.4	2.40±0.07	1.13±0.04	2.3±0.1	177±7

Table 12: (Cont.)

Specimen	Distance from fracture face (cm)	Cs	Ba	La	Ce	Nd	Sm	Eu
9A	-18.6	1.8±0.1	538±36	24±2	45±2	19±4	3.5±0.2	0.79±0.03
8A	-15.8	2.1±0.1	589±40	49±2	85±3	34±5	6.4±0.2	0.84±0.03
7A	-13.0	2.1±0.1	608±40	38±2	74±3	31±5	5.9±0.2	0.79±0.03
6A	-10.8	1.7±0.1	638±40	30±2	54±2	19±3	4.6±0.2	0.77±0.03
5A	- 8.8	1.6±0.1	480±36	26±2	55±2	22±3	3.9±0.1	0.69±0.03
4A	- 7.0	1.9±0.1	506±37	40±3	73±3	24±3	4.9±0.2	0.69±0.03
3A	- 5.0	1.9±0.1	571±39	26±2	44±2	17±3	4.0±0.1	0.74±0.03
2A	- 3.9	1.8±0.1	475±33	22±2	41±2	14±2	3.5±0.1	0.75±0.03
1	- 2.0	1.9±0.1	505±31	50±3	93±4	32±4	5.6±0.2	0.78±0.03
2B	- 0.4	2.0±0.1	403±26	46±3	86±3	30±4	6.4±0.2	0.71±0.03
3B	+ 0.6	2.1±0.2	483±30	44±3	47±2	35±5	5.7±0.2	0.76±0.03
4B	+ 2.2	2.3±0.2	555±36	44±2	70±2	37±5	7.3±0.2	0.88±0.03
5B	+ 3.4	2.0±0.1	493±33	44±2	83±3	27±4	5.9±0.2	0.73±0.03
6B	+ 4.8	2.1±0.2	601±48	50±3	99±4	32±4	6.7±0.2	0.86±0.04
7B	+ 6.4	2.1±0.2	495±39	35±2	69±3	21±3	5.1±0.2	0.73±0.03
8B	+ 7.8	1.9±0.1	567±46	43±3	69±3	22±3	4.8±0.2	0.80±0.03
9B	+ 9.2	1.9±0.1	555±47	26±2	48±2	18±3	4.4±0.2	0.67±0.03
10B	+10.8	2.0±0.1	572±38	37±2	62±3	25±5	4.9±0.2	0.75±0.03

Table 12: (Cont.)

Specimen	Distance from fracture face (cm)	Tb	Lu	Hf	Ta	Th	Mn
9A	-18.6	0.35±0.03	0.34±0.09	3.6±0.1	1.4±0.1	16±1	270.00±9.3
8A	-15.8	0.67±0.04	0.50±0.13	5.3±0.2	2.4±0.1	19±1	n.d.
7A	-13.0	0.46±0.03	0.49±0.12	4.5±0.1	2.4±0.1	16±1	290.7 ±9.8
6A	-10.8	0.36±0.02	0.36±0.09	5.0±0.2	1.8±0.1	18±1	272.2 ±9.5
5A	- 8.8	0.19±0.02	0.27±0.07	2.9±0.1	1.6±0.1	18±1	300.0 ±9.2
4A	- 7.0	0.23±0.02	0.33±0.09	4.1±0.1	1.5±0.1	18±1	401.3 ±13.3
3A	- 5.0	0.21±0.02	0.34±0.09	3.4±0.1	1.6±0.1	13±1	390.4 ±12.7
2A	- 3.9	0.18±0.02	0.36±0.09	3.8±0.1	1.7±0.1	13±1	328.7 ±10.3
1	- 2.0	0.20±0.02	0.36±0.09	4.4±0.1	1.7±0.1	23±1	343.8 ±11.3
2B	- 0.4	0.28±0.02	0.49±0.12	3.8±0.1	2.3±0.1	23±1	343.9 ±12.4
3B	+ 0.6	0.32±0.02	0.48±0.12	5.3±0.2	2.2±0.1	18±1	n.d.
4B	+ 2.2	0.48±0.03	0.59±0.15	5.7±0.2	3.2±0.2	20±1	375.7±11.3
5B	+ 3.4	0.33±0.02	0.39±0.10	4.4±0.1	1.9±0.1	21±1	300.9 ±9.0
6B	+ 4.8	0.50±0.03	0.42±0.11	4.8±0.2	2.0±0.1	24±1	280.8 ±8.4
7B	+ 6.4	0.42±0.03	0.42±0.11	5.3±0.2	1.8±0.1	20±1	278.1 ±8.3
8B	+ 7.8	0.42±0.03	0.39±0.11	3.8±0.1	1.6±0.1	21±1	260.8 ±8.0
9B	+ 9.2	0.43±0.04	0.35±0.09	3.8±0.1	1.6±0.1	14±1	300.8 ±9.0
10B	+10.8	0.49±0.03	0.39±0.10	4.6±0.2	1.8±0.1	20±1	300.6 ±8.4

$$x = \sqrt{\frac{Dp}{Rp}\ \Delta t}$$

where x is the distance (m)
Dp is the diffusion coefficient (m^2s^{-1})
Rp is th retardation factor
t is the time (s).

Utilising the data of HADERMANN and ROESEL (1985), where Dp and Rp are estimated to be 10^{-10} m^2s^{-1} and 10^5 respectively, producers an interaction depth of some 18 cm from the fracture in 10^6 years (as the radioactive decay of ^{238}U can be ignored when $t < 10^7$ years) - in excellent agreement with the 10-20 cm U migration observed in this core.

It may, however, be more realistic to use SHEA'S (1984) Da (apparent diffusivity =Dp/Rp) values calculated for uranium under reducing conditions. Here Da = 10^{-16} to 10^{-19} m^2s^{-1}, producing diffusion controlled penetration depths of 5.6 to 0.18 cm respectively - up to two orders of magnitude less than observed for this core. This implies that some form of advective transport, in a micro-fractured zone in the immediate vicinity of the main fracture, cannot be ruled out for core SB80.001. Unlike the core discussed in the previous section, however, there are no data available on the extent of microfracturing in this core, although the granite is pervasively altered and includes lineations of secondary minerals which are not dissimilar to those observed in core AU96.90W (see section 2). Clearly, a detailed study is required of the connected porosity of core SB80.001 but it is not inconceivable that advective transport, of the type described for core AU96.90W in the previous section, has occurred in the vicinity of the main fracture.

The presence of microfractures in this core would certainly help to explain the rather erratic and noisy $^{226}Ra/^{230}Th$ profile (Fig. 30) with reaction perhaps occurring in the close vicinity of the microfractures (although it is also worth noting that the analytical uncertainties are large). A closer examination of the 0 to + 8 cm section of SB80.001 would be useful to ascertian the presence of sites of preferential ^{226}Ra deposition such as micas chlorites and even secondary Fe-oxyhydroxides (cf. section 5.2).

5.4 Kråkamåla drillcore K1

This particular drillcore has been discussed, in less detail, in SMELLIE et al. (1986b). The contents of U and its daughter decay products in core K1 are detailed in Figure 32 and listed in Table 13 and the distribution of Fe, Mn, Co, Cs and the REE's La, Ce, Eu and Lu are displayed in Figure 33 and presented in Table 14 along with Na, K, Sc, Rb, Ba, Hf, Ta and Th (by INAA) and the REE's Nd and Sm.

The U concentration in the granite ranges from 12.13 to 23.26 ppm and the Th content ranges from 48.02 to 89.42 ppm (mean Th/U = 4.38) while U and Th in the fracture material are 20.13 ppm and 46.37 ppm (Th/U = 2.30). The U and Th values for the granite are in rough agreement with previous analyses of the Götemar granite (SMELLIE and STUCKLESS, 1985) but are high compared with both the two Grimsel cores described previously and average granites world-wide (CLARK et al., 1966; IVANOVICH and HARMON, 1982).

A general loss of U from the Götemar granite has been demonstrated istopically by SMELLIE and STUCKLESS (1985). This is in agreement with the KRESTEN and CHYSSLER (1976) study which also demonstrate that most of the remaining U in the granite is associated with zircon, monazite, sphene, magnetite, haematite and ilmeno-rutile type phases and that only subordinate amounts of U are associated with dispersed intergranular sericite, epidote and Fe-oxyhdroxides (cf. THIEL et al., 1983; MICHEL, 1984; GUTHRIE and KLEEMEN, 1986).

The distributions of U and Th in core K1 are quite distinctive with the U concentration falling from the fracture material to the granite (Fig. 32) where the level then remains low and unchanging until about 8 cm from the fracture where a peak exists over some 4 cm. Th, in comparison, increases from the fracture material and then displays an irregular pattern until 8 cm from the fracture where it also broadens into a peak similar to that of U. The distribution pattern of Th is mimicked by the REE (see Fig. 33 for example) and all other elements analysed (except Fe, Mn and Cs) suggesting that this is a reflection of the original mineralogy. That the Ce distribution follows that of Th especially closely suggests monazite as a possible control on the Th distribution. Certainly monazites can contain up to 30 wt % Th (DEER et al., 1966; FRONDEL et al., 1967).

Figure 32: Distribution of natural decay series radionuclides in core k1 (Kråkamåla)

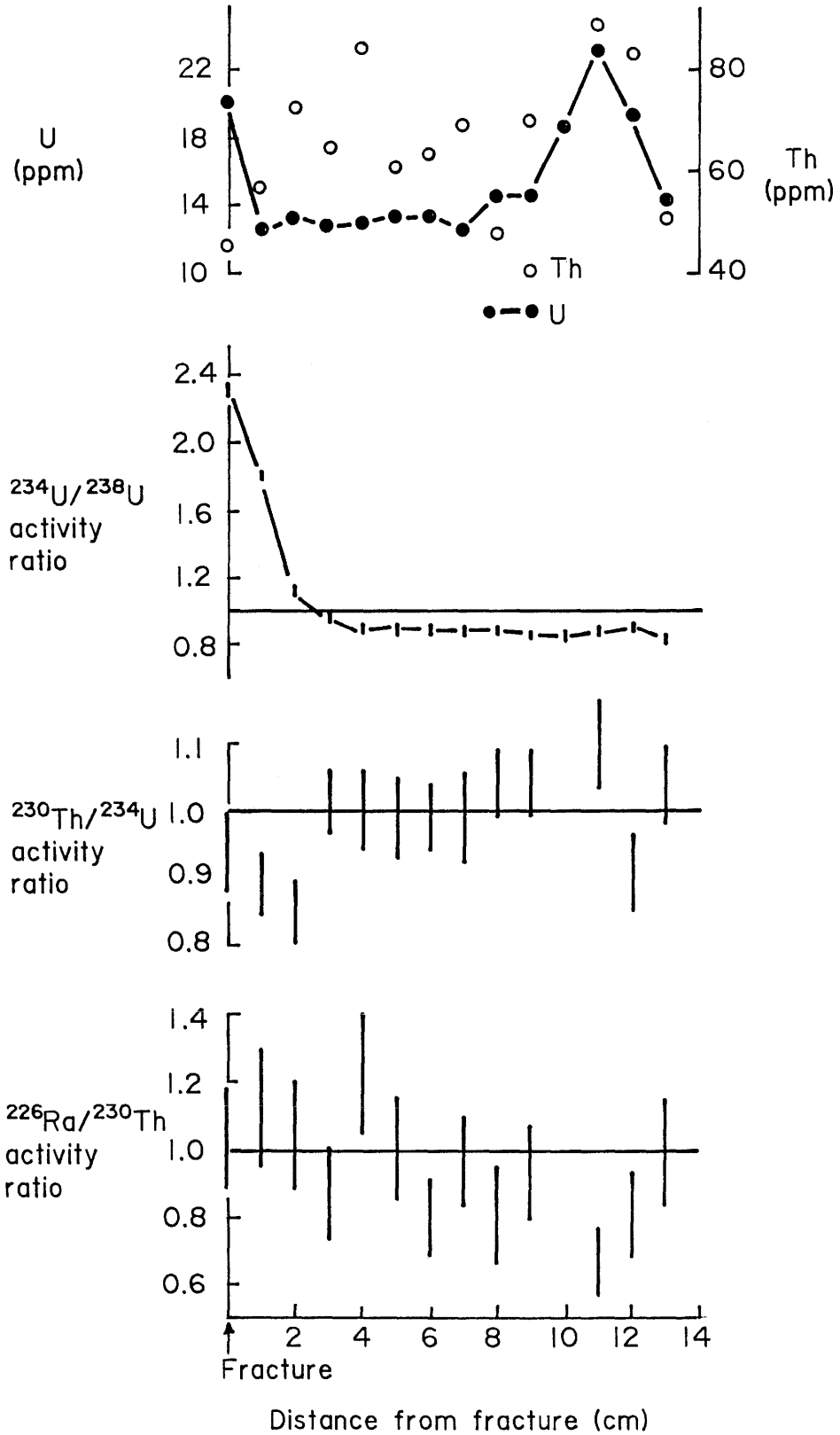

Table 13: Natural decay series results for core K1 from Kråkamåla, Sweden

Specimen	Distance from fracture face (cm)	U(*) (ppm)	Th(*) (ppm)	Th/U	^{238}U (Bq kg^{-1})	^{234}U (Bq kg^{-1})	$^{234}U/^{238}U$	^{230}Th (Bq kg^{-1})	$^{230}Th/^{234}U$	^{226}Ra (Bq kg^{-1})	$^{226}Ra/^{230}Th$	^{232}Th (Bq kg^{-1})
KIA-1	surface scrapings	20.13±0.54	47.37±0.54	2.3	246.7±6.7	565.0±13.3	2.29±0.07	531.7±16.7	0.94±0.06	545.0±81.7	1.03±0.15	186.7±8.3
KIA-2	1	12.51±0.41	57.96±1.24	4.6	153.3±5.0	278.3±5.0	1.81±0.05	246.7±5.0	0.89±0.05	276.6±41.7	1.12±0.17	233.3±5.0
KIA-3	2	13.19±0.27	74.52±2.07	5.6	161.7±3.3	181.7±3.3	1.12±0.02	155.0±5.0	0.85±0.05	161.6±25.0	1.04±0.16	300.0±8.3
KIA-4	3	12.78±0.41	65.83±0.83	5.2	156.7±5.0	150.0±5.0	0.96±0.03	151.7±3.3	1.01±0.05	130.0±20.0	0.86±0.13	265.0±3.3
KIA-5	4	12.92±0.41	84.46±2.07	6.5	158.3±5.0	141.7±5.0	0.89±0.04	141.7±5.0	1.00±0.06	173.3±26.7	1.22±0.18	340.0±8.3
KIA-6	5	13.46±0.41	61.69±1.24	4.6	158.3±5.0	145.0±5.0	0.88±0.03	143.3±3.3	0.99±0.06	143.3±21.7	1.00±0.15	248.3±5.0
KIA-7	6	13.46±0.27	64.17±1.24	4.8	165.0±3.3	143.3±3.3	0.87±0.03	141.7±3.3	0.99±0.05	113.3±16.7	0.80±0.12	258.3±5.0
KIA-8	7	12.65±0.27	69.13±1.24	5.5	155.0±3.3	131.6±3.3	0.85±0.03	130.0±5.0	0.99±0.07	125.0±18.3	0.96±0.14	278.3±5.0
KIA-9	8	14.55±0.27	48.02±1.24	3.3	178.3±3.3	156.7±3.3	0.88±0.02	163.3±5.0	1.04±0.05	126.7±18.3	0.78±0.12	193.3±5.0
KIA-10	9	14.42±0.27	69.97±1.24	4.9	176.7±3.3	148.3±3.3	0.84±0.02	155.0±3.3	1.04±0.05	143.3±5.0	0.92±0.14	281.7±5.0
KIA-11	10	(18.63±0.54	-	-	228.3±6.7	190.0±5.0	0.83±0.03	-	-	-	-	-
		(19.31±0.41	-	-	236.7±5.0	190.0±3.3	0.80±0.02	-	-	160.0±23.3	-	-
KIA-12	11	23.26±0.68	89.42±2.48	3.8	285.0±8.3	245.0±8.3	0.86±0.03	268.3±10.0	1.10±0.07	180.0±26.7	0.67±0.10	360.0±10.0
KIA-13	12	19.31±0.54	83.21±2.07	4.3	236.7±6.7	208.3±6.7	0.88±0.03	190.0±5.0	0.91±0.06	153.3±23.3	0.81±0.12	335.0±8.3
KIA-14	13	14.14±0.41	51.34±0.83	2.7	173.3±5.0	141.7±5.0	0.82±0.03	146.7±3.3	1.04±0.06	145.0±21.7	0.99±0.15	206.7±3.3
KIA-15	43	18.90±0.27	72.45±2.48	3.8	231.7±3.3	201.7±3.3	0.87±0.02	190.0±6.7	0.94±0.06	153.3±23.3	0.81±0.12	291.7±10.0

*Determined by radioisotope dilution and α-spectrometry

It is of note that SMELLIE et al. (1986b) suggest that the absence of any sympathetic U-Th relationship in the 0 - 8 cm zone of the core may be due to leaching of U from monazite during a (second) hydrothermal event. There are, indeed, partially altered monazites in this portion of the core but, if they are the source of the leached U, then the lack of mobilisation of Th suggests that U and Th are present in different sites in the monazite. Alternatively the later hydrothermal event was of too low a temperature (<400 Celsius; GABLEMANN, 1977; STUART et al., 1983) to also mobilise the Th and/or the (hydrothermal) fluids were enriched in carbonate, F^- and Cl^- all of which would preferentially leach the U from the monazite (LANGMUIR, 1978; MAYNARD, 1983).

The clear U increase in the vicinity of the fracture may be an accumulation of the U leached from the granite but it may equally represent uptake from the water moving in the fracture. Similar U increases in fracture material have been reported by SHIRVINGTON (1983) associated with kaolinite in weathered schists and by KAMINENI et al. (1986) in association with haematite and goethite in altered granites. The fracture material from core K1 includes haematite, chlorite, clays and Fe-oxyhydroxides (section 2), implying low temperature alteration of the previous hydrothermal assemblage in the vicinity of the fracture.

There is quite clearly significant disequilibrium between ^{234}U and ^{238}U in this core (Fig. 32). The $^{234}U/^{238}U$ activity ratio remains around 0.86 for the major length of the core (including the sample from 43 cm) then increases rapidly over the last 3 cm to the fracture reaching 1.81 at 1 cm and 2.29 in the fracture material. This is accompanied by a relatively invariant $^{230}Th/^{234}U$ activity ratio of unity which does, however, drop to 0.85 at 2 cm before rising slightly to 0.94 in the fracture material. There is a large amount of variation in the $^{226}Ra/^{230}Th$ activity ratios with perhaps a suggestion of random removal of some ^{226}Ra throughout the length of the core, to at least 43 cm from the fracture (cf. section 5.2).

Excluding for the moment the zone marginal to the fracture, the whole rock core displays a depletion of both ^{234}U and ^{230}Th relative to ^{238}U and a (slight) depletion of ^{226}Ra relative to ^{230}Th. A possible explanation for this is a sudden (that it to say over a time very much less than the half-lives of the isotopes involved; see section 4 for discussion) preferential loss of ^{234}U (by removal of intergranular U; by leaching of granular U by groundwaters; by recoil loss of ^{234}U etc.) on the order of 1 Ma ago followed by re-equilibration of ^{230}Th. The system then remained undisturbed until there was a sudden (for example) loss of ^{226}Ra from the rock some few thousand years ago.

According to the discussion presented in section 4, a similar effect may be induced by a slow, continuous process in each case such as groundwater leaching following the opening of the rock porosity initiated by tectonic rebound (due to glacial unloading) around 10^4 y. BP. Using the same nomenclature as before,

Figure 33: Distribution of Fe, Mn, Co, Cs, Ce, La, Eu and Lu in core K1 (Kråkamåla)

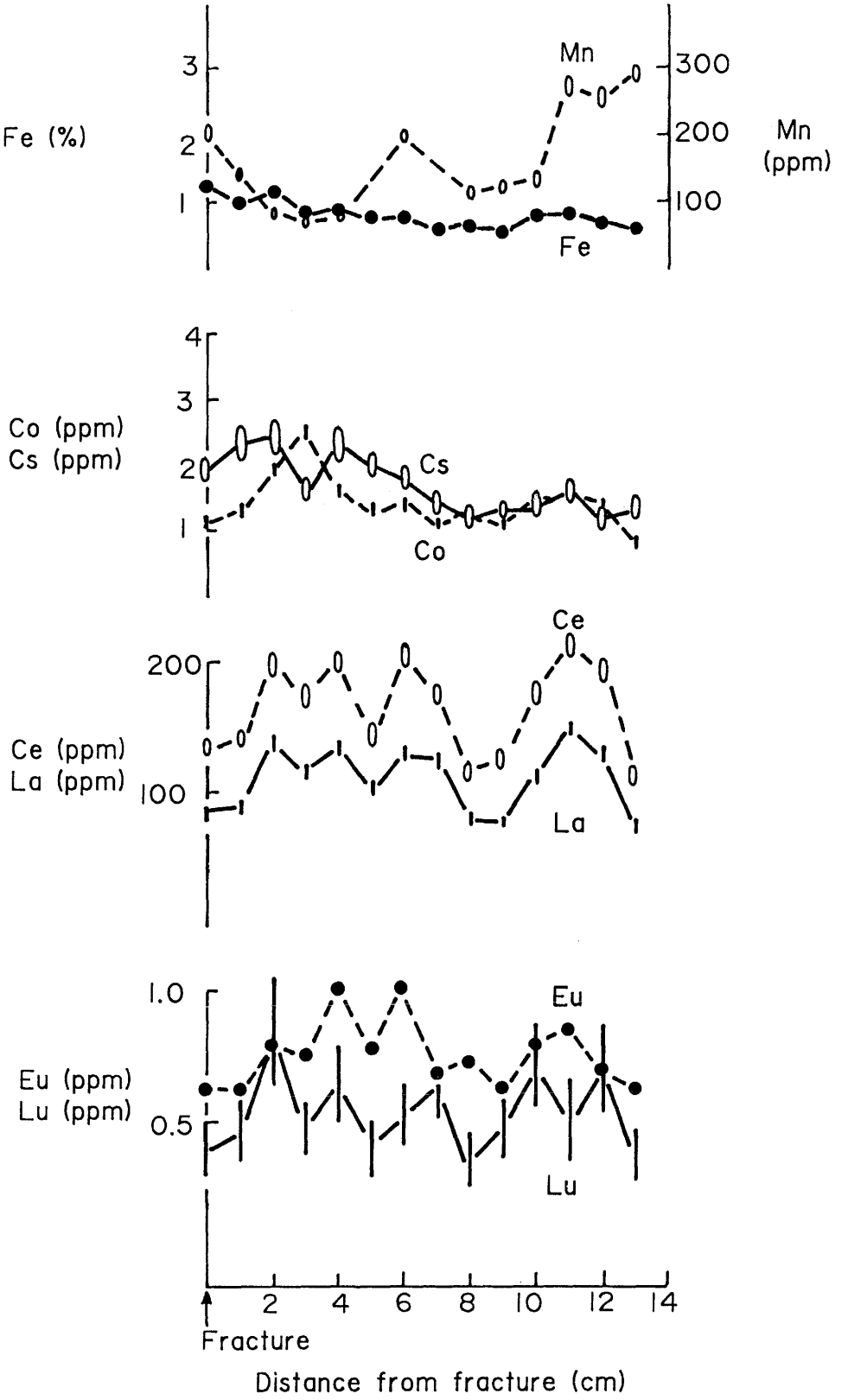

Table 14: INAA results for core K1 from Kråkamåla, Sweden

(all concentrations are ppm unless otherwise stated)

Specimen	Distance from fracture face (cm)	Na%	K%	Sc	Fe%	Co	Rb	Cs
KIA-1	surface scrapings	2.30±0.08	4.5±0.3	8.6±0.3	1.25±0.04	1.1±0.1	375±15	1.9±0.2
KIA-2	1	2.47±0.09	4.9±0.3	7.4±0.3	0.95±0.04	1.3±0.1	418±16	2.3±0.3
KIA-3	2	2.83±0.10	5.5±0.4	14.1±0.5	1.16±0.04	1.9±0.1	466±18	2.4±0.3
KIA-4	3	2.22±0.08	3.8±0.3	9.1±0.3	0.80±0.03	2.5±0.1	330±13	1.6±0.2
KIA-5	4	2.80±0.10	5.0±0.4	10.5±0.4	0.88±0.03	1.6±0.1	422±16	2.3±0.3
KIA-6	5	2.88±0.10	5.3±0.4	6.0±0.2	0.75±0.03	1.3±0.1	421±16	2.0±0.2
KIA-7	6	2.70±0.09	5.0±0.4	6.2±0.2	0.75±0.03	1.4±0.1	434±17	1.8±0.2
KIA-8	7	2.83±0.10	4.8±0.4	4.7±0.2	0.59±0.02	1.1±0.1	347±14	1.4±0.2
KIA-9	8	3.03±0.11	5.1±0.4	6.0±0.2	0.60±0.02	1.2±0.1	398±15	1.2±0.2
KIA-10	9	2.37±0.08	4.0±0.3	7.9±0.3	0.53±0.02	1.1±0.1	316±12	1.3±0.1
KIA-11	10	2.64±0.09	5.8±0.4	8.1±0.3	0.76±0.03	1.5±0.1	445±17	1.3±0.2
KIA-12	11	2.67±0.09	5.7±0.5	12.5±0.4	0.82±0.03	1.5±0.1	470±18	1.6±0.2
KIA-13	12	2.43±0.08	3.5±0.3	13.0±0.5	0.68±0.02	1.4±0.1	290±11	1.2±0.2
KIA-14	13	2.90±0.10	4.0±0.3	5.0±0.2	0.55±0.02	0.8±0.1	348±14	1.3±0.2
KIA-15	43	2.60±0.09	3.8±0.4	12.0±0.4	0.63±0.03	1.2±0.1	373±14	1.5±0.2

Table 14: (Cont.)

Specimen	Distance from fracture face (cm)	Ba	La	Ce	Nd	Sm	Eu
KIA-1	surface scrapings	313±29	84±4	136±8	36±5	3.7±0.2	0.63±0.06
KIA-2	1	246±26	88±4	140±08	34±4	3.6±0.1	0.62±0.04
KIA-3	2	298±35	139±6	197±11	46±6	5.3±0.2	0.80±0.07
KIA-4	3	213±22	117±5	173±9	44±5	4.4±0.2	0.75±0.05
KIA-5	4	266±36	135±5	197±10	44±6	5.3±0.2	1.01±0.08
KIA-6	5	324±27	103±4	144±8	34±5	4.1±0.2	0.77±0.05
KIA-7	6	375±29	130±5	206±11	45±6	5.1±0.2	1.06±0.06
KIA-8	7	239±23	125±5	173±10	42±6	4.8±0.2	0.68±0.05
KIA-9	8	227±22	80±4	117±7	41±5	3.5±0.1	0.73±0.05
KIA-10	9	214±26	78±3	126±7	33±4	3.7±0.2	0.62±0.05
KIA-11	10	294±25	113±5	176±10	41±5	5.0±0.2	0.79±0.05
KIA-12	11	312±24	148±6	212±11	60±7	6.2±0.2	0.86±0.05
KIA-13	12	165±30	131±5	192±10	53±6	5.2±0.2	0.69±0.06
KIA-14	13	246±22	76±3	112±6	34±4	3.3±0.1	0.62±0.04
KIA-15	43	284±34	118±5	170±9	40±5	4.7±0.2	0.77±0.06

Table 14: (Cont.)

Sample	Distance from fracture face (cm)	Lu	Hf	Ta	Th	Mn
KIA-1	surface scrapings	0.39±0.11	5.0±0.4	2.3±0.2	46±2	199.1 ± 15.6
KIA-2	1	0.46±0.11	6.5±0.5	2.4±0.2	64±2	141.5 ± 10.3
KIA-3	2	0.85±0.20	9.3±0.7	3.0±0.3	96±3	80.3 ± 6.2
KIA-4	3	0.48±0.11	5.2±0.4	1.3±0.1	62±2	63.6 ± 5.2
KIA-5	4	0.64±0.15	9.0±0.6	2.3±0.2	92±3	74.2 ± 6.3
KIA-6	5	0.39±0.11	7.0±0.5	1.8±0.2	58±2	n.d.
KIA-7	6	0.52±0.13	7.4±0.5	2.0±0.2	77±3	196.8 ± 14.9
KIA-8	7	0.62±0.15	7.5±0.5	2.3±0.2	71±2	n.d.
KIA-9	8	0.34±0.10	4.9±0.4	1.1±0.1	48±2	109.6 ± 9.2
KIA-10	9	0.46±0.11	5.7±0.5	2.0±0.2	61±2	119.3 ± 9.1
KIA-11	10	0.71±0.17	7.7±0.6	2.5±0.2	78±3	132.2 ± 10.2
KIA-12	11	0.52±0.13	7.7±0.5	2.3±0.2	89±3	276.3 ± 19.2
KIA-13	12	0.70±0.17	7.3±0.5	2.6±0.2	74±3	253.6 ± 17.6
KIA-14	13	0.32±0.10	4.9±0.4	1.1±0.1	46±2	286.3 ± 21.9
KIA-15	43	0.55±0.13	6.5±0.5	2.0±0.2	71±2	323.2 ± 21.5

$A_3/A_2 \simeq 1$ and $A_2/A_1 \simeq 0.85$ (Tab. 13)

and assuming a steady state has been reached.

Then, because $A_3/A_2 = \dfrac{\lambda_3}{\lambda_3 - \lambda_1'} \simeq 1$, λ_1' must be small.

If the upper analytical error is assumed for A_3/A_2 i.e. take

$A_3/A_2 = 1.05 = \dfrac{\lambda_3}{\lambda_3 - \lambda_1'}$

so that $\lambda_1' = 4.4 \times 10^{-7}$ y^{-1}.

Also, $0.85 = \dfrac{\lambda_2}{\lambda_2 + \lambda_2' - \lambda_1'}$, so that $\lambda_2' - \lambda_1' = 5.0 \times 10^{-7}$ y^{-1}

which gives $\lambda_2' = 9.4 \times 10^{-7}$ y^{-1}. Allowing A_3/A_2 to be 1.01 along the core would give $\lambda_1' = 9.1 \times 10^{-8}$ y^{-1} and $\lambda_2' = 5.9 \times 10^{-7}$ y^{-1}.

Thus we have a removal probability, for the more mobile species, of about 10^{-7} y^{-1} - similar to that of core SB80.001 in section 5.3. This is in accord with the conclusions of SMELLIE and STUCKLESS (1985) who suggest that pervasive open system modifications of the rock chemistry (of this core) have occurred, probably as a result of large scale hydrothermal alteration. Unfortunately, as we are unaware of any porosity or permeability data for the granite, we are unable to confirm whether the U transport through the rock is predominantly diffusive or advective (cf. ALEXANDER et al., 1989b; section 5.3).

In the granite marginal to the fracture and in the fracture material all four nuclides are enriched (although Th drops slightly in the fracture: Tab. 13) although the levels fall off rapidly over 0-3 cm. The $^{234}U/^{238}U$ activity ratios indicate a clear accumulation of U, preferentially ^{234}U, which is occurring sufficiently rapidly to prevent re-equilibration of the ^{230}Th daughter with ^{234}U so forcing the $^{230}Th/^{234}U$ activity ratio below unity. Simple mass balance calculations (which considers the core variations in only a one-dimensional sense) indicate that there is about three times more "excess" ^{234}U in the 0-3 cm zone of the core than could be provided from the ^{234}U deficit in the 3-13 cm zone of the core (as displayed in Fig. 32). This may be because the excess ^{234}U was supplied from the water moving in the fracture. However, the $^{234}U/^{238}U$ activity ratio for sample K1A-15, at 43 cm from the fracture, still displays a deficit of ^{234}U (Tab. 13), indicating that there is a ^{234}U deficit at depth in the granite so implying that all of the excess ^{234}U in the vicinity of the fracture could have come from the granite rather than the water. Again this is in agreement with the observations of SMELLIE and STUCKLESS (1985) noted above.

There is also a small increase in the $^{226}Ra/^{230}Th$ activity ratio (Tab. 13) in the vicinity of the fracture indicating preferential deposition of ^{226}Ra, presumably in association with the increased clay content of this zone of the core (cf. AU96.90W in section 5.2). As with the previous core, the excess ^{226}Ra may also be

associated with the secondary Fe phases in the vicinity of the fracture (see KAMINENI et al., 1986). It is not possible to rule out this mechanism in core K1 and it may well be worth considering such an association in future. Again, arguments similar to those mentioned in section 5.3 may be advanced for the timing of the various migration events.

As was mentioned above, Fe, Mn, Cs and U behave in a manner which is dissimilar to Th (and therefore to all other elements analysed) in this core. This grouping of elements is of interest because of the known redox-sensitivity of Fe, Mn and U in natural groundwaters (eg. STUMM and MORGAN, 1981; EDMUNDS et al., 1984; BROOKINS, 1987). Consequently their distribution patterns in the whole rock could indicate, by means of concentration minima and maxima analagous to those seen in marine sediment (eg. ALLER, 1980; COLLEY et al., 1984; COLLEY and THOMSON, 1985; UPSTILL-GODDARD et al., 1989), redox fronts between, for example, "anoxic" water flowing in the fracture system and the "oxic" granite-water system (or vice versa).

Redox buffering reactions within the rock matrix have been invoked within the Swedish KBS-3 project (cf. NERETNIEKS, 1983, 1986) and thus information about such processes is directly relevant to repository safety assessment. Buffering of radiolytically produced oxidant within the rock matrix is not only directly significant in terms of decreasing the solubility and mobility of some important radionuclides, but if such a "redox front" (cf. sandstone roll-front U deposits; COWART, 1980) is predominantly confined within the (micro-)porous structure of the host rock then the potential formation of colloids at this location could be less problematic.

In this core the Fe levels slowly increase from 10 cm depth to the fracture as does the concentration of Cs, although in not quite such a clear manner. The Cs level drops at 3 cm and then again in the fracture material. The Mn distribution is slightly more random in nature although the pattern is not unlike that of Th in the 5-14 cm zone of the core. At 4-5 cm from the fracture, the Mn concentration drops to a minimum before climbing steadily towards the fracture.

SMELLIE et al. (1986b) note that the increase in Fe levels coincide with an increase in Fe-oxyhydroxides which are dispersed throughout the rock along with an increase in the amount of chlorite and haematite associated with the numerous microfractures which parallel the main fissure. The main fracture also consists of haematite and chlorite along with Fe-oxyhydroxides and clays (see section 2). Although Cs is not, itself, redox sensitive it is known to be closely associated with secondary Fe minerals in ore bodies and it is likely that this is the case in this core (see also the Fe-Cs association in core WT 121, ALEXANDER et al., 1987c). In future studies it would appear worthwhile to check if any other of the many elements which are also known to sorb onto secondary Fe minerals behave in a manner similar to that of Cs. There is also a direct correlation between the Fe-oxyhydroxide phases and

intergranular U throughout the 0-3 cm zone of this drillcore. Fission track analysis shows that the U impregnation pattern corresponds with the dispersion of Fe-oxyhdroxides and alteration products (such as sericite) in this zone (SMELLIE et al., 1986b). This dispersion pattern also corresponds with the degree of alteration of the granite which, although pervasive, is strongly controlled by the irregular pattern of microfractures, grain boundaries and crystallographic planes (in the feldspars mainly). These results are in agreement with other field and laboratory studies of U immobilisation by Fe-phases (e.g. WEIJDEN et al., 1976; HO and DOERN, 1985; HSI and LANGMUIR, 1985; AIREY, 1986; KAMENINI, 1986; HOFMANN, 1988a,b).

The source of the Mn increase in the part of the core peripheral to the fracture is less clear although it is possible that secondary epidotes (after muscovite) determine the distribution of Mn in this zone (SMELLIE, pers. comm.). However, the coincidences in the profiles of Fe, U and Mn in the near fracture zone along with the well established mechanism of co-precipitation of Mn with Fe-oxyhydroxide (e.g. GIOVANOLI, 1980; HALBACH et al., 1980), suggests that it is as likely that the Mn exists in the oxide phase in association with the Fe-oxyhydroxides. Mn oxides can also play a part in adsorbing U in this zone (eg. TEWARI et al., 1972; BALISTRIERI and MURRAY, 1986) but it is likely that the Fe adsorption process will dominate in most cases (WEIJDEN et al., 1976; HALBACH et al., 1980).

Clearly then there is some form of redox control on the U distribution in this core in that the formation of Fe-oxyhydroxides is dependent on the redox potential of the system. It is not possible, however, to establish whether the association of U (and Mn) with Fe is also directly controlled by the redox potential of the system or simply by co-precipitation with and/or sorption on the Fe-phases. By analogy with sandstone roll-front deposits one would expect a spatial separation of the Fe and U "fronts" if the former process were dominant; unfortunately the sample intervals of this core do not allow definition of such fine structures (cf. Figs. 32 and 33). This is an important point because if, in fact, the latter process of U control dominates then it strongly suggests that further work, along the lines of TORSTENFELT et al. (1983), on the relationship between the Fe content, Fe form and reducing capacity of granites may be worth considering when evaluating the geochemistry of possible repository sites.

5.5 Böttstein drillcore BOE 618

Preliminary reports on this drillcore have already appeared elsewhere (SMELLIE et al., 1986b; ALEXANDER et al., 1988) and they are summarised here along with some new information and comments.

Although the fracture of interest lies in the middle of a pegmatite vein in the granite, the rock on only one side of the fracture has been examined for indications of rock-water interactions.

The distribution of U and its daughter decay products throughout the rock drillcore are displayed in Figure 34 and listed in Table 15. The levels of Fe, Mn, Co, Cs and the REE's La, Ce, Eu and Lu are shown in Figure 35 and are tabulated in Table 16 along with Na, K, Sc, Rb, Sb, Ba, Hf, Ta, Th (by INAA) and the REE's Nd, Sm, and Tb. The presence of the pegmatite-granite contact (as defined by the mineralogy of the core (decreased mafic content etc.), by the increase in Na and Ta levels and by the associated decrease in K and Rb concentrations on moving from the granite into the pegmatite) is marked on both Figures by a vertical, dashed line.

U and Th are relatively invariant in the granite until the pegmatite contact is reached where there is a jump in the U content to the core maximum with an associated increase in the Th content. Both U and Th then fall sharply in the pegmatite with Th decreasing continuously to the fracture while U increases once more in the last two centimetres before dropping again in the fracture material.

The U and Th contents of the fracture material are 2.4 ppm and 0.9 ppm respectively (Th/U ratio = 0.4) while in the associated pegmatite the U concentration ranges from 2.68 to 4.20 ppm with Th displaying a much larger concentration range of 0.74 to 12.58 ppm (mean Th/U ratio of 0.7). In the granite adjacent to the pegmatite, the U content ranges from 3.37 to 5.73 ppm and the Th content ranges from 21.44 to 34.69 ppm (mean Th/U ratio of 6.5). Fresh, unaltered granite from elsewhere in the drillcore displays a range in U concentrations of 8.6 to 10.4 ppm and a range in Th concentration of 19.8 to 29.3 ppm; mean Th/U ratio of 2.6 (PETERS et al., 1986) indicating a significant depletion of U in the study granite with Th seemingly immobile.

It has been reported (SMELLIE et al., 1986b) that the core mineralogy indicates that the granite has been subject to a hydrothermal event, presumably in association with the intrusion of the adjacent pegmatite. The alteration extends for at least 8 cm into the granite from the pegmatite contact with strong argillisation producing illite, smectite, calcite (in K-feldspar) and dispersed Fe-oxhydroxides as secondary phases. It is likely that this event remobilised and leached at least part of the original U in the granite (cf. BROOKINS, 1983, 1986). There has

Figure 34: Distribution of the natural decay series radionculides in core BOE (Böttstein)

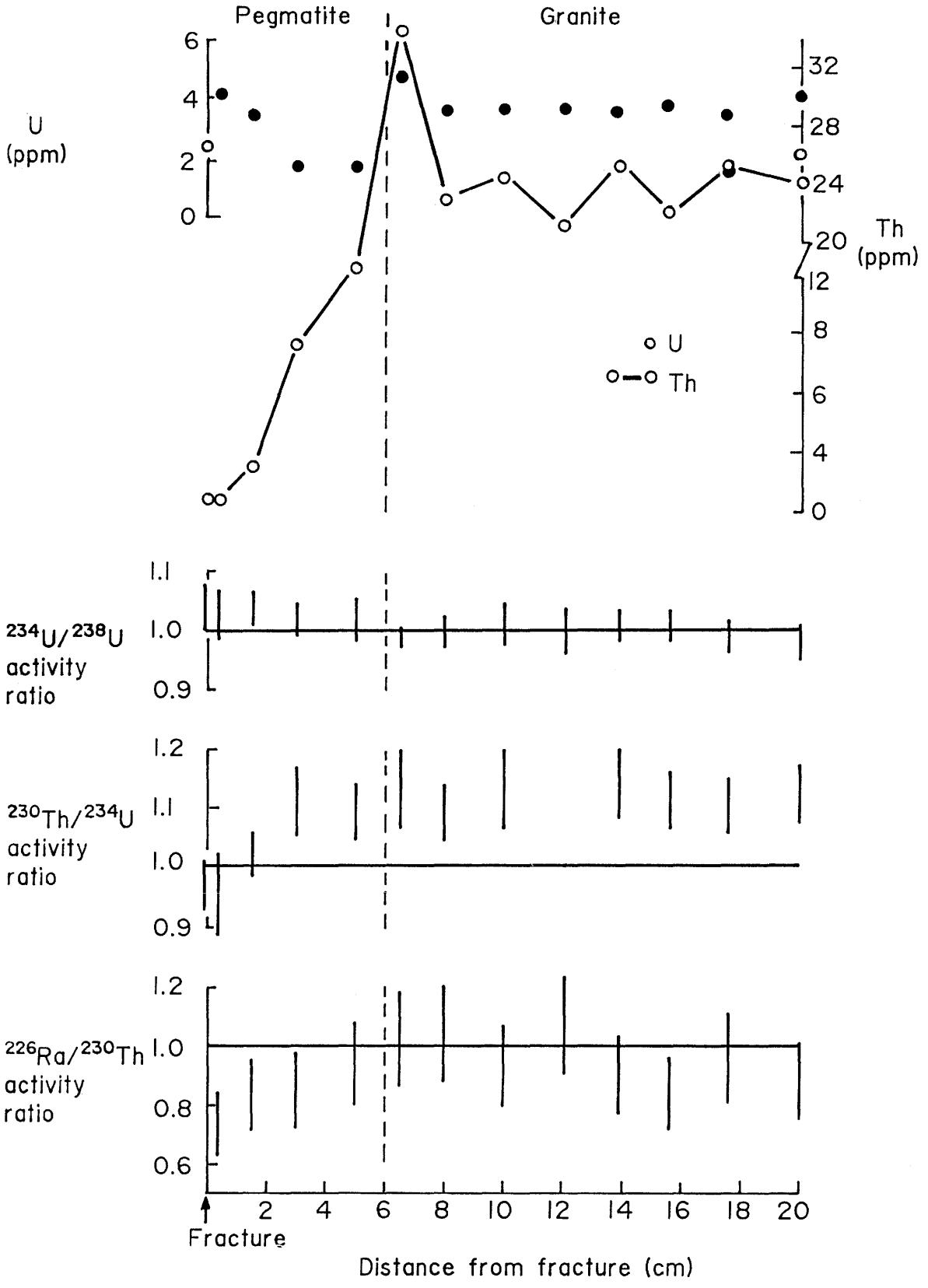

Table 15: Natural decay series results for core BOE from Böttstein, Northern Switzerland

Specimen	Distance from fracture face (cm)	U(a) (ppm)	Th(a) (ppm)	Th/U	^{238}U (Bq kg^{-1})	^{234}U (Bq kg^{-1})	$^{234}U/^{238}U$	^{230}Th (Bq kg^{-1})	$^{230}Th/^{234}U$	^{226}Ra (Bq kg^{-1})	$^{226}Ra/^{230}Th$	^{232}Th (Bq kg^{-1})
BOE 3396	fracture material a,b	2.42	0,99	0.4	29.73	30.73	1.04±0.04	29.73	0.97±0.04	-	-	4.00
BOE-1	fracture slice a,b	4.20±0.11	0.95±0.12	0.2	51.60±1.34	52.94±1.37	1.03±0.04	50.10±2.00	0.95±0.07	36.74±5.01	0.73±0.11	4.00±0.50
	0.4	3.98±0.11	0.74±0.25	0.2	48.93±1.34	44.26±1.33	0.90±0.05	47.09±1.84	1.06±0.08	-	-	3.06±0.99
BOE-2	1.5 a,c	3.41±0.08	3.27±0.12	1.0	41.92±0.84	43.42±0.84	1.04±0.03	44.26±0.83	1.02±0.04	36.74±5.01	0.83±0.12	13.19±0.50
BOE-3	3.0 a,c	2.68±0.05	7.32±0.29	2.7	32.90±0.67	33.57±0.67	1.02±0.03	37.24±1.34	1.11±0.06	31.73±5.01	0.85±0.13	29.56±1.17
BOE-4	5.0 a,c	2.71±0.04	12.58±0.29	4.6	33.23±0.50	34.07±0.50	1.02±0.04	37.24±1.00	1.09±0.05	35.07±5.01	0.94±0.14	50.77±1.17
BOE-5	6.5 a,d	5.73±0.08	34.69±0.87	6.1	70.31±1.00	69.30±1.00	0.99±0.02	77.32±0.50	1.12±0.05	78.49±11.69	1.02±0.15	139.95±3.51
BOE-6	8.0 a,d	3.59±0.07	23.27±0.58	6.5	44.09±0.84	44.26±0.83	1.00±0.03	48.26±1.34	1.09±0.05	50.10±6.68	1.04±0.16	93.85±2.34
BOE-7	10.0 a,d	3.60±0.10	24.63±0.75	6.8	44.26±1.17	44.59±1.17	1.01±0.04	50.27±2.00	1.13±0.07	46.76±6.68	0.93±0.14	99.36±3.00
BOE-8	12.1 a,d	(3.60±0.10	21.44±0.62	6.0	44.26±1.17	44.09±1.17	1.00±0.04	42.08±1.67	0.95±0.07	45.09±6.68	1.07±0.16	86.51±2.51
		(3.40±0.14	23.52±0.70	6.9	41.75±0.80	41.25±1.67	0.99±0.05	46.43±1.34	1.13±0.07	-	-	94.86±2.84
BOE-9	13.9 a,d	3.55±0.07	25.50±0.75	7.2	43.59±0.89	43.92±0.83	1.01±0.03	49.93±2.00	1.14±0.06	45.09±6.68	0.90±0.14	102.87±3.00
BOE-10	15.6 a,d	3.79±0.05	22.27±0.41	5.9	46.59±0.89	47.09±0.67	1.01±0.03	52.27±1.67	1.11±0.05	43.42±6.68	0.83±0.12	89.85±1.67
BOE-11	17.6 a,d	3.37±0.07	25.30±0.50	7.5	41.42±0.84	41.08±0.83	0.99±0.03	45.09±1.17	1.10±0.05	43.42±6.68	0.96±0.15	102.04±2.00
BOE-12	20.0 a,d	4.09±0.08	24.18±0.58	5.9	50.27±1.03	49.10±0.98	0.98±0.03	54.95±1.67	1.12±0.05	48.43±6.68	0.88±0.13	97.53±2.34

a Determined by radioisotope dilution and α-spectrometry
b (PEARSON 1988)
c Pegmatite
d Granite

also been some remobilisation and reconcentration of U and Th in the granite at the pegmatite-granite contact reflecting the high temperatures experienced in this zone (pegmatite fluid temperatures have been estimated at 400-600 Celsius; HATCH et al., 1975). The contact is also characterised by an increase in mafic mineral content in the granite.

Apart from a possible rise in the $^{234}U/^{238}U$ ratio in the pegmatite section of core BOE (Fig. 34), the pattern effectively indicates secular equilibrium throughout. There is, however, significant deviation from unity in the $^{230}Th/^{234}U$ activity ratio with average ratios of 1.1 to 1.5 throughout most of the core. There is a rapid drop, within the pegmatite, over the last 3 cm to the fracture with the fracture slice and fracture material both slightly less than unity. A similar pattern occurs in the distribution of the $^{226}Ra/^{230}Th$ activity ratios although in this case the activity ratios are unity throughout most of the drillcore and fall over the last few centimetres approaching the fracture to a minimum of 0.73 in the fracture slice (Fig. 34, Tab. 15).

The REE's generally mimic the distribution of Th although there is also a systemic decrease in the REE levels from 14 cm to 8 cm where there is then a sharp increase in concentration associated with the pegmatite-granite contact. Similar redistribution of the REE as a product of hydrothermal alteration have been reported for a range of environments (CORLISS, 1971; NESBITT, 1979; CLAUER et al., 1984; PALACIOS et al., 1986) although other low temperature mechanisms could also produce such changes (HUMPHRIS, 1984; JONASSON et al., 1988).

Fe, Mn, Co, Cs, (Fig. 35), Ba, Sc, Sb, and Hf (Tab. 16) display similar patterns with little variation throughout the granite followed by a sharp decrease across the pegmatite-granite contact. Unlike U, Th and the REE there is no comparable reconcentration of any of these elements (nor K, Na, Rb and Ta; Tab. 16) at the contact and this presumably reflects the differing mineral associations of these two groups. Unfortunately fission track analyses are not available for these samples but U and Th (and the REE) were probably associated with zircon and apatite originally (SMELLIE et al., 1986b) although the abundance of mafic minerals at the pegmatite-granite contact suggests an association with these constituents now (ALEXANDER et al., 1988).

Figure 35: Distribution of Fe, Mn, Co, Cs, Ce, La, Eu and Lu in core BOE (Böttstein)

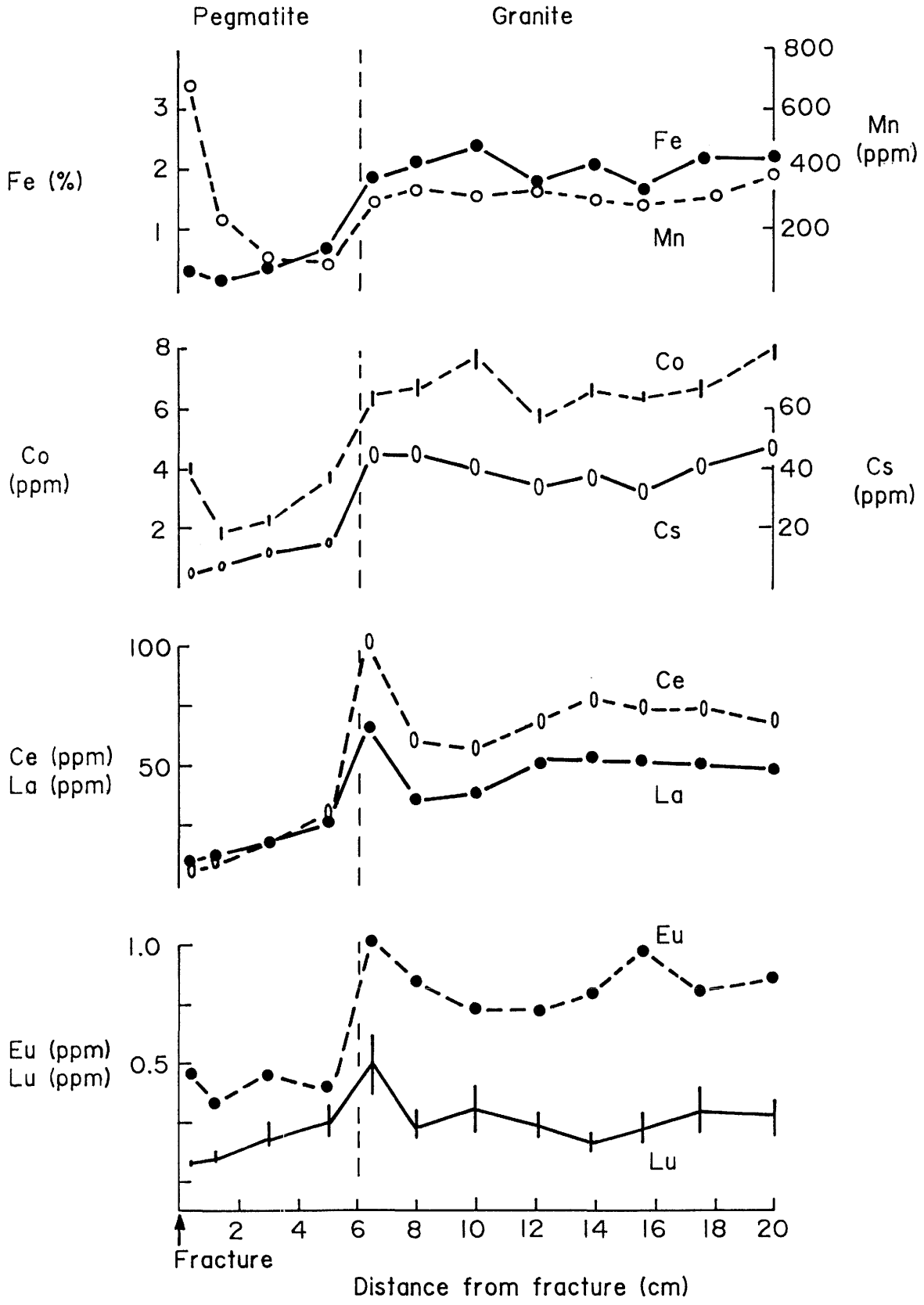

Table 16: INAA results for core BOE from Böttstein, Northern Switzerland

(All concentrations are in ppm unless stated otherwise)

Specimen	Distance from fracture face (cm)	Na%	K%	Sc	Fe%	Co	Rb
BOE-1	0.4 (fracture	1.92±0.06	1.3±0.1	1.39±0.05	0.30±0.01	3.0±0.1	106±4
BOE-2	1.5 slice)	2.60±0.09	3.5±0.3	1.45±0.05	0.13±0.01	1.9±0.1	243±10
BOE-3	3.0	2.25±0.08	3.9±0.3	2.82±0.09	0.35±0.01	2.1±0.1	255±11
BOE-4	5.0	1.64±0.06	2.6±0.2	2.58±0.09	0.64±0.02	2.7±0.1	179±8
BOE-5	6.5	1.09±0.04	4.0±0.3	7.95±0.27	1.84±0.06	6.4±0.3	325±14
BOE-6	8.0	1.15±0.04	5.0±0.3	8.62±0.29	2.10±0.07	6.7±0.3	391±16
BOE-7	10.0	1.01±0.03	5.1±0.4	9.83±0.33	2.38±0.08	7.7±0.3	381±16
BOE-8	12.1	1.04±0.04	4.8±0.3	7.40±0.25	1.76±0.06	5.8±0.2	362±15
BOE-9	13.9	1.06±0.04	5.2±0.4	8.39±0.28	2.04±0.07	6.6±0.3	396±17
BOE-10	15.6	1.02±0.03	5.5±0.4	6.96±0.24	1.69±0.06	6.4±0.2	350±15
BOE-11	17.6	0.99±0.03	5.0±0.4	8.61±0.29	2.17±0.08	6.7±0.3	387±16
BOE-12	20.0	0.98±0.03	5.3±0.4	9.32±0.32	2.15±0.07	7.9±0.3	400±16

Table 16: (Cont.)

Specimen	Distance from fracture face (cm)	Sb	Cs	Ba	La	Ce	Nd	Sm
BOE-1	0.4 (fracture	0.69±0.05	5.2±0.5	448±30	9.3±1.6	5.8±0.2	10±3	2.2±0.1
BOE-2	1.5 slice)	0.61±0.06	7.4±0.7	130±18	12.0±2.3	8.1±0.3	ND	1.7±0.1
BOE-3	3.0	0.67±0.06	11.6±1.1	84±21	18.7±2.3	17.2±0.6	ND	2.1±0.1
BOE-4	5.0	0.67±0.07	14.8±1.3	114±25	26.5±2.2	31.3±1.1	18±3	3.3±0.1
BOE-5	6.5	1.48±0.10	43.3±4.0	448±42	66.8±3.1	102.9±3.5	59±12	10.5±0.4
BOE-6	8.0	1.56±0.09	43.3±4.0	461±37	36.9±2.0	60.9±2.1	39±9	7.5±0.3
BOE-7	10.0	1.29±0.10	40.0±3.7	533±55	38.2±2.1	57.9±2.0	40±11	5.8±0.2
BOE-8	12.1	0.99±0.06	34.5±3.2	432±38	51.6±2.5	69.7±2.4	41±8	6.4±0.2
BOE-9	13.9	1.04±0.09	37.1±3.5	496±55	51.9±2.5	77.9±2.6	41±6	6.4±0.2
BOE-10	15.6	0.93±0.06	31.8±3.0	939±64	51.3±2.6	72.5±2.5	39±10	5.8±0.2
BOE-11	17.6	1.13±0.09	40.7±3.8	415±54	50.3±2.5	72.8±2.5	62±16	6.7±0.2
BOE-12	20.0	1.21±0.08	46.8±4.4	528±51	47.5±2.5	68.1±2.3	78±14	7.0±.3

Table 16: (Cont.)

Specimen	Distance from fracture face (cm)	Eu	Tb	Lu	Hf	Ta	Th	Mn
BOE-1	0.4 (fracture	0.46±0.02	0.14±0.01	0.08±0.02	0.64±0.03	1.0±0.1	0.58±0.0	678.6±19.9
BOE-2	1.5 slice)	0.33±0.02	0.16±0.02	0.10±0.03	0.64±0.05	1.7±0.1	5.9 ±0.2	229.0±8.1
BOE-3	3.0	0.46±0.03	0.19±0.02	0.19±0.06	1.2 ±0.7	3.0±0.2	7.4 ±0.3	99.6±3.9
BOE-4	5.0	0.39±0.03	0.33±0.03	0.26±0.08	0.63±0.06	1.0±0.1	11.0 ±0.4	93.0±2.9
BOE-5	6.5	1.03±0.05	0.80±0.06	0.49±0.14	5.3 ±0.2	1.3±0.1	37±1	287.7±9.2
BOE-6	8.0	0.86±0.04	0.60±0.05	0.24±0.07	5.8 ±0.2	1.7±0.1	28±1	338.7±11.1
BOE-7	10.0	0.73±0.04	0.52±0.05	0.31±0.09	6.2 ±0.2	1.9±0.2	21.4 ±0.7	314.7±10.9
BOE-8	12.1	0.72±0.03	0.48±0.04	0.23±0.07	5.1 ±0.2	1.7±0.1	23.1 ±0.8	325.2±11.0
BOE-9	13.9	0.79±0.04	0.66±0.07	0.17±0.06	4.6 ±0.2	1.9±0.2	23.7 ±0.8	299.6±10.5
BOE-10	15.6	0.98±0.04	0.54±0.05	0.22±0.07	5.7 ±0.2	1.5±0.1	19.6 ±0.7	280.0±9.5
BOE-11	17.6	0.80±0.04	0.77±0.07	0.29±0.09	6.6 ±0.2	2.0±0.2	25.3 ±0.9	309.5±9.2
BOE-12	20.0	0.86±0.04	0.81±0.06	0.27±0.08	6.5 ±0.2	2.0±0.2	24.8 ±0.8	372.5±12.7

Overall, core BOE provides evidence of several stages of mobilisation of a range of elements including U, Th and, the actinide analogues, REE's. Considering only the granite to begin with, if it is assumed that the Th is immobile under most natural water conditions (see above for qualifications), the average $^{230}Th/^{234}U$ activity ratio of $\sim$1.1 clearly indicates a loss of ^{234}U from the rock. However, as the $^{234}U/^{238}U$ activity ratios are unity, the removal of U, over the length of the drillcore, was non-fractionated with ^{238}U equally as mobile as the ^{234}U.

We can once again utilise the nomenclature of section 4 here. Thus $A_2/A_1 \simeq 1$ and $A_3/A_2 \simeq 1.1$. As in the case of SB80.001, if we assume equilibrium removal of U over a period which is >0.2 My then a steady state is attained and so $\lambda' = \sim 8 \times 10^{-7} y^{-1}$ (i.e. a probability of removal for U of some $10^{-7} y^{-1}$ - the same as for cores SB80.001 and K1. Once again, as in the case of core SB80.001, it must be conceded that a similar balance of the $^{234}U/^{238}U$ and $^{230}Th/^{234}U$ activity ratios could be produced if a higher rate of U loss has been proceeding for a shorter time or if the activity ratios are attempting to re-equilibrate after a recent, sudden removal of U. The fact that the $^{226}Ra/^{230}Th$ activity ratios are unity in the granite would tend to suggest that the U loss has been a slow, continuous process. At a probability of U loss of $10^{-7} y^{-1}$ it is not possible to see any effect on the ^{226}Ra simply due to the U migration (see SCOTT and MacKENZIE, 1989).

Repeating the exercise carried out on the data of core SB80.001, it is also possible to gain an insight into the dominance of diffusional or advective transport of the mobilised U in the granite section of this core. Once again the estimated Dp and Rp of HADERMANN and ROESEL (1985) produce excellent agreement with the analytical data while the, probably more realistic, Da values of SHEA (1984) underestimate the diffusion controlled interaction depth. Clearly then an advective component (acting in the vicinity of the main fracture by transport in associated microfractures) cannot be ruled out for the U migration in this core.

If this is the case then previous repository safety assessment calculations which assume only limited matrix diffusion (although they would certainly be conservative), may have to be re-assessed. Admittedly this granite has undergone a hydrothermal alteration (possibly associated with the Permian (?) pegmatite emplacement) and the argillisation has probably initiated conditions which have allowed easy access of geologically recent ground waters to U-bearing phases (perhaps via the numerous microfractures clearly visable in Fig. 18). Nevertheless, the significance of the continuous U advection throughout the length of this and the two previous drillcores to safety assessment models, indicating as it does the presence of a large volume of the rock matrix which is accessible to radionuclides migrating in the granite groundwater system of a radioactive waste repository, should not be underestimated.

Within the pegmatitic part of the core (0-6 cm) there is clearly a change in the distribution of the natural decay series radionuclides. With decreasing distance from the fracture there is a decrease in both the $^{230}Th/^{234}U$ and $^{226}Ra/^{230}Th$ activity ratios with the suggestion of a concommitant increase in the $^{234}U/^{238}U$ activity ratios. An input of U (which may be slightly enriched in ^{234}U) to the rock in the vicinity of the fracture, possibly by solution to solid ^{234}U α-recoil (FLEISCHER and RAABE, 1978; ROSHOLT, 1983) or more likely by a sorption mechanism (HSI and LANGMUIR, 1985; BARNEY et al., 1985), could simultaneously produce the observed $^{234}U/^{238}U$ and $^{230}Th/^{234}U$ activity ratios.

This deposition of ^{238}U and ^{234}U obviously occurred recently enough to prevent re-equilibration of ^{230}Th with its parent ^{234}U suggesting a slow continuous input of U over a longer period. It is important to note that there is also an apparent loss of ^{226}Ra in the vicinity of the fracture with the $^{226}Ra/^{230}Th$ activity ratios dropping below unity (cf. core AU96.90W). However, examination of the data in Table 15 indicates that the ^{226}Ra level is constant (around 35 Bq kg^{-1}) throughout the pegmatite and, rather, there is an increase in the ^{230}Th content of the pegmatite towards the fracture. The simplest explanation for this would be a solution to rock transfer of ^{230}Th (produced in a ^{234}U rich solution) which has occurred recently enough to prevent re-equilibration of ^{226}Ra with its parent (cf. the case for U and Th above). Again the mechanism is unclear although a solubility control seems most likely in this case (LANGMUIR and HERMANN, 1980).

Along with the uptake of U and ^{230}Th in the fracture zone there is a large decrease, from the pegmatite/granite interface to the fracture, of all other elements analysed (apart from Na and Ta). It is tempting to suggest that the compositional changes observed across the pegmatite are associated with the presence of the fracture (see Fig. 34), however, a more reasonable explanation is that the changes are simply a reflection of the mineralogical zoning previously described in some pegmatites (e.g. HATCH et al., 1975; CERNY et al., 1985; WALKER et al., 1986). This is believed to be a product of either the initial sequence of crystallisation of the pegmatite (granite/pegmatite border followed by a pegmatite wall zone then an intermediate zone and finally the pegmatite core (e.g. STAATZ et al., 1955) or the repeated passage of fluids, of varying composition, along a particular route during pegmatite crystallisation (QUIRKE and KREMERS, 1943). Although, from the examination of hand specimens and thin sections, there are no obvious mineralogical zones in the pegmatite of core BOE this clearly does not preclude a chemical zonation of the type described in pegmatites by previous researches (e.g. WALKER et al, 1986; JOLLIFF et al., 1987 and references therein) being produced by either (or both) of the above mechanisms.

The chondrite normalised diagram (Fig. 36) for the REE displays the changes across the pegmatite very clearly (note that the samples from the granite proper have not been plotted as they all lie very close to sample BOE-5 at 6.5 cm from the fracture). Clearly there is a significant change in the behaviour of Ce and Eu (and possibly Tb) across the pegmatite with an increasing depletion (with respect

to chondritic material) of both these REE as the fracture is approached. This is almost certainly a reflection of the original fluid composition (see, for example, SCHREIBER et al., 1980; HENDERSON, 1984; MOELLER and MUECKE, 1984, for details). While it is acknowledged that the redox state of the original fluid can also influence the behaviour of Ce and Eu (e.g. DRAKE, 1975; ELDERFIELD and SHOLKOVITZ, 1987), this mechanism seems unlikely in this case since most other elements analysed (including those which are not redox sensitive) display a pattern similar to that of the REE in the pegmatite (see Figs. 34 and 35).

It is of note, however, that the zone of U and ^{230}Th (and possibly Fe, Mn and Co?) uptake in the pegmatite coincides with that portion of the rock which displays the most intense Ce and Eu anomalies, possibly indicating that a primary feature of the pegmatite is involved in enhancing the fixation of radionuclides in the vicinity of the fracture. There are no obvious mineralogical or textural zones in this pegmatite (as mentioned above) but the ubiquitousness of pegmatites (and other late stage magmatic features) in most granites and their frequent rôle as water conducting zones in the host rock strongly suggests that further studies be carried out on pegmatites in general (and this core in particular) to determine more fully their potential rôle in retarding radionuclides in the vicinity of water conducting fractures.

Figure 36: Chondrite normalised REE diagram of core BOE (Böttstein). Note that the samples from the granite proper have not been plotted as they all lie very close to sample BOE-5 (6.5 cm).

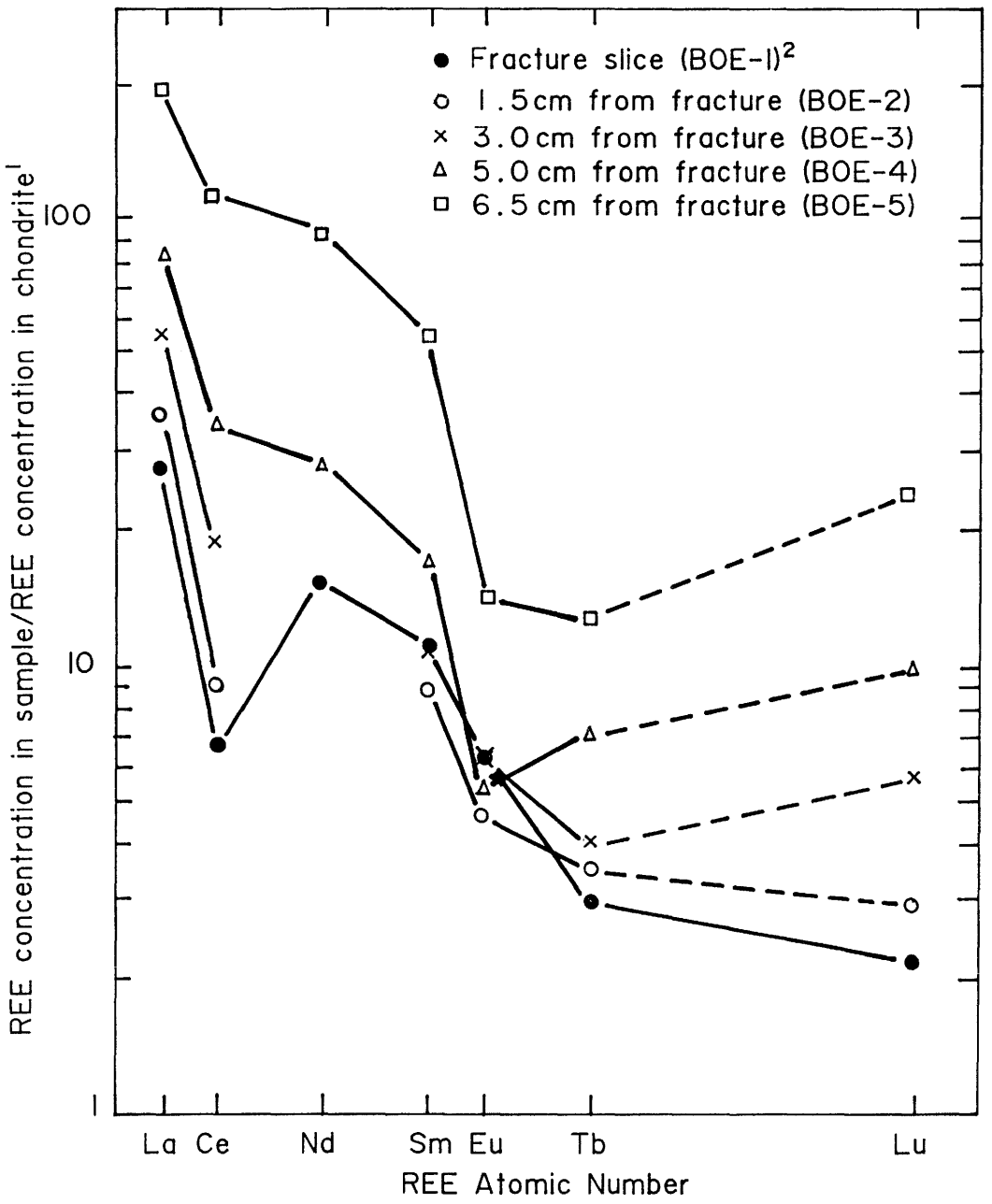

1. Laul and Schmitt, 1975 2. Sample numbers from table 15

SUMMARY

The main points arising from this study can be summarised as:

1) Disequilibrium studies, as used in the natural analogue approach, provide the best evidence to date for an interconnected porosity extending from fissures in crystalline rock into the rock matrix. Such a pore network may extend 50 cm into the matrix of heavily altered granite but it may be more restricted in a granite which has experienced less weathering or hydrothermal activity. For the Swiss case, the assumed connected pore distance of 1 mm in the Project Gewähr 1985 fracture flow model (NAGRA, 1985a) appears to be very conservative - a value of 1 cm would be sufficiently conservative and 5 cm could be considered as realistic. In the Swiss granites, at least, there is no evidence of matrix diffusion extending throughout the granite (as assumed, for example, in KBS 3 [KBS, 1983]). The timescale of the diffusion studied is inherently limited by the natural series nuclide half-lives, however, and hence the penetration distances observed are only lower limits.

   The only caveat on the application of the "diffusion distances" observed is the possible perturbation caused by leaching during sample preparation. The consistency of elemental and radionuclide profiles and the agreement between such profiles and observed microporosity in thin section, however, argue against such perturbation being significant.

   In terms of profile interpretation, the difficulties of quantitative analysis have been summarised by HERZOG (1987). The Ra profile from the FLG migration site, nevertheless, argues strongly for solute transport through micropores parallel to the main fissure by advection rather than diffusion. As far as repository safety analysis is concerned, it makes little difference if general advective flow occurs through a fissure zone several cm thick or if advection is confined to the fissure with diffusion into a surrounding zone of high diffusivity (HADERMANN and ROESEL, 1985). The description of transport on a microscale is, however, essential to interpretation of the Grimsel migration experiment (McKINLEY et al., 1988). Excavation of the fissure after the migration experiment with depth profiling of sorbed nuclides would shed more light on this aspect.

2) Sorption of U-series radioisotopes on fracture infill material is clearly indicated with increased concentrations of U and Ra in this zone. This sorption is probably associated with minerals such as plagioclase, sericite, chlorite, muscovite and clays (illite and smectite). Iron oxides and oxyhydroxides may also be important sorbing phases although their rôle as redox buffers, causing subsequent precipitation, may be equally significant. In this regard, it should be noted that the procedure for determination of in-situ distribution coefficients from natural series measurements proposed by IVANOVICH et al. (1988) is

grossly oversimplified. This procedure does not distinguish between sorbed and precipitated phases and hence retardation factors derived are not only wrong but also non-conservative in a safety assessment sense. Despite the more sophisticated sequential leaching and mineralogical analysis in the present study, it is not possible to unequivocably distinguish between sorption, precipitation and co-precipitation as immobilisation mechanisms and hence there has been no attempt to derive "Kd" values (see McKINLEY et al., 1989, for further comments).

3) A general observation is that the analytical data is consistent with Th and the REE being immobile under ambient conditions and any removal of Th and the REE can be attributed to earlier high temperature hydrothermal events. Although generally supporting the assumption of low mobility of the III and IV valent actinides in such environments, it should be stressed that the low mobility observed is predominantly due to the presence of these elements in resistate mineral phases and not to high retardation of dissolved species in the vicinity of a fracture.

Based on these findings, some areas for future research can be proposed:

a) From measurements of radionuclide concentrations and activity ratios in water (especially $^{234}U/^{238}U$ and ^{226}Ra) and careful extraction/leaching of fracture infill it may be possible to determine in-situ sorption. Such work needs to be very closely associated with detailed mineralogy in order to distinguish between desorption of sorbed phases and dissolution of secondary precipitates (see McKINLEY et al., 1989).

b) A preliminary box model to examine quantitatively the consequences of various transport/retardation mechanisms is currently under consideration. It would be worth further development as predictions would be testable in the event of excavation of the FLG migration experiment fissure. The input data required for such a model would be provided by the measurements proposed in a) above together with basic hydrologic characteristics which are currently being measured at the FLG.

c) Finally, it should be noted that the techniques employed here are equally applicable to fissured sedimentary rocks which are of interest to the Swiss radwaste programme (e.g. marls). Although such rocks have a relatively high porosity, preliminary data indicate that water-carrying fractures are sealed by secondary minerals (e.g. calcite, quartz). Natural series radionuclide profiles through such features may unambigously demonstrate solute transport from the matrix to the fissure thus justifying the assumption of matrix diffusion in the safety analysis. This analysis would also be appropriate to formations with significant gas content, indicating the extent of solute exchange between the unsaturated rock matrix and the major water-carrying fractures.

ACKNOWLEDGEMENTS

Special thanks to J.A.T. SMELLIE for his involvment in the early stages of this project and his continued support throughout. Thanks are also due to the many colleagues in Scotland and Switzerland who contributed to this work, especially T.M. SHIMMIELD and R.M. MALCOLMSON (both SURRC) who analysed many of the samples (with great enthusiasm and care). Thanks also to A.E. FALLICK, G. COOK, I. HARRIS (SURRC) and J. MULGREW (British Coal) for many useful discussions and comments.

We would like to thank U. FRICK and K. SIEGRIST (NAGRA) for their invaluable aid throughout the duration of this work and J. HADERMANN and K. BISCHOFF (both PSI) for general encouragement and profitable discussion. Many thanks to the Mineralogisch-petrographisches Institut, Universität Bern for their considerable efforts towards this study, notably T.J. PETERS, M. MAZUREK, B. HOFMANN and H. DOLLINGER. Special thanks to J. MEYER, of the same institute, for his attention to detail and cogent comments.

The manuscript was greatly improved by reviews by A. LATHAM (University of Liverpool) and J. HADERMANN (PSI) but the opinions expressed herein remain the sole responsibility of the authors.

This work was jointly funded by NAGRA and SKB and we are grateful to both organisations for their support. We would also like to thank NAGRA for their encouragement to publish work from this study in the open literature, which we have done under SMELLIE et al. (1984; 1985; 1986 a,b), MACKENZIE et al. (1986), ALEXANDER et al. (1987, 1988, 1989b), ALEXANDER and SHIMMIELD (1989), McKINLEY et al. (1988) and SCOTT and MACKENZIE (1989).

8. REFERENCES

ABELIN, H., BIRGERSSON, L., GIDLAND, J., MORENO, L., NERETNIEKS, I. and TUNBRANT, S. (1986): Flow and tracer experiments in crystalline rocks: results from several Swedish in-situ experiments. - Sci. Basis Nucl. Waste Manag. IX, pp 627-639. - Ed. L.O. Werme

ÅBERG, G. (1978): Precambrian geochronology of south-eastern Sweden. - Geol. Fören. Stockholm Förh. 100, pp 125-154.

ACEÑA, M.L. and CRESPO, M.T. (1988): On the use of ^{232}U and it's daughters for the determination of ^{226}Ra in water samples. - J. Radioanalyt. Nucl. Chem. Lett. 126, pp 77-85.

AIREY, P.L. (1986): Radionuclide migration around uranium ore bodies in the Alligator Rivers region of the Northern Territory of Australia - Analogue of radioactive waste repositories - a review. - Chem. Geol. 55, pp 255-268.

AIREY, P.L. and IVANOVICH, M. (1986): Geochemical analogues of high-level radioactive waste repositories. - Chem. Geol. 55, pp 203-214.

ALEXANDER, W.R. (1985): Inorganic diagenesis in anoxic sediments of the Tamar estuary. - Unpubl. PhD thesis, Univ. of Leeds, 268 pp.

ALEXANDER, W.R. and SHIMMIELD, T.M. (1989): Microwave oven dissolution of granites and marine sediments: implications for natural decay series analyses. - J. Radioanalyt. Nucl. Chem. Lett. (submitted).

ALEXANDER, W.R., SCOTT, R.D., MacKENZIE, A.B.and McKINLEY, I.G. (1987): Natural analogue studies at Grimsel, southern Switzerland. - Proc. Symp. on Natural Analogues in Radioactive Waste Disposal, Brussels 28-30 April 1987. - Ed. B. Côme and N.A. Chapman. CEC Report No. EUR 11037 EN.

ALEXANDER, W.R., SCOTT, R.D., MacKENZIE, A.B. and McKINLEY, I.G. (1988): A natural analogue study of radionuclide migration in a water-conducting fracture in crystalline rock. - Radiochimica Acta 44/45, pps 283-289.

ALEXANDER, W.R., BAEYENS, B. and UPSTILL-GODDARD, R.C. (1989a): FLG-MI site laboratory support studies: Redox buffering capacity of the granitic rock-water system. - PSI internal report, TM-43-89 (in prep), PSI, Villigen, Switzerland.

ALEXANDER, W.R., McKINLEY I.G., MacKENZIE, A.B. and SCOTT, R.D. (1989b): Attempted verification of matrix diffusion in granite by means of natural decay series disequilibria in a profile across a water-conducting fracture in granitic rock - Sci. Basis Nucl. Waste Manag. (in press)

ALLER, R.C. (1980): Diagenetic processes near the sediment-water interface of Long Island Sound. II. Fe and Mn. - Advances in Geophysics 22, pp 351-415.

ANDREWS, J.N. and KAY, R.C.F. (1982): $^{234}U/^{238}U$ activity ratios of dissolved uranium in ground waters from a Jurassic limestone aquifer in England. - Earth Planet. Sci. Lett. 57, pp 139-151.

ANON (1986): Operating instructions for Parr microwave acid digestion bombs. - Bulletins 4781, 4745 and 243M. - Parr Inst. Coy, Illinois, USA.

BACON, M.P. and ROSHOLT, J.N. (1982): Accumulation rates of ^{230}Th and ^{231}Pa and some transition metals in the Bermuda Rise. - Geochim. Cosmochim. Acta 46, pp 651-666.

BAEYENS, B., BRADBURY, M.H. and AKSOYOGLU, E.S. (1989): Sorption processes in the AU126 mylonite. - Ch. 4 in. - The laboratory support for the Grimsel test site migration experiment: Mineralogy, groundwater chemistry and rockwater interaction (ed. M.H. Bradbury). - NAGRA NTB 88-23, Baden, Switzerland.

BAJO, C. (1980): Extraction du Th et de l'U des granites Suisses. - Unpubl. PhD thesis, Federal Inst. of Tech. Zurich, No. 6738.

BALISTRIERI, L.S. and MURRAY, J.W. (1986): The surface chemistry of sediments from the Panama Basin: The influence of Mn-oxides on metal adsorption. - Geochim. Cosmochim. Acta 50, pp 2235-2243.

BARENBLATT, G. I. ZHELTOV, Iu, P. and KOCHINA, I.N. (1960): Basic concepts in the theory of seepage of homogenous liquids in fissured rocks. J. Appl. Math. Mech. 24 pp 1286.

BARNEY, G.S., LANE, D.L., ALLEN, C.C. and JONES T.E. (1985): Sorption and desorption reactions of radionuclides with a crushed basalt-bentonite packing material. - Rockwell, Hanford Report No. RHO-BW-SA-416P.

BARRETTO, P.M.C. and FUJIMORI, K. (1986): Natural analogue studies: geology and mineralogy of Morro do Ferro, Brazil. - Chem. Geol. 55, pp 297-312.

BATH, A.H., CHRISTOFI, N., NEAL, C., PHILP, J.C., CAVE, M.R. McKINLEY, I.G. and BERNER U. (1987): Trace element and microbiological studies of alkaline groundwaters in Oman, Arabian Gulf: A natural analogue for cement pore waters. - NAGRA NTB 87-16, Baden, Switzerland.

BERGER, L.C. and TRUOG, E. (1944): Boron tests and determination for soils and plants. - Soil Sci. 57, pp 25-36.

BIRGERSSON, L. and NERETNIEKS, I. (1988): Diffusion in the matrix of granitic rock. Field test in the Stripa mine. Final report. - SKB Technical Report 88-08, Stockholm, Sweden.

BRADBURY, M.H. (1989): (editor) The laboratory support for the Grimsel test site migration experiment: Mineralogy, ground water chemistry and rock-water interaction. - NAGRA NTB 88-23, Baden, PSI Report No. 28, Villigen, Switzerland.

BROOKINS, D.G. (1983): Trace element studies of the Oklo natural reactor, Republic of Gabon. - in. The significance of trace elements in solving petrogenetic problems and controversies. - Ed. S.S. Augustithis, Theophrastus Publications, Athens.

BROOKINS, D.G. (1986): Natural analogues for radwaste disposal: elemental migration in igneous contact zones. - Chem. Geol. 55, pp 337-344.

BROOKINS, D.G. (1987): Sandstone uranium deposits: analogue for SURF disposal in some sedimentary rocks. - Proc. Symp. Natural Analogues in Radioactive Waste Disposal, Brussels, 28-30 April, 1987. - Ed. B. Côme and N.A. Chapman. CEC Report No. EUR 11037 EN.

CANTILLANA, R., QUINIF, Y. and MAIRE, R. (1986): Uranium-thorium dating of stalagmites applied to study the Quaternary of the Pyrénées (France): the example of the "Gouffre de la Pierre-Saint-Martin". - Chem. Geol. 57, pp 137-144.

CERNY, P., MEINTZER, R.E. and ANDERSON, A.J. (1985): Extreme fractionation of rare element granitic pegmatites: selected examples of data and mechanisms, Can. Mineral. 23, pp 381-421.

CHAO, T.T. (1972): Selective dissolution of manganese oxides from soils and sediments with acidified hydroxylamine hydrochloride. - Soil Sci. Soc. Am. Proc. 36, pp 764-768.

CHAPMAN, H.D. (1965): Methods of Soil Analysis. - pp 891-904. - Ed. C.A. Black. - American Society of Agronomy, Madison, Wis. USA.

CHAPMAN, N.A., McKINLEY, I.G. and SMELLIE, J.A.T. (1984): The potential of natural analogues in assessing systems for deep disposal of high-level radioactive waste. - NAGRA NTB 84-41, Baden, Switzerland (also SKB TR 84-16).

CHERDYNSTEV, V.V. (1955): Trans. Proc. 3RD Session Comm. on absolute age determinations of geological formations. - Moscow, 1954, pp 175.

CHERDYNSTEV, V.V. (1971): Uranium-234. Israel Programme for Scientific Translations, Jerusalem, pp 234. - (Translation of Uran-234, Atomizodat, Moscow, 1969).

CHESTER, R. and HUGHES, M.J. (1967): A chemical technique for the separation of ferro-manganese minerals, carbonate minerals and adsorbed trace elements from pelagic sediments. - Chem. Geol. 2, pp 249-262.

CHOUKROUNE, P. and GAPAIS, D. (1983): Strain pattern in the Aar Granite (Central Alps): orthogenesis developed by bulk inhomogenous flattening. - J. Struct. Geol. 5, pp 411-418.

CLARK, S.P., PETERMANN, Z.E. and HEIER, K.S. (1966): Handbook of physical constants. - Ed. S.P. Clark. - Geol. Soc. Amer. Mem. 97, pp 521. Geological Society of America, Boulder, Colorado.

CLAUER, N., STILLE, P., BONNOT-COURTOIS, C. and MOORE, W.S. (1984): Nd-Sr isotopic and REE constraints on the genesis of hydrothermal manganese crusts in the Galapagos. - Nature 311, pp 743-745.

COLLEY, S. and THOMSON, J. (1985): Recurrent uranium relocations in distal turbidites emplaced in pelagic conditions. - Geochim. Cosmochim. Acta 49, pp 2339-2348.

COLLEY, S., THOMSON, J., WILSON, T.R.S. and HIGGS, N.C. (1984): Post-depositional migration of elements during diagenesis in brown clay and turbidite sequences in the N.E. Atlantic. - Geochim. Cosmochim. Acta 48, pp 1223-1235.

CORLISS, J.B. (1971): The origin of metal-bearing submarine hydrothermal solutions. - J. geophys. Res. 76, pp 8128-8138.

COTTENIE, A., CAMERLYNCK, R., VERLOS, M. and DHAESE, A. (1979): Fractionation and determination of trace elements in plants, soils and sediments. - Pure and Appl. Chem. 52, pp 45-53.

COWART, J.B. (1980): The relationship of uranium isotopes to oxidation/reduction in the Edwards carbonate aquifer of Texas. - Earth Planet. Sci. Lett. 48, pp 277-283.

DEER, W.A., HOWIE, R.A. and ZUSSMAN, J. (1966): An introduction to the rock-forming minerals. - pp 528. Longman, London.

DRAKE, M.J. (1975): The oxidation estate of europium as an indicator of oxygen fugacity. Geochim. Cosmochim. Acta 39, pp 55-64.

EDMUNDS, W.M., MILES, D.L. and COOK, J.M. (1984): A comparative study of sequential redox processes in three British aquifers. - in Hydrochemical Balances of Freshwater Systems. Ed. E. Eriksson, pp. 55-70. - I.A.H.S. Publication No. 150.

ELDERFIELD, H. and SHOLKOVITZ, R.E. (1987): REE's in the pore waters of reducing nearshore sediments. - Earth. Planet. Sci. Lett. 82, pp 280-288.

EYAL, Y. and FLEISCHER, R.L. (1985): Preferential leaching and the age of radiation damage from alpha decay in minerals. - Geochim. Cosmochim. Acta 49, pp 1155-1164.

FLEISCHER, R.L. and RAABE, O.G. (1978): Recoiling alpha-emitting nuclei. Mechanisms for uranium-series disequilibrium. - Geochim. Cosmochim. Acta 42, pp 973-978.

FOLLET, E.A.C., McHARDY, W.J., MITCHELL, B.D. and SMITH, B.F.L. (1965): Chemical dissolution techniques in the study of soil clays: Parts I and II. - Clay Mineral 6, pp 23-34.

FRONDEL, J.W., FLEISCHER, M. and JONES, R.S. (1967): Glossary of U and Th bearing minerals. - 4th Edit. U.S. Geol. Surv. Bull 1250, pp 69.

GABLEMAN, J.W. (1977): Migration of U and Th. - Am. Assoc. Petrol. Geol., Studies in Geology 3, pp 168.

GASCOYNE, M. (1985): Uranium series disequilibrium studies of Precambrian Shield rocks and groundwaters. - AECL Report, TR-299, pp 634-641. AECL, Pinowa, Canada.

GASCOYNE, M. and SCHWARCZ, H.P. (1986): Radionuclide migration over recent geologic time in a granitic pluton. - Chem. Geol. 59, pp 75-85.

GIOVANOLI, R. (1980): Layer structured Mn oxide hydroxides VI: Recrystallisation of synthetic buserite and the influence of amorphous silica and ferric hydroxide on its nucleation. - Chimia 34, pp 308-310.

GLUECKAUF, E. (1980): The movement of solutes through aqueous fissures in porous rock. - AERE Report 9823, UKAEA, Harwell, UK.

GREY, D. (1986): The geochemistry of U and Th during weathering. - Unpubl. PhD thesis, Univ. of Sydney.

GRISAK, G.E. and PICKENS, J.F. (1980): Solute transport through fractured media. Part 1: The effect of matrix diffusion. - Water Resour. Res. 16, pp 719-730.

GUPTA, S.K. and CHEN, K.Y. (1975): Partitioning of trace metals in selective chemical fractions of nearshore sediments. - Environ. Lett. 10, pp 129-158.

GUTHRIE, V.A. and KLEEMAN, J.D. (1986): Changing U distributions during weathering of granite. - Chem. Geol. 54, pp 113-126.

HADERMANN, J. and ROESEL, F. (1985): Radionuclide chain transport in inhomogenous crystalline rocks: limited matrix diffusion and effective surface sorption. - NAGRA Technical Report 85-40, Baden, Switzerland.

HALBACH, P., VON BORSTEL, D. and GUNDERMANN, K.D. (1980): The uptake of U by organic substance in a peat bog environment on granitic bedrock. - Chem. Geol. 29, pp 117-138.

HARRIS, I. (1985): Unpubl. SURRC internal report. - SURRC, Glasgow, U.K.

HATCH, F.H., WELLS, A.K. and WELLS, M.K (1975): Textbook of Petrology vol. 1: petrology of the ignenous rocks. - 13th edition, Thomas Murby and C^{o}, London.

HENDERSON, P. (1984): Developments in geochemistry 2: REE geochemistry. - Elsevier, Amsterdam.

HERZOG, F. (1987): Modelling isotope distributions in borecores. - Proc. Symp. on Natural Analogues in Radioactive Waste Disposal, Brussels 28-30 April, 1987. Eds. B. Côme and N.A. Champan. CEC Report No. EUR 11037 EN.

HO, C.H. and DOERN, D.C. (1985): The sorption of uranyl species on a haematite sol. - Can. J. Chem. 63, pp 1100-1104.

HOFMANN, B. (1988a): Genese, Alteration und rezentes Fliess-System der Uranlagerstätte Krunkelbach (Menzenschwand, Südschwarzwald). - Unpubl. PhD thesis, Univ. Bern.

HOFMANN, B. (1988b): Geochemical analogue study in the Krunkelbach mine, Menzenschwand, Southern Germany: 1. Geology and water-rock interaction. - Sci. Basis, Nucl. Waste Manag. XII pp 921-926.

HSI, C.-K.D. and LANGMUIR, D. (1985): Adsorption of uranyl onto ferric oxyhydroxides: application of the surface complexation site binding model. - Geochim. Cosmochim. Acta. 49, pp 1931-1941.

HUMPHRIS, S.E. (1984): The mobility of REE's in the earth's crust. - Ch. 9 (pp 317-342) in REE Geochemistry. - Ed. P. Henderson, Vol. 2 Developments in Geochemistry, Elsevier, Amsterdam.

IVANOVICH, M. and HARMON, R.S. (eds.) (1982): Uranium series disequilibrium: applications to environmental problems. - Oxford University Press, Oxford.

IVANOVICH, M. and WILKINS, M.A. (1984a): Harwell report on the analysis of NAGRA groundwater samples from deep boreholes: Uranium series disequilibrium measurements. - AERE Report G3135, UKAEA, Harwell, UK.

IVANOVICH, M. and WILKINS, M.A. (1984b): Harwell report on the analysis of NAGRA rock and fracture infilling samples from Böttstein core: Uranium series disequilibrium measurements. AERE Report G3371, UKAEA, Harwell, UK.

IVANOVICH, M., WILKINS, M.A. and DEARLOVE, J. (1986a): Analysis of uranium series disequilibrium data in NAGRA's deep borehole solid and liquid samples. - AERE Report 12482, UKAEA, Harwell, UK.

IVANOVICH, M., DEARLOVE, J. and LEVER, D.A. (1986b): Uranium series disequilibrium profiles from reduction haloes in Permian red-beds of Northern Switzerland. - AERE Report 12483, UKAEA, Harwell, UK.

IVANOVICH, M., LONGWORTH, G., WILKINS, W.A., HASLER, S.E. and LLOYD, M.J. (1988): Measurement of effective K_d factors for long-lived uranium and thorium isotopes in samples of London Clay (Bradwell) and Mudrock (Fulbeck). - NIREX Tech. Rep. NSS-R117, U.K.

JOLLIFF, B.L., PAPIKE, J.J. and SHEARER, C.K, (1987): Fractionation trends in mica and tourmaline as indicators of pegmatite internal evolution: Bob Ingersoll pegmatite, Black Hills, South Dakota. - Geochim. Cosmochim. Acta 51, pp 519-534.

JONASSON, R.G., BANCROFT, G.M. AND BOATHER L.A. (1988): Surface reaction of synthetic end member analogues of monazite, xenotime and rhabdophane, and evolution of ground waters. - Geochim. Cosmochim. Acta 52, pp 767-770.

KAMINENI, D.C. (1986): Distribution of U and Th and REE's in the Eye-Dashwa Lakes pluton - a study of some analogue elements. - Chem. Geol. 55, pp 361-373.

KAMINENI, D.C., CHUNG, C.F., DUGAL, J.J.B. and EJECKAM R.B. (1986): Distribution of U and Th in core samples from the underground research laboratory lease, southeastern Manitoba, Canada. - Chem. Geol. 54, pp 97-111.

KBS (1983): Final storage of spent nuclear fuel. - SKB/KBS 3. - Stockholm, Sweden.

KRALIK, M. (1984): Effects of cation-exchange treatment and acid leaching on the Rb-Sr system of illite from Fithian, Illinois. - Geochim. Cosmochim. Acta 48, pp 527-533.

KRESTEN, P. and CHYSSLER, J. (1976): The Götemar massif in south-eastern Sweden: a reconnaissance survey. - Geol. Fören. Stockholm Förh. 98, pp 155-161.

KRISHNASWAMI, S. and SEIDEMANN, D.E. (1988): Comparative study of ^{222}Rn, ^{40}Ar, ^{39}Ar and ^{37}Ar leakage from rocks and minerals: Implications for the role of nanopores in gas transport through natural silicates. - Geochim. Cosmochim. Acta 52, pp 655-658.

LABHART, T.P. (1977): Aarmassiv and Gotthardmassiv. - Sammlung geol. Führer vol. 63, Borntraeger, Berlin.

LABHART, T.P. and RYBACH, L. (1976): Radioaktivitätsprofile durch den Zentralen Aaregranit im Bereich der Schweizer Geotraverse. - Schweiz. mineral. petrogr. Mitt. 56, pp 669-673.

LAFLAMME, B.D. and MURRAY, J.W. (1987): Solid/solution interaction: the effect of carbonate alkalinity on adsorbed thorium. - Geochim. Cosmochim. Acta 51, pp 243-250.

LAMOTHE, P.J., FRIES, T.L. and CONSUL, J.J. (1986): Evaluation of a microwave oven system for the dissolution of geologic samples. - Anal. Chem. 58, pp 1881-1886.

LANGEVALD VAN, A.D., GAAST VAN DER, S.J. and EISMA, D. (1978): A comparison of the effectiveness of eight methods for the removal of organic matter from clay. - Clays and Clay Miner. 26, pp 361-364.

LANGMUIR, D. (1978): Uranium solution-mineral equilibria at low temperatures with applications to sedimentary ore deposits. - Geochim. Cosmochim. Acta 42, pp 547-569.

LANGMUIR, D. and HERMAN, J.S. (1980): The mobility of thorium in natural waters at low temperatures. - Geochim. Cosmochim. Acta 44, pp 1753-1766.

LATHAM, A.G. and SCHWARCZ, H.P. (1987a): The relative mobility of U, Th and Ra isotopes in the weathered zones of the Eye - Dashwa Lakes granite pluton, northwestern Ontario, Canada. - Geochim. Cosmochim. Acta 51, pp 2787-2793.

LATHAM, A.G. and SCHWARCZ, H.P. (1987b): On the possibility of determining rates of removal of uranium from crystalline igneous rocks using U-series disequilibria. -1: A U-leach model and its applicability to whole-rock data. - Appl. Geochem. 2, pp 55-65.

LATHAM, A.G. and SCHWARCZ, H.P. (1987c): On the possibility of determining rates of removal of uranium from crystalline igneous rocks using U-series disequilibria. -2: Applicability of a U-leach model to mineral separates.- Appl. Geochem. 2, pp 67-71.

LAUL, J.C. and SCHMITT, R.A. (1975): Dunite 72417: A chemical study and interpretation. - Proc. 6th Lunar Sci. Conf., pp 1231-1254.

LAUL, J.C. and SMITH, M.R. (1988): Disequilibrium study of natural radionuclides of uranium and thorium series in cores and briny groundwaters from Palo Duro Basin, Texas. - Rad. Waste Manag. Nucl. Fuel Cycle 11, pp 169-225.

LAUL, J.C., SMITH, M.R. and HUBBARD, N. (1985): $^{234}U/^{230}Th$ ratio as an indicator of redox state, and U, Th and Ra behaviour in briney aquifers. - Sci. Basis Nucl. Waste Manag. IX, pp 673-680. - Ed. L. Werne.

LOWSON, R.T., SHORT, S.A., DAVEY, B.G. and GRAY, D.J. (1986): $^{234}U/^{238}U$ and $^{230}Th/^{234}U$ activity ratios in mineral phases of a lateritic weathered zone. - Geochim. Cosmochim. Acta 50, pp 1697-1702.

MacKENZIE, A.B., SCOTT, R.D., McKINLEY, I.G. and WEST, J.M. (1983): A study of long term (10^3-10^4 y) elemental migration in saturated clays and sediments. - FLPU 83-6, IGS London, UK.

MacKENZIE, A.B., BOWDEN, P. and KINNAIRD, J.A. (1984): Combined neutron activiation and particle track analysis of element distributions in a rock slice of mineralized granite. - J. Radioanaly. Chem. 82, pp 341-352.

MacKENZIE, A.B., SCOTT, R.D. and SMELLIE, J.A.T. (1986): A comparison of neutron activation and alpha-spectroscopy analyses of thorium in crystalline rocks. - J. Radionanalyt. Nucl. Chem. Lett. 103, pp 321-330.

McKINLEY, I.G., ALEXANDER, W.R., BAJO, C., FRICK, U., HADERMANN, J., HERZOG, F.A. and HOEHN, E. (1988): The radionuclide migration experiment at the Grimsel rock laboratory, Switzerland. - Sci. Basis Nucl. Waste Manag. XI, pp 178-187.

McKINLEY, I.G., ALEXANDER, W.R. and HERZOG, F.A. (1989): A critical review of the in situ K_D concept (in prep.).

MAGNUSSON, K.A. and DURAN, O. (1984): Comparative study of geological, hydrological and geophysical borehole investigations. Div. KBS, SKBF, Stockholm, Tech. Rep. No. 84-09.

MANSKAYA, S.M. and DROZDOVA, T.V. (1968): Geochemistry of Organic Substances. - Pergamon Press. Oxford, pp 345.

MAYNARD, J.B. (1983): Geochemistry of Sedimentary Ore Deposits. - Springer-Verlag, Berlin, pp 305.

MEYER, J., MAZUREK, M. and ALEXANDER, W.R. (1989): Geology of the FLG migration site (AU96). Ch. 2 in The laboratory support for the Grimsel test site migration experiment: Mineralogy, ground water chemistry and rock-water intraction (ed. M.H. Bradbury). - NAGRA NTB 88-23, Baden, Switzerland.

MICHEL, J. (1984): Redistribution of uranium and thorium series isotopes during isovolumetric weathering of granite. - Geochim. Cosmochim. Acta 48, pp 1249-1255.

MOELLER, P. and MUECKE, G.K. (1984): Significance of europium anomalies in silicate melts and crystal-melt equilibria: a re-evaluation. Contrib. Mineral. Petrol. 87, pp 242-250.

MORTON, J.P. and LONG, L.E. (1980): Rb-Sr dating of Paleaozoic glauconite from the Llano region, central Texas. - Geochim. Cosmochim. Acta 44, pp 663-672.

NAGRA, (1981): Sondierbohrungen Juchlistock - Grimsel. - NAGRA, NTB 81-07, Baden, Switzerland, pp 79.

NAGRA, (1984): Erläuterung zur Geologischen Karte der zentralen Nordschweiz. - NAGRA, NTB 84-25, Baden, Switzerland.

NAGRA, (1985a): Nukleare Entsorgung Schweiz: Konzept und Uebersicht über das Projekt Gewähr 1985. - NAGRA, NGB 85-01 to 08, Baden, Switzerland.

NAGRA (1985b): Felslabor Grimsel: Rahmenprogramm und Statusbericht. - NAGRA, NTB 85-34, Baden, Switzerland, pp 148.

NAGRA (1985c): Sondierbohrung Böttstein - Untersuchungsbericht - NAGRA, NTB 85-01, Baden, Switzerland.

NERETNIEKS, I. (1980): Diffusion in the rock matrix: An important factor in radionuclide retardation? - J. geophys. Res. 85, pp 4379-4397.

NERETNIEKS, I. (1983): The movement of a redox front downstream from a repository for nuclear waste. - Nucl. Technol. 62, pp 110-115.

NERETNIEKS, I. (1986): Some uses for natural analogues in assessing the function of a HLW repository. - Chem. Geol. 55, pp 175-188.

NESBITT, H.W. (1979): Mobility and fractionation of rare earth elements during weathering of granodiorite. - Nature 279, pp 206-210.

O'CONNER, T.P. and KESTER, D.R. (1975): Adsorption of Cu and Co from fresh and marine systems. - Geochim. Cosmochim. Acta 39, pp 1531-1543.

OHSE, W. (1983): Lösungs- und Fällungserscheinungen im System oberflächennähes unterirdisches Wasser/gesteinsbildende Minerale - eine Untersuchung auf der Grundlage des chemischen Gleichgewichts - Thermodynamik. - Unpubl. PhD. thesis, Univ. of Kiel.

PALACIOS, C.M., HEIN, U.F. and DULSKI, P. (1986): Behaviour of REE's during hydrothermal alteration at the Buena Esperanza copper-silver deposit, northern Chile. - Earth Planet. Sci. Lett. 80, pp 208-216.

PETERS, T.J., MATTER, A., BLAESI, H.R. and GAUTSCHI, A. (1986): Sondierbohrung Böttstein Geologie. - NAGRA, NTB 85-02, Baden, Switzerland.

QUIRKE, T. and KREMERS, H. (1943): Pegmatite crystallization. - Am. Mineral. 28, pp 571-580.

RAMA T. and MOORE, W.S. (1984): Mechanism of transport of U-Th series radioisotopes from solids into groundwater. - Geochim. Cosmochim. Acta 48, pp 395-399.

ROSHOLT, J.N. (1982): Mobilization and Weathering. Ch. 7 in Uranium series disequilibrium: applications to environmental problems. Eds. M. Ivanovich and R.S. Harmon. - Oxford Science Publications, Oxford (1982).

ROSHOLT, J.N. (1983): Isotopic composition of U and Th in crystalline rocks. - J. geophys. Res. 88, pp 7315-7330.

SCHREIBER, H.D., LAUER, H.V. and THANYASIRI, T. (1980): The redox state of cerium in basaltic magmas: an experimental study on iron-cerium interactions in silicate melts. Geochim. Cosmochim. Acta 44, pp 1599-1612.

SCHWARCZ, H.P., GASCOYNE, M. and FORD, D.C. (1982): Uranium series disequilibrium studies of granitic rocks. - Chem. Geol. 36, pp 87-102.

SCOTT, R.D. and MacKENZIE, A.B. (1984): Detection of ^{222}Rn by use of silicon surface-barrier detectors. - Int. J. Appl. Radiat. Isot. 35, pp 301-303.

SCOTT, R.D. and MacKENZIE, A.B. (1985): Measurement of low ^{222}Rn activities by means of surface barrier detectors. - Nucl. Instr. and Meth. A238, pp 160-164.

SCOTT, R.D. and MacKENZIE, A.B. (1989): The intrepretation of U-Th ratios in non-ideal systems. - (in prep.).

SHEA, M. (1984): Uranium migration at some hydrothermal veins near Marysvale, Utah: a natural analog for waste isolation. Sci. Basis Nucl. Waste Manag. VII.

SHIRVINGTON, P.J. (1983): Fixation of radionuclides in the ^{238}U decay series in the vicinity of mineralised zones: 1. The Austatom uranium prospect, Northern Territory, Australia. - Geochim. Cosmochim. Acta 47, pp 403-412.

SMELLIE, J.A.T. and ROSHOLT, J.N. (1984): Radioactive disequilibria in mineralised fracture samples from two uranium occurrences in northern Sweden. Lithos 17, pp 215-225.

SMELLIE, J.A.T. and STUCKLESS, J.S. (1985): Element mobility studies of two drillcores from the Götemar granite (Kråkemåla test site), S.E. Sweden. - Chem. Geol. 51, pp 55-78.

SMELLIE, J.A.T., MacKENZIE, A.B. and SCOTT, R.D. (1984): Natural analogues to the conditions around a final repository for high-level radioactive waste. in J.A.T. Smellie (ed.) - SKB/KBS Technical Report 84-18 Stockholm, Sweden.

SMELLIE, J.A.T., MacKENZIE, A.B. and SCOTT, R.D. (1985): An analogue validation study of natural radionuclide migration in crystalline rocks using uranium-series disequilibrium: preliminary results. - Sci. Basis Nuc. Waste Manag. IX, pp 91-98 - Ed. L.O. Werme.

SMELLIE, J.A.T., MacKENZIE, A.B. and SCOTT, R.D. (1986a): I. An analogue validation study of natural radionuclide migration in crystalline rock using uranium-series disequilibrium studies. - II. A comparison of neutron activation and alpha-spectroscopy analyses of Th in crystalline rocks. - SKB Technical Report 86-01, Stockholm, Sweden.

SMELLIE, J.A.T., MacKENZIE, A.B. and SCOTT, R.D. (1986b): An analogue validation study of natural radionuclide migration in crystalline rocks using U-series disequilibrium studies. - Chem. Geol. 55, pp 233-254.

SMITH, C.W. and STEGER, H.F. (1983): ^{226}Ra in certified U reference ores DL-1a, BL-4a, DH-1a and BL-5. - CANMET Report 83-9E: CANMET (Energy, Mines and Resources), Ottawa, Canada.

STAATZ, M.H., MURARA, K.J. and GLASS, J.J. (1955): Variation of composition and physical properties of tourmaline with its position in the pegmatite. - Amer. Mineral. 40, pp 780-804.

STALDER, H.A. (1964): Petrographische und mineralogische Untersuchungen im Grimselgebiet. - Schweiz. mineral. und petrog. Mitt. 44/1, pp 187-398.

STECK, A. (1968): Die alpidischen Strukturen in den Zentralen Aaregraniten des westlichen Aarmassivs. - Eclogae geol. Helv. 61, pp 19-48.

STUART, E.J., BORNHORST, T.J., ROSE W.I. and NOBLE, D.C. (1983): Distribution and mobility of U and Th in the peralkaline soldier meadow tuff, NW Nevada. - Econ. Geol. 78, pp 353-358.

STUMM, W. and MORGAN, J.J. (1981): Aquatic Chemistry. - John Wiley and Sons, New York.

TAMM, O. (1934a): Oxalate method in chemical examination of soils. - Medd. Stat. Skogsforsoksanst 27, pp 1-20 (Chem. Abstr. 29:59692).

TAMM, O. (1934b): Rapid mineralogical examination of soil. - Sven, Skogsvardsford. Tids. No. 1-2, 231 (Chem. Abstr. 29:59692).

TANNER, A.B. (1964): Radon migration in the ground: a review. - in The Natural Radiation Environment. - eds J.A.S. Adams and W.M. Lowder, Univ. Chicago Press, Chicago.

TESSIER, A., CAMPBELL, P.G.C. and BISSON, M. (1979): Sequential extraction procedure for the speciation of particulate trace metals. - Anal. Chem. 51, pp 844-851.

TESSIER, A., CAMPBELL, P.G.C. and BISSON, M. (1980): Trace metal speciation in the Yamaska and St. François rivers (Québec). - Can. J. Earth Sci., 17, pp 90-105.

TESSIER, A., RAPIN, F. and CARIGNAN, R. (1985): Trace metals in oxic lake sediments: possible adsorption onto iron oxhydroxides. - Geochim. Cosmochim. Acta 49, pp 183-194.

TEWARI, P.H., CAMPBELL, A.B. and LEE, W. (1972): Adsorption of cobalt (+2), by oxides from aqueous solution. - Can. J. Chem. 50, pp 1642-1648.

THIEL, K., VORWERK, R., SAAGER, R. and STUPP, H.D. (1983): ^{235}U fission tracks and ^{238}U-series disequilibria as a means to study recent mobilisation of uranium in Archaean pyritic conglomerates. - Earth Planet Sci. Lett. 65, pp 249-262.

TORSTENFELT, B., ALLARD, B., JOHANNSON, W. and ITTNER, T. (1983): Iron content and reducing capacity of granites and bentonite. - KBS Technical Report 83-36, Stockholm.

UPSTILL-GODDARD, R.C., ALEXANDER, W.R., ELDERFIELD, H. and WHITFIELD, M. (1989): Chemical diagenesis in the Tamer Estuary. - Contrib. to Geochem. 16, pp 1-49.

WALKER, R.J., HANSON, G.N., PAPIKE, J.J. O'NEIL, J.R. and LAUL, J.C. (1986): Internal evolution of the Tin Mountain pegmatite, Black Hills, South Dakota. - Amer. Mineral. 71, pp 440-459.

WEIJDEN, C.H., ARTHUR R.C. and LANGMUIR, D. (1976): Sorption of uranyl by haematite: theoretical and geochemical implications. - Geol. Soc. Am. Annual. Meeting, Denver, USA.

ZIELINSKI, R.A., BLOCH, S. and WALKER, T.R. (1983): The mobility and distribution of heavy metals during the formation of First Cycle Red Beds. - Econ. Geol. 78, pp 1574-1589.

ZUKIN, J.G., HAMMOND, D.E., KU, T.L. and ELDERS, W.A. (1987): U-Th series radionuclides in brines and reservoir rocks from two deep geothermal borheoles in the Salton Sea Geothermal Field, southeastern California. - Geochim. Cosmochim. Acta 51, pp 2719-2721.

Appendix A: Data for the mylonite AU126 which has not been discussed in the text

INAA analyses

Element	Concentration (ppm unless otherwise stated)
Na	2.31±0.12 (%)
K	3.23±0.45 (%)
Sc	7.60±0.39
Fe	2.30±0.13 (%)
Co	5.7±0.7
Cs	11.4±0.8
La	54±4
Ce	132±10
Nd	57±3
Sm	8.1±0.4
Eu	1.45±0.28
Lu	0.87±0.10
Hf	7.2±0.5
Ta	2.0±0.4
Th	33±2
Mn	287.4±18.6